Elucidation of the Aqueous Equilibrium System of $IrH_2(PMe_3)_3Cl$ and Periodic Trends of the Iridium (III) dihydrido tris(trimethylphosphino) Series, $IrH_2(PMe_3)_3X$

by

Kelly E. Matthews

Dissertation submitted to the Faculty of the
Virginia Polytechnic Institute and State University
in partial fulfillment of the requirements for the degreee of

DOCTOR OF PHILOSOPHY
in
CHEMISTRY

APPROVED:

Joseph S. Merola, Chairman

Karen Brewer

John Dillard

James Glanville

Brian Hanson

July 1994
Blacksburg, Virginia

Elucidation of the Aqueous Equilibrium System of $IrH_2(PMe_3)_3Cl$ and Periodic Trends of the Iridium (III) dihydrido tris(trimethylphosphino) Series, $IrH_2(PMe_3)_3X$

by
Kelly E. Matthews
Joseph S. Merola, Committee Chairman
Department of Chemistry
(ABSTRACT)

The complex, $IrH_2(PMe_3)_3Cl$ (**1**), was previously found to be, not only unexpectantly water-soluble but also an effective homogeneous catatyst for the hydrogenation of unsaturates in water. The results of extensive ^{31}P NMR studies on the aqueous system of (**1**) indicate that (**1**) is in equilibrium with the iridium(III) dihydrido "aquo" complex, $[IrH_2(PMe_3)_3(H_2O)]^+$, and not the μ-chloro bridged complex, $\{[IrH_2(PMe_3)_3]_2Cl\}^+$ (**2**), as previously reported. The calculated K_{eq} value for the aqueous equilibrium is (0.0037 ± 0.0003) M. Thermodynamic data (ΔH = 30.8 kJ/mol, ΔS = 56.0 J/(Kmol), and ΔG = 14.1 kJ/mol) obtained from variable temperature ^{31}P NMR studies are consistent with the proposed equilibrium system.

The complexes $IrH_2(PMe_3)_3X$ (X = O_2CPh (**3**), I (**4**), and Br (**6**) were synthesized and examined. The complexes $IrH_2(PMe_3)_3X$ (X = H_2O and F) could not be isolated. (**3**) was determined to dissociate completely in water to form the iridium(III) dihydrido "aquo" complex, $[IrH_2(PMe_3)_3(H_2O)]^+$, seemingly explaining the greater catalytic activity of (**3**). Solubility of the halo complexes decreased from moderately soluble (**1**), to slightly soluble (**6**), to very slightly soluble (**4**). The solubilities of (**4**) and (**6**) were too low to allow quantification of their equilibria.

Finally it was observed that linear relationships exist between the electronegativity of the ligand, **X**, and the ^1H and ^{31}P NMR chemical shifts of the hydrides and the phosphines for the complexes, $IrH_2(PMe_3)_3X$. These relationships are consistent with the findings of Birnbaum.

This dissertation is dedicated to my father —
who had the sense of humor to wait until after I was born to decide
he didn't want more children.

Acknowledgements

I wish to specifically thank Joseph Merola, for his time, patience, and understanding; my committee members, Karen Brewer, John Dillard, Jim Glanville, and Brian Hanson for their assistance.

Acknowledgement goes to the National Science Foundation, the Petroleum Research Fund, and the Department of Chemistry at Virginia Tech for their financial support.

Personal thanks to Chris Roy, without whom I would have shot everyone.

Table of Contents

Illustrations

Tables

Chapter 1 - Introduction

The general thrust of the Merola Group research effort has been the activation of various E-H bonds (E = B, C, N, O) by the complex $[Ir(PMe_3)_3(cod)]Cl$ (cod = 1,5-cyclooctadiene), and subsequent analysis of the reactivity and physical characteristics of the resultant complexes shown below.

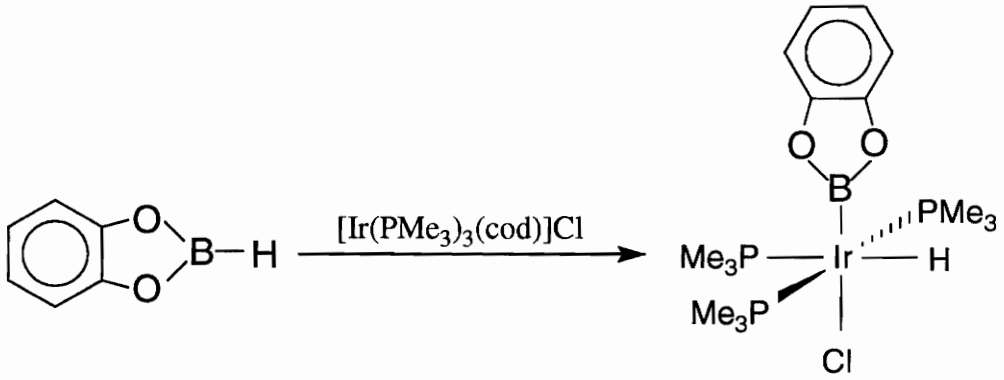

Organometallics, 9, 3008, **1990**

(1.1)

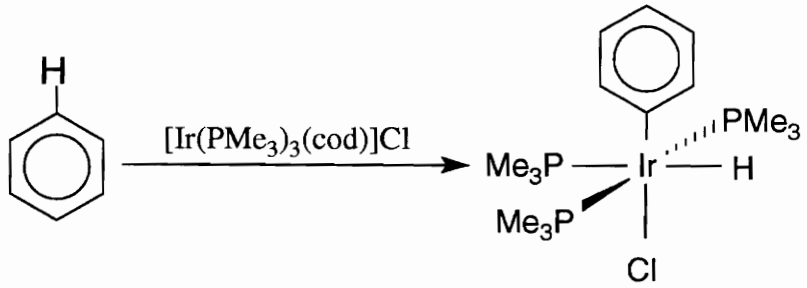

Polyhedron, 11, 2912, **1992**

(1.2)

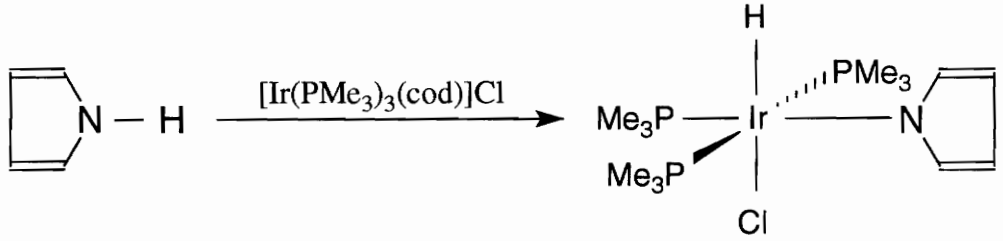

Inorg. Chem., 29, 4172, **1990**

(1.3)

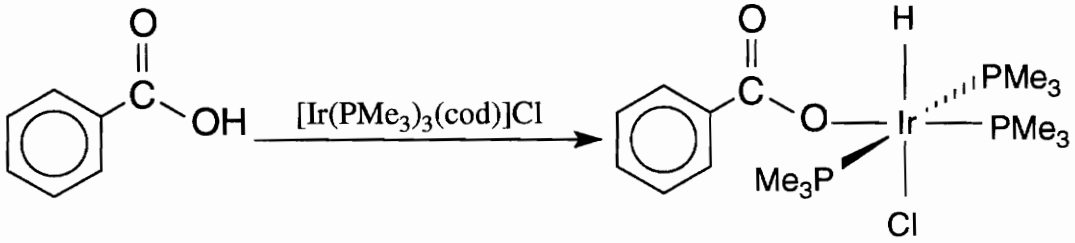

Inorg. Chem., 32, 1681, **1993**

(1.4)

In 1992, Le synthesized $IrH_2(PMe_3)_3Cl$ (**1**), by hydrogenating $[Ir(PMe_3)_3(cod)]Cl$ with molecular hydrogen.[11] X-ray crystallography and ^1H NMR and ^{31}P NMR spectroscopy in CD_2Cl_2 determined that (**1**) was a classical organometallic dihydride.

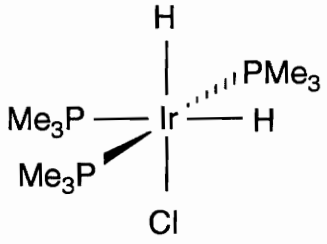

(1)

Organometallics, 12, 3798 **1993**

However during the investigation of the reactivity of $IrH_2(PMe_3)_3Cl$, Le discovered that, surprisingly, (**1**) was moderately soluble in water. Subsequent studies showed that aqueous solutions of (**1**) would easily insert unsaturates under mild conditions to form iridium vinyl monohydride complexes. Performing the same experiments under hydrogen atmosphere led to the formation and recovery of alkanes, alkenes, and the starting material (**1**), indicating (**1**) was able to catalyze the hydrogenation of unsaturates *in water.* Catalytic control studies of (**1**) in the typical organic solvents often used with other catalytic dihydrides showed no reaction. Thus it was inferred that the catalytic activity of (**1**) was somehow intimately connected to water.

^1H NMR and ^{31}P NMR studies of (**1**) in D_2O or H_2O indicated the presence of two distinct species in aqueous solution. Very crude experiments led to the belief that the two complexes were in equilibrium. The material presented in the following chapters describes background of dihydride complex chemistry, the elucidation of the specific aqueous equilibrium system of (**1**) and the involved species, synthesis and reactivity of other related iridium(III) dihydrides, and discussion of the periodic trends of these dihydride complexes.

Chapter 2 - Literature Review

Transition Metal Dihydride Chemistry

Even though the first transition metal hydrides, $H_2Fe(CO)_4$ and $HCo(CO)_4$ were discovered in 1934 by Hieber, the instability of these complexes prevented transition metal hydrides from becoming more than laboratory curiosities until the late 1950's. In 1955 Wilkinson and Birmingham synthesized $HRe(C_5H_5)_2$ and Fischer, Hafner, and Stahl synthesized $HM(C_5H_5)(CO)_3$ (M = Cr, Mo). After the 1957 discovery of *trans* – $HPtCl(PEt_3)_2$ by Chatt, Duncanson, and Shaw, hydride chemistry developed rapidly. By 1965 more than 300 papers had been written on hydrides and more than 200 derivatives had been characterized. At that time hydrides began to be recognized as intermediates and catalysts in, among others, hydrogenation, olefin isomerization, and hydroformylation reactions. By 1971 when Kaesz and Saillant's review of hydrides was written, over 400 new articles had appeared and 500 new hydride complexes had been synthesized, and coordinatively unsaturated complexes of all metals, with the exception of Cd and Hg, had been shown to bind to molecular hydrogen in some way.[1] This burst of activity has continued to the present, as the role of hydrides in heterogeneous and homogeneous catalysis as well as other synthetically useful reactions continues to be explored.

Most of the hydride complexes synthesized, excluding binary metal hydrides which are not included in this review, contain either phosphino or carbonyl ligands, because of the ability of these ligands to stabilize the metal–hydrogen bond by decreasing the electron density on the metal.[2] A comprehensive review of the transition metal hydrides known to

date is beyond the scope of this review. However, as dihydride complexes are an integral part of this thesis, an overview of transition metal dihydride complex synthesis and reactivity follows in the next section.

An Overview of Dihydride Complexes and Reactions

Dihydrides (and hydrides by default) can be synthesized by five noticeably different synthetic pathways.[1]

1) Reactions with molecular hydrogen (H_2) to form neutral complexes.
2) Reactions of metal complexes with complex hydrides.
3) Hydrogen transfer from solvent or coordinated groups.
4) Protonation.
5) Oxidative addition of H_2 and HX to cationic metal centers.

This review will present significant dihydride complexes and their syntheses grouped according to this scheme.

1) Reactions with Molecular Hydrogen

Several methods are available to make dihydride complexes by reaction with molecular hydrogen. The first of these is the direct hydrogenation of the metal at elevated temperatures and pressures as in the reaction of iron metal with hydrogen and bisdiethylphosphinoethane (depe) (eq. 2.1).

$$Fe + depe + H_2 \xrightarrow{200\ C} H_2Fe(depe)_2 \quad \textbf{(2.1)}$$

Kruck *et. al.*, took this synthesis one step farther by synthesizing hydridometal trifluorophosphine complexes from metal salts, a halogen acceptor, a ligand, and hydrogen[3,4]. (Eq. 2.2)

$$FeI_2 + Zn + H_2\,(100\ atm) + PF_3 \xrightarrow{250\ C} H_2Fe(PF_3)_4 \quad \textbf{(2.2)}$$

L'Eplattenier and Calderazzo[5,6] synthesized $H_2Os(CO)_4$ in a number of ways. (Eq. 2.3)

$$\begin{aligned} OsO_4 + CO + H_2 &\xrightarrow[\text{heptane, 6 hr}]{\text{180 atm, 160 C}} \\ Os(CO)_5 + H_2 &\xrightarrow[\text{heptane, 10 hr}]{\text{180 atm, 170 C}} H_2Os(CO)_4 \\ Os_3(CO)_{12} + H_2 &\xrightarrow[\text{6 hr}]{\text{80 atm, 100 C}} \end{aligned} \quad \textbf{(2.3)}$$

Dihydrides can also be made by replacement of a coordinated ligand with H_2, as in Equation 2.4, where a CO ligand was replaced. L'Eplattenier and Calderazzo synthesized the ruthenium analog, $H_2Ru(CO)_2(PPh_3)_2$, in a similar manner.[6]

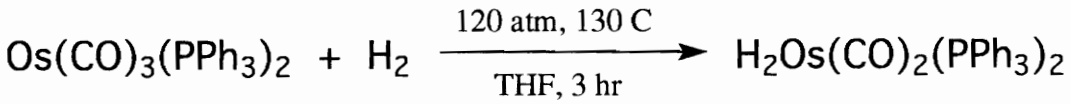

(2.4)

In 1983 Kubas, *et. al.* [7] postulated the existence of, then later[8] found clear evidence for, $W(CO)_3(P^iPr_3)_2(\eta^2\text{–}H_2)$ (^{i}Pr = isopropyl), the first documented case of a non–classical (dihydrogen σ–bonded) dihydride complex. Kubas *et. al.* observed that when triisopropylphosphine was added to a yellow solution of $M(CO)_3$(cht) (M=W, Mo; cht = cycloheptatriene) under nitrogen atmosphere, the solution evolved a gas and became orange when SO_2 was added. When the initial complex solution was placed under an argon atmosphere, instead of nitrogen, *and* no SO_2 was added, the solution turned purple instead of orange. It was also found that H_2 added reversibly to the purple solution of

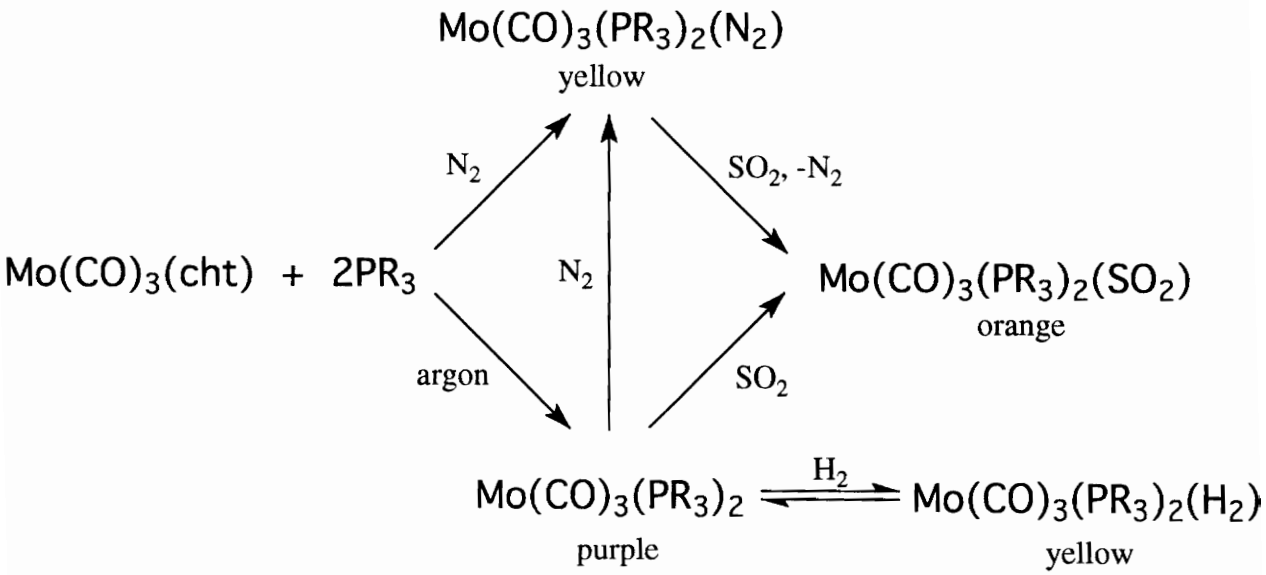

Figure 2.1 Kubas's Mechanism for the Formation of $Mo(CO)_3(PR_3)_2(H_2)$

$M(CO)_3(PR_3)_2$ giving yellow complexes with properties similar to those of the N_2 adducts. (Fig. 2.1) These new complexes failed to catalyze SO_2 or ethylene hydrogenation. IR spectra of these complexes were not indicative of classical seven–coordinate dihydride structures. After X–ray crystallography failed to determine the positions of the hydrides within the complex, single–crystal neutron diffraction finally provided the first unequivocal proof of the non–classical η^2–dihydrogen bond, in the complex $W(CO)_3(PR_3)_2(H_2)$.

More recently Schubert and Knorr[9] synthesized a mixed phosphino–carbonyl iron dihydride complex photochemically, (Eq. 2.5) after having already made the dihydrido complex from a monohydridosilyltetracarbonyliron complex. (Eq. 2.6)

$$Fe(CO)_3(dppe) + H_2 \xrightarrow[\text{toluene, -35 C}]{h\upsilon} H_2Fe(CO)_2(dppe) \qquad \textbf{(2.5)}$$

$$Fe(CO)_4(H)SiPH_3 + dppe \xrightarrow[\text{benzene}]{\text{20 C}} H_2Fe(CO)_2(dppe) \qquad \textbf{(2.6)}$$

In 1990, Deutsch and Eisenberg[10] displaced an η^2–C_2H_4 ligand with H_2, forming $H_2Ir(Et)(CO)(dppe)$ (eq. 2.7). This compound was suggested to be one of the intermediates in the hydrogenation reaction of ethylene by $IrH_3(CO)(dppe)$. The results of their kinetic studies at 150 torr C_2H_4 and 300 torr H_2 at 80 °C indicated the individual

$$Ir(Et)(\eta^2\text{-}C_2H_4)(CO)(dppe) + H_2 \xrightarrow[\text{benzene}]{} H_2Ir(Et)(CO)(dppe) \qquad \textbf{(2.7)}$$

reactions that occur were unimolecular and have highly ordered transition states. The authors proposed the first step was the reversible loss of H_2, followed by the reversible η^2–coordination of ethylene and then hydride migration. H_2 then coordinated with subsequent loss of ethane. If this scheme is correct, then this dihydridoiridium complex is one of the few examples of an alkyldihydridometal complex directly involved in olefin hydrogenation.

Finally in 1992, Le[11] synthesized a dihydridoiridium complex from $Ir(COD)(PPh_3)_3Cl$ by displacing 1,5–cyclooctadiene with H_2 . (Eq. 2.8) This complex

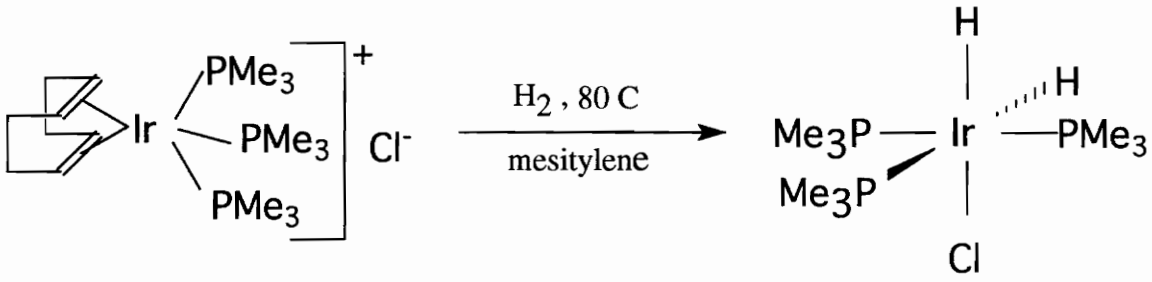

(2.8)

was unusual because it was soluble not only in solvents like benzene, chloroform, and methylene chloride, but also in water. It was also an active hydrogenation catalyst in water. A separate section in this review is reserved for a more in–depth discussion of this complex and its derivatives' properties, characteristics, and chemistry.

Oxidative addition of H_2 to a coordinatively unsaturated metal complex is another method utilized to synthesize dihydride complexes. Vaska and Rhodes[12] in 1965 showed treatment of the sixteen electron complex $IrCl(CO)(PPh_3)_2$ with H_2 gives the eighteen electron *cis* dihydrido complex shown below in Equation 2.9.

$$\textit{trans}\text{-}IrCl(CO)(PPh_3)_2 + H_2 \overset{1\ atm}{\rightleftharpoons} \textit{cis}\text{-}H_2IrCl(CO)\text{-}\textit{trans}\text{-}(PPh_3)_2 \quad \textbf{(2.9)}$$

In 1966, Osborn, *et. al.*[13] dissolved Wilkinson's catalyst, $RhCl(PPh_3)_3$, in either benzene, chloroform, ethyl acetate, or glacial acetic acid, causing the loss of a phosphine ligand to form a brilliant red solution, in which a solvent molecule was thought to be loosely bound to the metal complex $RhCl(PPh_3)_2$. (Eq. 2.10) When shaken with molecular hydrogen, the solution turns pale yellow. Upon sweeping this yellow solution

$$RhCl(PPh_3)_3 \overset{benzene}{\rightleftharpoons} RhCl(PPh_3)_2 + PPh_3 \quad \textbf{(2.10)}$$

with nitrogen the solution returns to its original red color, indicating the reversible uptake of hydrogen. (Eq. 2.11) Similar behavior was observed for the compounds $RhBr(PPh_3)_3$, and $RhI(PPh_3)_3$. All of these complexes were demonstrated to be catalysts in the homogeneous hydrogenation of non-conjugated olefins and acetylenes at ambient temperatures and pressures at or below 1 atm. Their findings indicate; 1) terminal olefins were reduced more rapidly than internal olefins; 2) *cis* –olefins were reduced faster than *trans* –; 3) conjugated olefins were not reduced at 1 atm, but can be reduced at higher pressures (*ca.* 60 atm.); 4) ethylene was not hydrogenated; and 5) functional groups such as carbonyls, nitriles, or azo– were not reduced under these conditions.

$$\underset{\text{red}}{RhCl(PPh_3)_2} + H_2 \overset{benzene}{\rightleftharpoons} \underset{\text{yellow}}{H_2RhCl(PPh_3)_2} \quad \textbf{(2.11)}$$

Magueand Wilkinson[14] also made the triphenylarsine and triphenylstibine derivatives and noted the chemistry of these complexes was similar to that of the triphenylphosphine derivative, although they were not as efficient hydrogenation catalysts as the triphenylphosphine analog, hydrogenating 1–hexene at only 2.5% of the rate of the triphenylphosphine complex , even at 40 °C. The dihydrido complex of the triphenylstibine complex was not stable in air like the others. Neither the arsine– or the stibine–dihydrido derivative would displace hydrogen when swept with an inert gas at 25 °C. This might indicate hydrogen was more strongly bound in these complexes, and thus less likely to facilitate hydrogenation.

Bennet and Milner[15] showed the phosphine ligand was not as readily lost in the analogous iridium complex, and the oxidative addition of H_2 to the complex was not reversible, and did not involve the loss of a phosphine ligand. $H_2IrCl(PPh_3)_2$ also did not catalyze the hydrogenation of olefins. These facts led to the conclusion that it was the ability of Wilkinson's catalyst to lose a phosphine ligand and loosely bind a solvent molecule in a labile coordination site that facilitates the coordination and subsequent hydrogenation of olefins.

More recently, Werner's group[16] synthesized the complexes $H_2MCl(P(^iPr)_3)_2$ (M=Rh, Ir) by the oxidative addition of H_2 to the corresponding 16–electron complexes, $[MCl(P(^iPr)_3)_2]$. The rhodium dihydrido complex could be reacted with cyclopentadiene to give low yields of $H_2Rh(C_5H_5)(P(^iPr)_3)$. However the authors also prepared the same cyclopentadienyl complex in higher yields by utilizing a reaction falling under the second category of general reactions resulting in dihydride complexes—the reaction of metal complexes with complex hydrides.

2) Reactions of Metal Complexes with Complex Hydrides

Werner[16] used the two following reactions (Eq. 2.12) to give $H_2Rh(Cp)(P(^iPr)_3)_2$ (Cp = cyclopentadienyl) in better yields than did the direct hydrogenation of $[RhCl(P(^iPr)_3)_2]$.

$$(Cp)Rh(OCOF_3)_2(P(iPr)_3) + Na[AlH_2(OC_2H_4OMe)_2]$$
$$\text{or}$$
$$(Cp)RhHCl(P(iPr)_3) + LiAlH_4$$
$$\downarrow$$
$$(Cp)RhH_2(P(iPr)_3 \qquad \textbf{(2.12)}$$

In 1970, Levison and Robinson synthesized $RuH_2(PPh_3)_4$ by heating an aqueous mixture of $RuCl_3$, triphenyl phosphine and $NaBH_4$. The complex $RuH_2(PPh_3)_4$ was made simply by adding formaldehyde to the mixture.

Earlier Angoletta and Caglio[17] added $LiAlH_4$ to $HIrX_2L_3$ to form dihydrides and trihydrides, while Freni, *et. al.*,[18] made the complex $H_2ReX(dppe)_2$ (X=Cl, I, Br) by the prolonged reaction of $LiAlH_4$ with $ReX_2(dppe)_2$ in warm THF. These dihydrido halides did not show any basic character as they did not evolve hydrogen gas and could be recovered unchanged when treated with acids at room temperature.

3) Hydrogen Transfer from Solvent or Ligand

Another method for synthesizing hydrides is to transfer hydrogen from solvent molecules or from groups coordinated to the metal center. The earliest of these techniques took advantage of reducing agents such as hydrazine and alcohols in the presence of

ligands or bases. In this reaction primary alcohols are oxidized to aldehydes, while secondary alcohols are oxidized to ketones.[1] An important point of this reaction, recognized by Chatt and Shaw, and also by Vaska was the transfer to the metal of the α–hydrogen from the alcohol.[1] This was the reverse of the reaction process found in the reduction of aldehydes and ketones, as illustrated by the following figure. (Fig. 2.2) It was obvious the β–hydrogen shift seen in the elimination of olefins from metal alkyls,

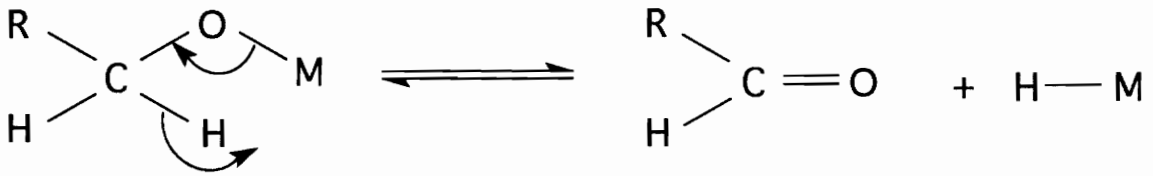

Figure 2.2 Reduction of Aldehydes and Ketones

and also its microscopic reverse, the addition of olefins to metal hydrides, (shown below in Figure 2.3) were closely related to this reaction.

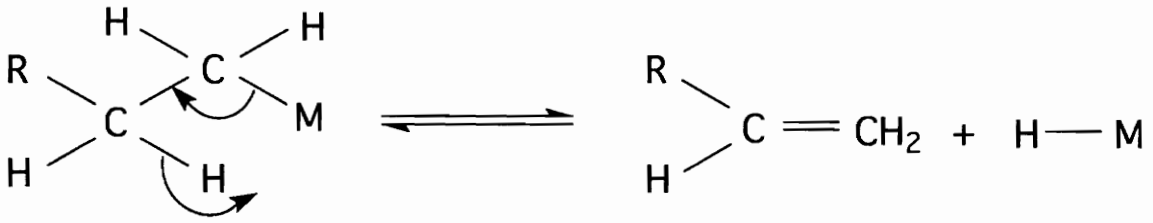

Figure 2.3 Elimination of Olefins from Metals

Dewhirst, *et. al.*,[19] used hydrazine, ethanol, and hydrogen to make ruthenium dihydridotetrakisdimethylphenylphosphine from the cation $Ru_2Cl_3L_6^+$.

In 1981 Pearson, Walker, Mauermann, and Ford[20] performed the reaction below (Eq. 2.13) as part of a kinetics study to explain the unusual lability of $HCo(CO)_4$

$$[HRu(CO)_4^-](PPN^+) + MeOH \longrightarrow H_2Ru(CO)_4 + MeO^- \quad \textbf{(2.13)}$$

versus $XCo(CO)_4$, and $HMn(CO)_5$ versus $XMn(CO)_5$ to ligand substitution. The authors concluded a hydride shift to a carbonyl group was responsible for the initial opening of a coordination site for substitution, followed by loss of a carbonyl group and then back–migration of the hydrogen to form the final substituted product. The authors also noted, upon comparing similar hydride compounds throughout the first–, second–, and third–row transition metals, the hydrides of first–row metals underwent rapid ligand substitution, but second–row metal complexes, with the exception of one ruthenium complex, and third–row metal complexes were substitutionally inert. This follows evidence from surface studies[21] establishing third–row metal–hydrogen bonds were stronger than first–row metal–hydrogen bonds, leading to lower probability of migration.

Chatt, Coffey, and Shaw[22] treated *mer* – $HIrCl_2(PPh_3)_3$ with KOH and EtOH and isolated *cis* – $H_2IrCl(PPh_3)_3$, instead of the *trans* – H_2 isomer, (Eq. 2.14) which the authors postulated undergoes dehydrohalogenation under these reaction conditions.

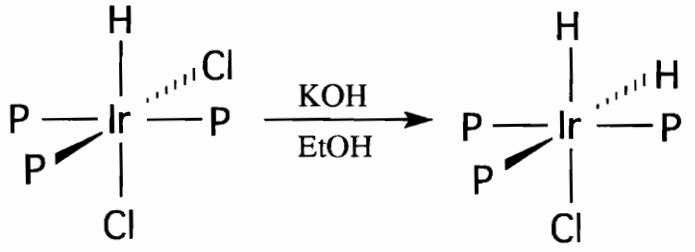

cis - H_2, *mer* - P_3 **(2.14)**

This explanation was consistent with previous work of Shaw.[23,24] An iridium complex with *trans* – P_2, *cis* – Cl_2 stereochemistry dehydrohalogenated in a base (reductively eliminate HCl)

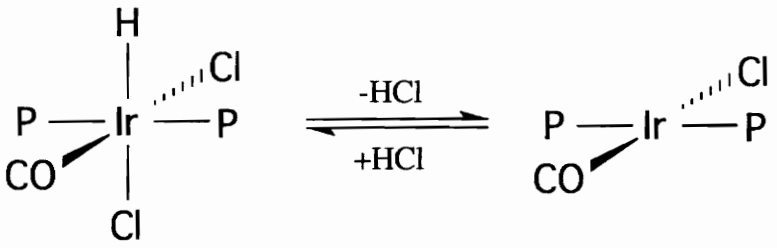

(2.15)

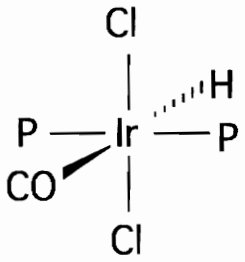

(stable in base)

mer -P_3, *cis* - H_2

(2.16)

to form a square planar complex, (Eq. 2.15) while the *trans* – P_2, *trans* – Cl_2 complex was stable under these conditions. (Eq. 2.16) Also, when a *mer* – P_3, *mer*– Cl_2 iridium complex was treated with KOH in EtOH, it first forms the *mer* – P_3, *trans* – Cl_2 complex, which then slowly isomerizes to the more thermodynamically stable *mer* – P_3, *cis* – Cl_2 complex. (Eq. 2.17)

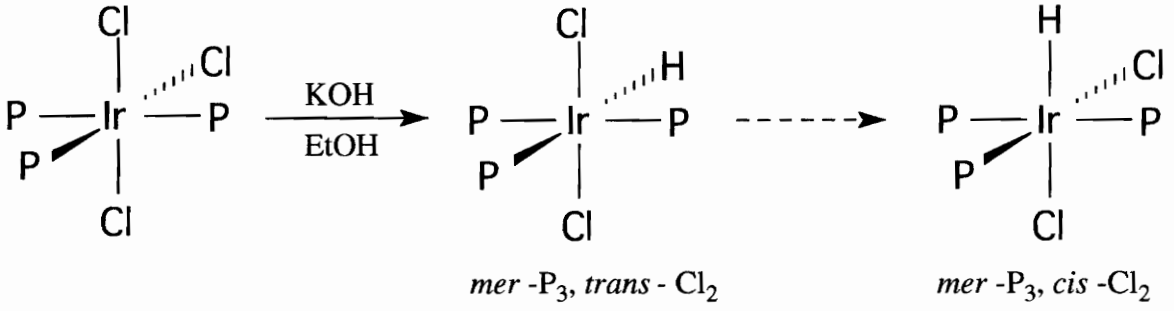

mer -P_3, *trans* - Cl_2 *mer* -P_3, *cis* -Cl_2

(2.17)

In 1991, Werner, Stahl, and Kohlmann[25] substituted sodium carbonate as the base under similar conditions to make a mixture of $(Mes)OsH(PPh_3)_3Cl$ and $(Mes)OsH_2(PPh_3)_3$ from $(Mes)Os(PPh_3)_3Cl_2$ (Mes = mesitylene).

The last method in this section involves reduction of a metal complex with silyl hydrides, and other group III hydrides. Harrod, *et. al.*,[26] determined from spectroscopic data, that silyl hydride added to $HIr(CO)L_3$ (L = PPh_3 and R_3Si = Cl_3Si, $MeCl_2Si$,

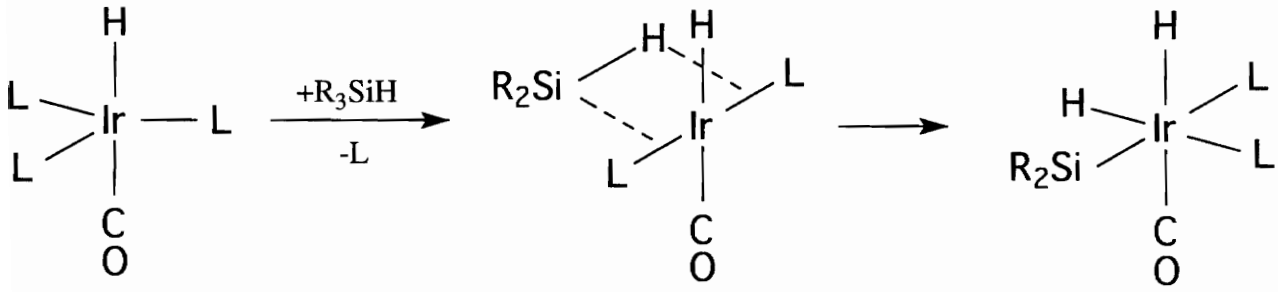

(2.18)

$(EtO)_3Si$, Ph_3Si, ME_2PhSi, Me_3Si) in a *cis* manner. (Eq. 2.18) A follow–up deuterium labeling experiment using $DIr(CO)L_3$ as the starting material found hydrogen equally distributed between the positions *trans* to L and *trans* to CO. The authors believed this to invalidate their *cis* – addition mechanism. However, Kaesz and Saillant[1] suggested if

either the five coordinate starting material or the square planar intermediate undergoing addition, geometrically isomerized, then the results were still consistent with a *cis* –addition mechanism. (Fig. 2.4)

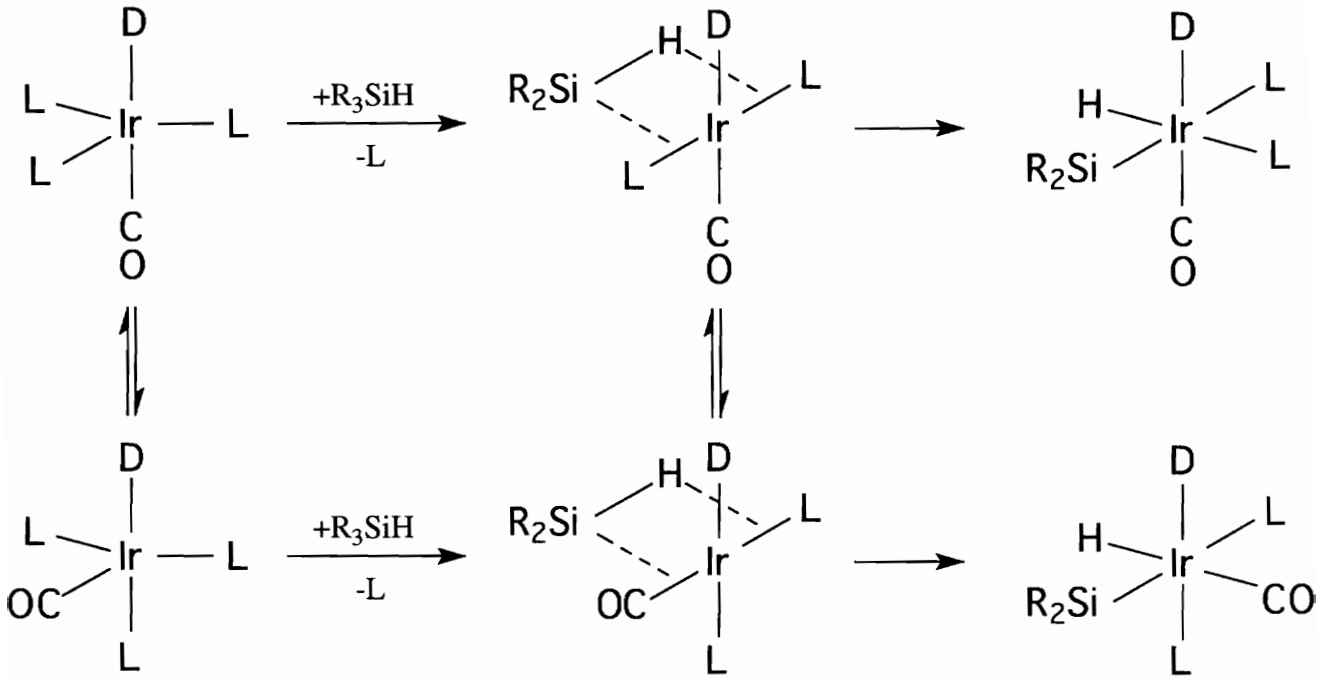

Figure 2.4 Mechanism for the *cis* - Addition of Silanes to Transition Metal Centers

Glockling and Wilbey[27] obtained the same type of Ir(III) adducts when they reduced *trans* –$IrCl(CO)L_2$ with trialkylgermanes. However when triarylgermanes were used, the product was the monohydride $HIrCl(GePh_3)(CO)PPh_3$ which crystallized with one molecule of solvent.

4) Protonation

Protonation of a metal complex usually will occur when all the low–lying orbitals become filled through interactions with donor ligands and the complex contains 18 electrons. In cases where the complex has fewer than 18 electrons, attempts to protonate lead to oxidative addition instead of protonation.

In 1955 Wilkinson and Birmingham[1] were the first to observe the protonation of a metal complex when they treated $HReCp_2$ with HCl to form $[H_2ReCp_2]^+$. They also determined the original complex was about as basic as ammonia.

Vaska[28] protonated $HIr(CO)(PPh_3)_3$ with HCl giving the *cis* – dihydride cation shown below. (Eq. 2.19)

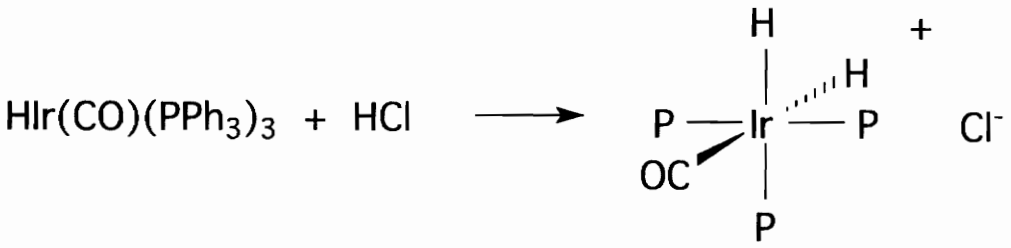

(2.19)

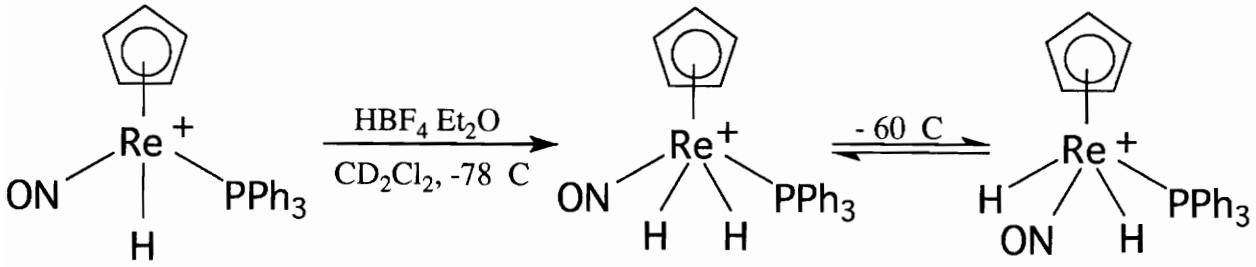

cis - *trans* -

(2.20)

Fernandez and Gladysz[29] monitored the treatment of $HRe(Cp)(NO)(PPh_3)$ with $HBF_4 \cdot Et_2O$ in methylene chloride at -78 °C by ^1H and ^{13}C NMR and observed a single product with two separate hydride resonances. Upon warming to -60 °C, a new product appeared with a single hydride resonance. These were determined to be the *cis* – dihydride at -78 °C, and then a mixture of the *cis*– and *trans* – dihydrides at -60 °C. (Eq. 2.20)

The last work to be described in this section is that of Chinn and Heinekey.[30] They synthesized cationic ruthenium complexes by protonation of a monohydride neutral ligand. (Eq. 2.21) In this report the authors determined from ^1H NMR, these complexes were

$$(\eta^5\text{-Cp}^{(*)})\text{Ru(L)(L')(H)} \xrightarrow[\text{CD}_2\text{Cl}_2,195\text{ K}]{\text{HBF}_4\ \text{Et}_2\text{O}} [(\eta^5\text{-Cp}^{(*)})\text{Ru(L)(L')}(\eta^2\text{-H}_2)]\text{BF}_4$$

(L) = CO

(L') = PCy_3 *, PPh_3, PMe_2Ph, PMe_3

(L)(L') = dmpe, $(PPh_3)_2$ *, (R)- prophos

* compounds with (*) were synthesized as both the C_5H_5 and the C_5Me_5 derivatives.

(Cy = cyano, dmpe = (dimethylphosphino)ethane, prophos = 1,2-bis(diphenylphosphino)propane)

(2.21)

dihydrogen complexes at -78 °C. When the initial monohydride complex was prepared as the monodeuteride and then protonated, the ^1H NMR showed a 1:1:1 triplet with J_{HD}= 22–32 Hz, strongly supporting the theory of a η^2–dihydrogen ligand, since classical dihydride complexes with terminal metal–to–hydride bonds normally exhibit J_{HH} = 2–5 Hz. In this study the authors uncovered evidence for a rapid equilibrium between dihydrogen and dihydride complexes (as had Kubas [31] and others previously). When the complexes with only mono–dentate phosphine ligands were heated to 0 °C, they decomposed to dimeric complexes. However, when the complexes with bidentate chelating phosphines were warmed to room temperature ^1H NMR indicated the dihydrogen products were in a rapid equilibrium with dihydride complexes. (Fig. 2.5)

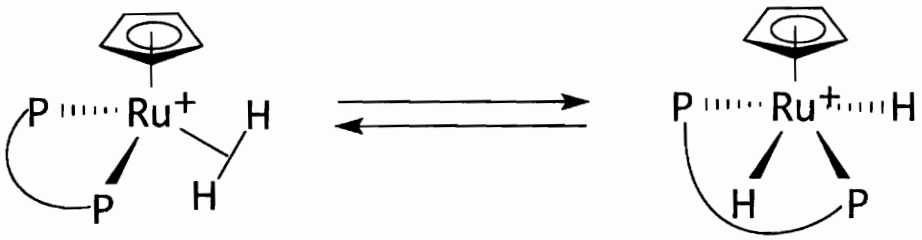

Figure 2.5 Dihydride/Dihydrogen Equilibrium of $[Ru(Cp)(P\text{-}P)H_2]^+$

Chinn and Heinekey, because they had available to them a means for systematically varying the ligands on the ruthenium centers, attempted to draw some conclusions about the effect of ligand variety on the dihydride and dihydrogen bonds. Generally the J_{HD} coupling constant decreases as the metal center of the dihydrogen complexes becomes more basic due to ligand environment. When viewed on purely electronic terms, this makes sense. As the metal center becomes more basic, more electron density becomes available to the 3–center–2–electron metal–dihydrogen bond, allowing it to become more like a terminal metal– hydride bond. However, when the more basic ligand pentamethylcyclopentadienyl

was substituted for cyclopentadienyl, J_{HD} increased. This suggested to the authors that factors other than metal basicity affect J_{HD}. Attempts to equate ligand basicity with the dihydrogen–dihydride equilibrium indicated steric effects rather than electronic were dominating the equilibrium.

5) Oxidative Addition of H_2 or HX to Metal Cationic Complexes

Finally, when H_2 or HX is added to a cationic metal center, protonated complexes are formed. Vaska and Catone[32], as well as Sacco, Rossi, and Nobile[33] formed the cationic $H_2M(diphos)_2^+$ (M=Co, Ir and diphos = bis(diphenylphosphino)ethane) when $M(diphos)_2^+$ was reacted with H_2 or HX (X=Cl, Br, I, ClO_4 and BPh_4). The analogous rhodium complexes did not add H_2 under similar conditions.

In 1968, Shapley, Schrock, and Osborn hydrogenated the cationic species, $[Ir(COD)(PPh_3)_2]^+$ in acetone to form $\{IrH_2(PPh_3)_2[(CH_3)_2CO]_2\}^+$,[34] which functioned as a hydrogenation catalyst under mild conditions. 5 mM acetone solutions of the cationic dihydrido complex catalytically hydrogenated 1,5-cyclooctadiene in the initial step to cyclooctene at a rate of approximately 0.1 M^{-1} hr^{-1}. The cyclooctene would then slowly be hydrogenated to cyclooctane. The authors also prepared the analogous rhodium complexes from $[Rh(NBD)(PPh_3)_2]^+$. These complexes were effective hydrogenation catalysts when dissolved in THF. Their studies noted that 1) catalytic activity of these complexes was greater for terminal versus internal olefins. 2) Acetylenes were hydrogenated faster then olefins. 3) Unsaturated ketones and esters were hydrogenated without reducing the carbonyl. 4) The hydrogenation cycle was inhibited by excess triphenylphosphine or solvent that are good donors, such as acetonitrile.

Butter and Chatt[35] reported *cis* addition of H_2 to $Rh(dmpe)_2^+$ to form $H_2Rh(dmpe)_2^+$, although HCl and HBr added in a *trans* fashion. (Eq. 2.22) Deeming and

Shaw[36] oxidatively added H_2 and HX to the five–coordinate complex $Ir(PMe_2Ph)_4(CO)^+$ to give the *cis* addition products illustrated in the following equation. When two of the dimethylphenylphosphine groups were

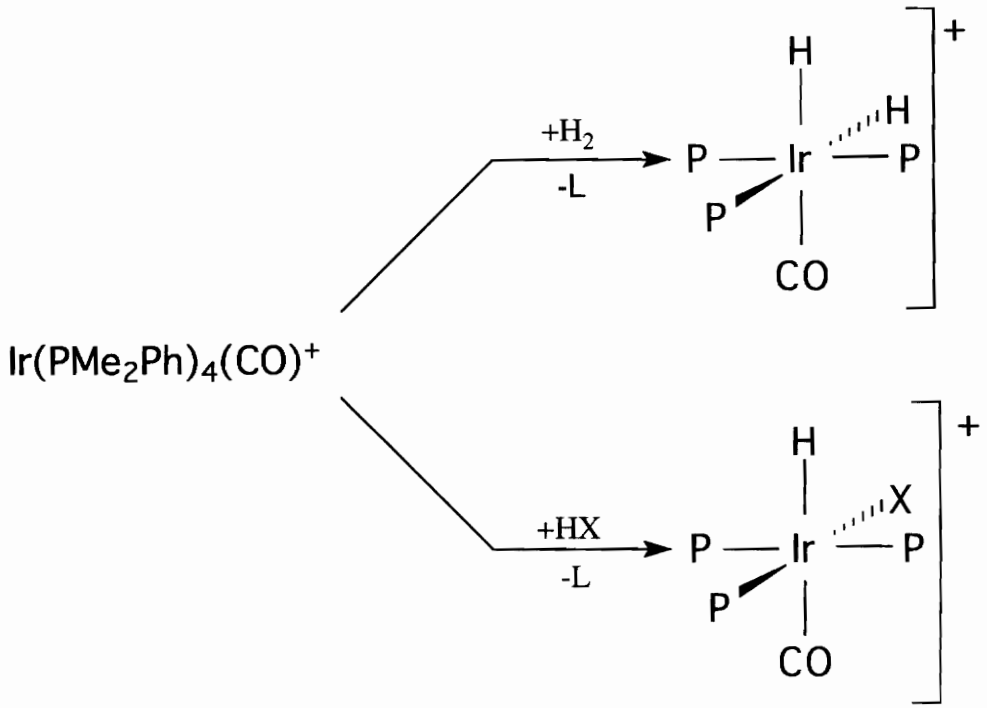

(2.22)

replaced with dimethylphenylarsine groups, the complex $H_2Ir(CO)(PMe_2Ph)(AsMe_2Ph)_2^+$ was formed with one of the arsine groups *trans* to the hydrogen. Similar displacement of ligand by H_2 was observed by Shapley, Schrock, and Osborn[37] in the complex $Rh(C_7H_8)L_2^+$ to form $H_2RhL_2S_2^+$ (S = solvent) with the loss of C_7H_8.

Bianchini, *et. al.*, synthesized the compounds $[(PP_3)Co(H_2)]PF_6$,[38] $[(PP_3)Rh(H_2)]BF_4$,[39] $[(PP_3)Ir(H_2)]BF_4$,[40] and $[(PP_3)Fe(H_2)]$ (PP_3 = $P(CH_2CH_2PPh_2)_3$) and performed interesting experiments on these complexes to determine whether they were classical or non–classical dihydrides. (Fig. 2.6)

The authors first examined the complexes by ^1H NMR. The cobalt complex $[(PP_3)Co(H_2)]PF_6$ had a temperature dependent T_1 that assumed a minimum value at 203 K. J_{HD} maximized at 27.8 Hz ($[(PP_3)Co(H_D)]PF_6$) at 300 MHz in d^8 – THF. These values were indicative of $\eta^2 - H_2$ coordination to cobalt. The rhodium complex is octahedral with terminal Rh – H bonds in the solid state, but heating above 173 K in solution converted it to the trigonal bipyramidal $\eta^2 - H_2$ complex, as indicated by NMR (T_1=120 ms, J_{HD} = 18 Hz). The iridium complex is a classical dihydride with octahedral structure in both solution and solid state. The complexes differ not only in their structures, but also in their reactivity. The results of adding DMMA (dimethylmaleonate, 1 mmol) to a stirred THF solution of the cobalt, rhodium, and iridium complexes are summarized in the following figure.

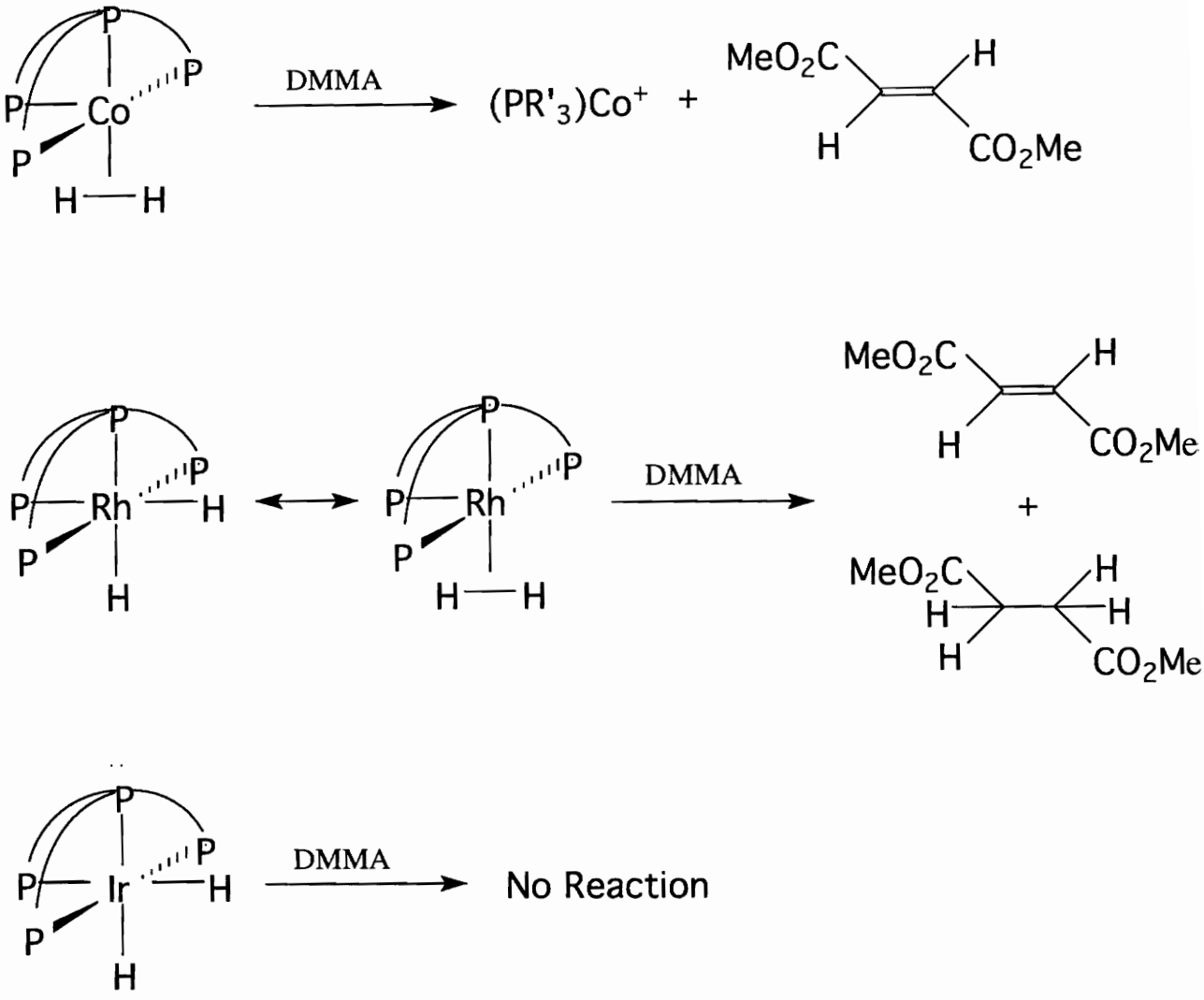

Figure 2.6 Dihydride/Dihydrogen Differences between Octahedral Co, Rh, and Ir Complexes

The authors explain the different reactivities of these complexes in terms of the nature and initial strength of the metal–hydrogen bonds. In the cobalt complex, the two hydrogens are strongly bond to each other and act like a labile ligand in the presence of the competing ligand DMMA. For the iridium complex the M–H bonds are too strong and no open coordination site is available to allow olefin insertion. The bonding in the rhodium

complex appears to fall in between the extremes of the cobalt and iridium complexes. These results and interpretations were consistent with Pearson's[20] and Morris's[41] findings, which present the case from the perspective of the lower ability of first–row metals to donate electrons from metal d orbitals into the σ^* orbitals of the dihydrogen ligand, compared to third– and, sometimes, second–row metals. The lower electron donation of the first–row metals results in a stronger H–H bond leading to a non–classical structure in which the dihydrogen ligand can be displaced, while in third–row metals, electron donation is greater, weakening the H–H bond enough to favor the classical dihydride structure with strong M–H terminal bonds and no open coordination sites.

The second method Bianchini used was to add the reagent [Au(PR_3)Cl] (R=Et, Ph) to room temperature solutions of the dihydride in THF.[42] This gold complex is useful as a diagnostic agent because it reacts differently with dihydride and dihydrogen complexes. [Au(PR_3)Cl] dissociates to form the electrophilic cation $[Au(PR_3)]^+$, which reacts with terminal M–H bonds to form M–H–Au(PR_3) adducts. [Au(PR_3)Cl] also contains the nucleophiles Cl^- and PR_3, which can either deprotonate or displace dihydrogen ligands. The authors treated [(PP_3)Co(H_2)]PF_6 with $[Au(PR_3)]^+$, forming [(PP_3)Co(PEt_3)]PF_6 with reduction of Au(I) to Au(0). When treated with [Au(PR_3)Cl], [(PP_3)CoCl] was formed along with evolution of hydrogen gas, while the $[Au(PR_3)]^+$ remained intact. The reaction of $[Au(PR_3)]^+$ with the rhodium analog gave similar results, while reaction with [Au(PR_3)Cl] resulted in the loss of HCl to form the binuclear compound [(PP_3)Rh(μ–H)Au(PPh_3)]PF_6. This reaction is thought to occur by heterolytic cleavage of dihydrogen promoted by the electrophilic $[Au(PR_3)]^+$, and the nucleophilic Cl^-, and PR_3 fragments.

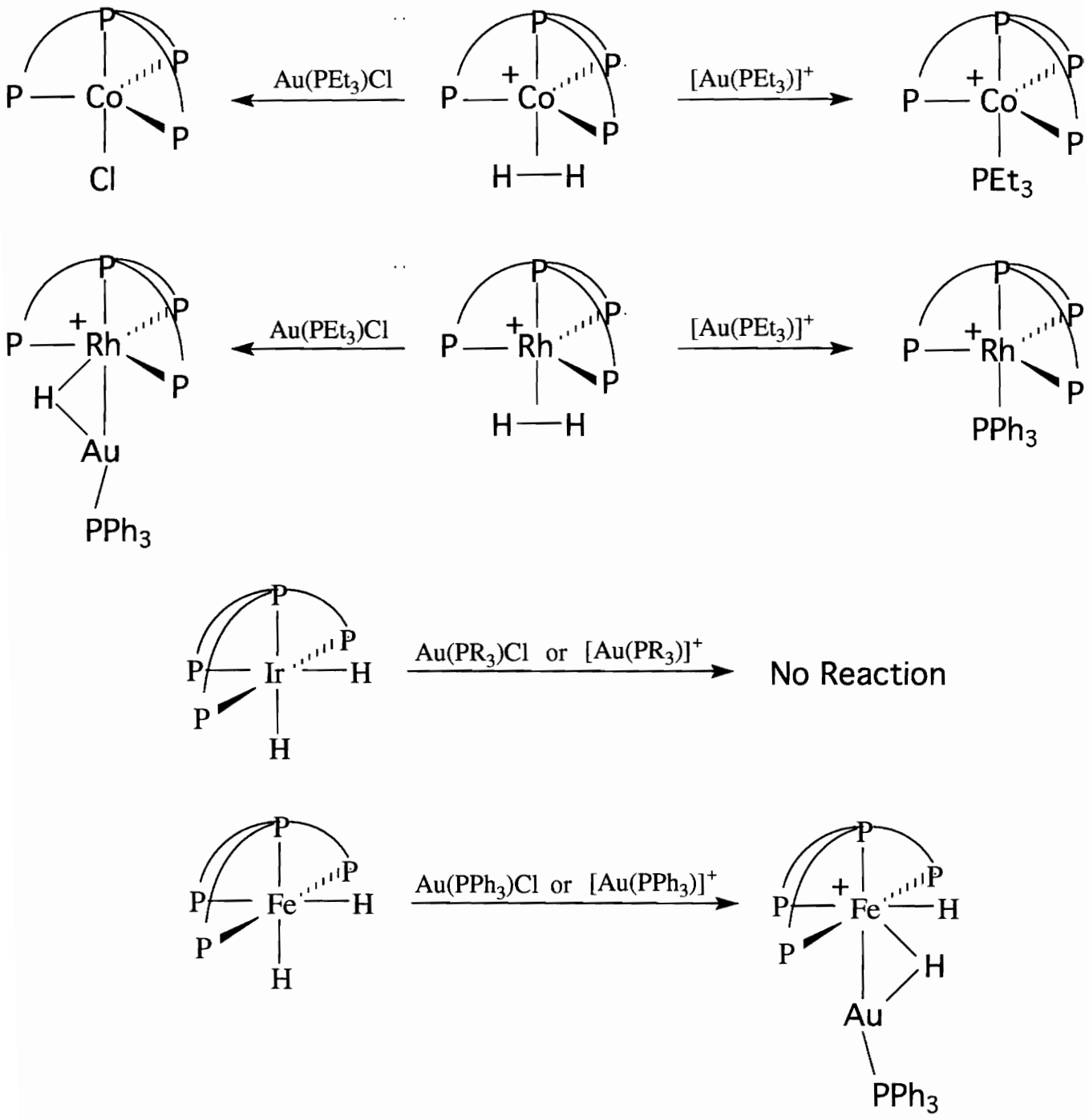

Figure 2.7 [Au(PR3)Cl] Used to Diagnose Dihydrogen versus Dihydride Complexes

$[(PP_3)Ir(H_2)]BF_4$ did not react with either $[Au(PR_3)]^+$ or $[Au(PR_3)Cl]$, while $[(PP_3)Fe(H)_2]$ reacted with both $Au(PR_3)]^+$ and $[Au(PR_3)Cl]$ to give the binuclear complex $[(PP_3)Fe(H)(\mu\text{–}H)Au(PPh_3)]$ as the PF_6^- or Cl^- salt. (Fig. 2.7) The authors suggest the stability of the $[(PP_3)Ir(H_2)]BF_4$ complex, compared to its rhodium and cobalt analogs, towards $[Au(PR_3)]^+$ is due to its lack of protic species, while its charge distinguishes it from the reactivity of the isoelectronic $[(PP_3)Fe(H_2)]$.

Electrochemistry is the last method used by Bianchini[43] to study classical versus non–classical dihydride structures. The redox properties of the same four $[(PP_3)M(H)_2]$ complexes were studied. The non–classical dihydride compounds, $[(PP_3)Co(H_2)]PF_6$ and $[(PP_3)Rh(H_2)]BF_4$ underwent irreversible one–electron oxidation in THF, resulting in the deprotonation of the H_2 ligand to form the corresponding monohydrides $[(PP_3)M(H)]^+$. On the other hand the classical dihydrides, $[(PP_3)Ir(H)_2]BPh_4$ and $[(PP_3)Fe(H)_2]$ showed no redox activity within the limitations of THF. The authors qualify these findings, stating that the redox–induced deprotonation of these dihydrogen compounds was probably not indicative of all dihydrogen compounds, since the complexes studied were d^8 L_4M fragments, while the majority of dihydrogen complexes belong to the d^6 L_5M family, for which the oxidation of the metal may be more difficult.

Transition Metal Dihydride Carboxylate Complexes

The chemistry, and subsequently the literature, of transition metal carboxylate complexes is quite extensive, but there are a very limited number of reports of transition metal monohydride carboxylates, and even fewer that deal with dihydride carboxylate complexes. This section of the review will deal only with dihydride complexes. Those wishing more general information on metal carboxylates might start with Mehrotra and Bohra's review *Metal Carboxylates* .[44]

Carboxylate ligands can generally bind in four different manners : 1) **Ionic**, which occurs with highly electropositive metals, *e.g.* sodium formate. 2) **Unidentate**, in which the metal binds to the singly bond oxygen, *e.g.* $[Co(NH_3)_5(O_2CCH_3)]$. 3) **Bidentate chelating** (symmetrical or asymmetrical). Symmetrical bidentate chelating, considered to be the least favorable of all the possible coordination types, forms a four-membered ring with two M-O bonds of equal length and has been identified in some zinc and uranyl complexes. Asymmetrical bidentate chelating is believed to occur in the complex $Sn(O_2CCH_3)_4$. The X-ray crystal structure of this compound indicates it is nearly eight coordinated, but the limited space around the metal center causes one of the M-O bonds in a single acetate group to lengthen. 4) **Bidentate bridging** occurs when the carboxylate ligand bonds to a separate metal through each of its oxygens, from which arise bi-, tri-, tetra-, and polymeric carboxylates.[44] Although unidentate bonding is the most common found throughout the literature, this is not necessarily the case for dihydrido complexes, as can be seen in the following section.[45] The dihydride carboxylate complexes were formed simply by adding a carboxylic acid, carboxylate salt or carboxylate ester to a dihydrido

metal complex in solution. Many of the complexes reported in this section have not been isolated and completely characterized, but instead their presence as reaction intermediates has been inferred from reaction products and isotopic labeling studies.

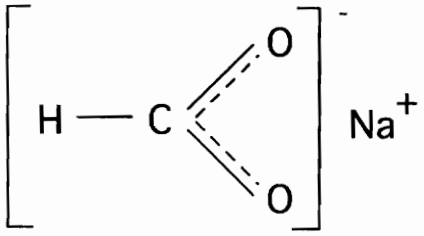

Ionic $Na(O_2CH)$

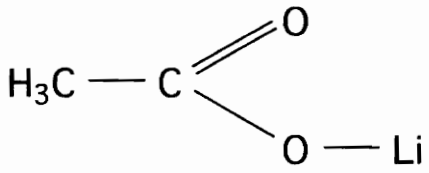

Unidentate $Li(O_2CCH_3)_3$

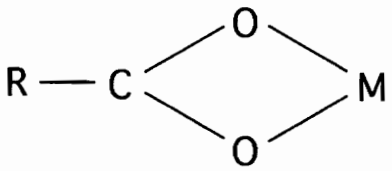

Symmetrical chelating

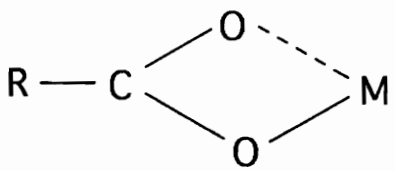

Assymmetrical chelating

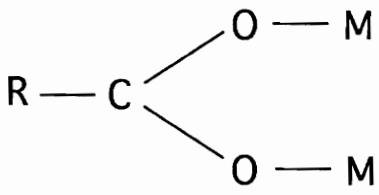

Bidentate bridging

In a 1972 paper Roundhill[46] reported the isolation and characterization of the iridium(III) complex $H_2Ir(CO)(PPh_3)_3(CF_3COO)_2H$ from the reaction of the corresponding iridium (I) monohydride complex with excess trifluoroacetic acid in methylene chloride. (Eq. 2.23) The structure of this complex was determined by

$$H(CO)(PPh_3)_3Ir + xsCF_3COOH \xrightarrow{CH_2Cl_2} H_2Ir(CO)(PPh_3)_3(CF_3COO)_2H \quad \textbf{(2.23)}$$

^1H NMR, and was similar to the spectra obtained by Shaw[36] and Wilkinson[47] from the reaction of $[(PMePh_2)_3Ir(CO)H_2]BPh_4$ and carboxylic acids. The carboxylate anion is believed to be a hydrogen-bonded dimer, as Vaska[28] found for $[(PPh_3)_3Ir(CO)H_2]HCl_2$, where HCl_2^- was the dimeric anion.

Komiya and Yamamoto[48] treated vinyl acetate with the dihydride complex $RuH_2(PPh_3)_4$ at room temperature. One mole of ethylene was liberated for each mol of $RuH_2(PPh_3)_4$ used and a light brown precipitate was recovered. The precipitate was identified by elemental analysis, IR, NMR, and other methods to be $RuH(O_2CMe)(PPh_3)_3$. No hydrogenation product of vinyl acetate or molecular hydrogen was detected in the reaction mixture. When allyl acetate was treated with $RuH_2(PPh_3)_4$, one mole of propylene and the same monohydride, $RuH(O_2CMe)(PPh_3)_3$ were recovered. The authors suspected that pre-dissociation of one phosphine ligand producing a coordinatively unsaturated species was necessary to initiate the reaction, because when the triphenyl phosphine ligands were replaced with either diphenyl phosphine or methyldiphenyl phosphines, the corresponding dihydrido complexes showed much less tendency to dissociate than the triphenyl phosphine complex, as shown by NMR studies. From these results the authors suggested the following mechanistic scheme. A phosphine ligand first

dissociates from the dihydride complex. The olefin then coordinates at the open site, forming the π-bonded carboxylate dihydride complex. Hydride insertion is followed by coordination of the doubly-bonded oxygen, and then C-O bond cleavage with ejection of ethylene, resulting in the bidental chelated carboxylate monohydride ruthenium complex.

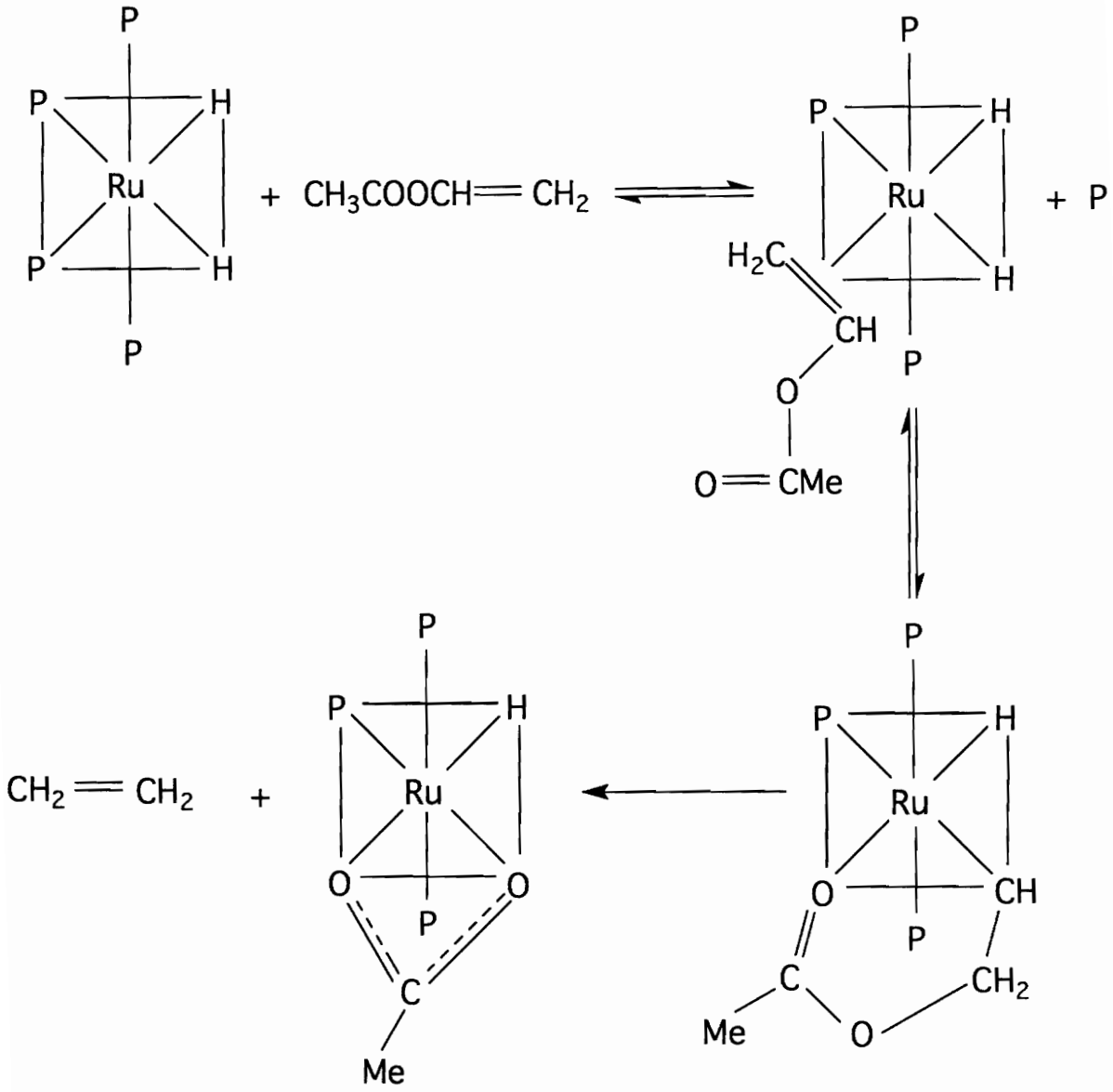

Figure 2.8 Insertion of Vinyl Acetate into $RuH_2(PPh_3)_4$

Further evidence for this mechanism was given by the authors in a later paper.[49] ^1H and ^{31}P NMR in deuterated pyridine and DMF showed that the phosphine *trans* to the hydride was the one that dissociates. Addition of the dihydridotetrakistriphenylphosphine

ruthenium complex with alkyl, instead of vinyl, acetates did not react, supporting the coordination of the carboxylate double bond *trans* to the hydride. Also, hydrido complexes such as $FeH_2(dppe)_2$ and $CoH_2(dppe)_2$ failed to react with vinyl acetate, presumably because the bidentate ligand will not dissociate.

Deuterium labeling experiments of the original complex ($RuD_2(PPh_3\text{-}d^6)_4$, (where the *ortho* protons of the phenyl groups were deuterated) indicate that isotopic exchange, and subsequent scrambling, is taking place between the insertion of the vinyl group into a Ru-D bond and the reverse ß-elimination.

In 1976 Marko, *et. al.*, synthesized the complexes $RhH_2(PPh_3)_2(OOCR)$ (R = n-C_5H_{11}, Ph, PhCH=CH, and $PhCH_2CH_2$) by reacting $[Rh(COD)Cl]_2$ with carboxylic acids with triethyl amine in a 1:1 benzene/methanol solution under a hydrogen atmosphere. These complexes were active olefin hydrogenation catalysts. Marko[50] later detected the complexes, $RhH_2(PPh_3)_2(OOCR)$ (where R gives the corresponding *L* (+)-mandelate and formate), by IR spectroscopy in a 1:1 benzene/methanol solution with a slight excess of PR_3, under hydrogen. The formate complex catalyzed the hydrogenation of olefins in the presence of phosphines, and behaved similarly to the *in situ* catalysts derived from the $[Rh(diene)_2X]_2$ catalysts of Horner and Siegel.[51] This suggested that the active species for the two systems were similar if not equivalent. The chiral complex derived from *L* (+)-mandelate was found to enantioselectively hydrogenate α-acetamidocinnamic acid methyl ester with high turnover (20 mol H_2/mol Rh/ min, although the maximum optical yield was only 13%. Marko suggested that the low optical yields were due to either loss of the chiral carboxylate ligand from $RhH_2(PPh_3)_2$(*L* (+)-mandelate) through reductive elimination of the carboxylic acid or dissociation of the carboxylate anion, leaving a non-chiral center. However, addition of excess *L* (+)-mandelic acid to the reaction mixture did not result in higher optical yields. This led the authors to propose that the presence of only one chiral ligand on the metal center was the cause of the enantioselectivity.

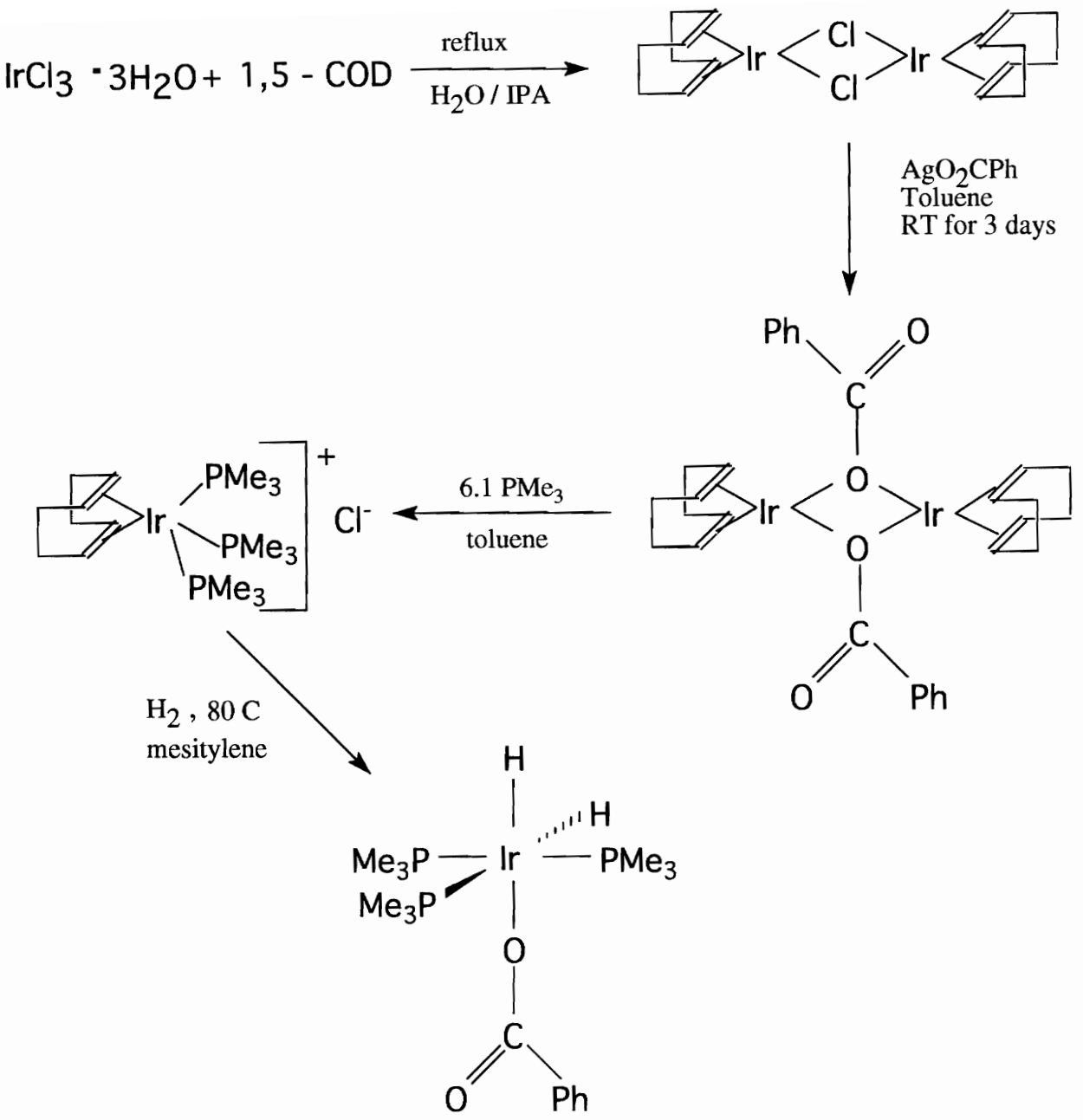

Figure 2.9 Synthesis of $IrH_2(PMe_3)_3O_2CPh$

Robinson and coworkers[52] detected $[IrH_2(CO)(PPH_3)_3][O_2CCCl_3]$ in the reaction mixture of $IrH(CO)(PPh_3)_3$, while thermally fragmenting perhaloacetate anions to form

dihalo-carbenes ($:CX_2$). The addition of excess CCl_3CO_2H to the mixture results in the stabilization of the salt $[IrH_2(CO)(PPH_3)_3][H(O_2CCCl_3)]_2$. Again, the anion is dimeric in form, as was found by Roundhill earlier in this section. Attempts to detect dihydrido intermediates from the $RhH(CO)(PPh_3)_3$ were unsuccessful, due most likely to the ease with which Rh complexes will reductively eliminate dihydrogen.

In 1990 Bianchini[53] synthesized the dihydrido carboxylato complexes $[(PP_3)Rh(H)_2][O_2CR]$ and $[(NP_3)Rh(H)_2][O_2CR]$ (R=Me, Ph) by protonating monohydride complexes, $[(PP_3)RhH]$ and $[(NP_3)RhH]$, with the corresponding carboxylic acid. The carboxylic anions were replaced with BPh_4 upon addition of $NaBPh_4$.

Finally, Le[11] synthesized $IrH_2(PMe_3)_3(O_2CPh)$ by first preparing $[Ir(COD)(O_2CPh)]_2$, oxidatively adding PMe_3 to make $[Ir(COD)(PMe_3)][O_2CPh]$, then hydrogenating in mesitylene at 80 °C. The benzoate ligand was unidentate bonded and the whole complex was soluble in water. This complex is integral to the results of this thesis and will be reviewed later in greater depth .

Water–Soluble Complexes with Water Soluble Ligands

The relatively high selectivity and activity of homogeneous versus heterogeneous catalysts makes such systems quite attractive. However, difficulties arising from separation of product from catalysts, recent rising costs of using and post–process recovery or disposal of typical organic solvents, and increasingly strident calls from the public and government for environmentally sound manufacturing techniques have led to increased interest in organometallic systems that function as homogeneous catalysts in aqueous medium. One does not normally associate the term water, let alone water soluble, with organometallic chemistry. In fact, water has normally been considered a "poison" to many reactions, including Grignard syntheses and polymerization reactions, to name a few. Prior to 1977, only a few organometallic complexes soluble in water and active as catalysts or catalyst precursors were known.[54] The majority of literature dealing with water soluble complexes catalytically active for hydrogenation involves coordinating water soluble phosphine ligands, containing SO_3^-, COOH, OH, or NH_2 functional groups to metal centers. Much of the research has centered on SO_3^-, presumably because of its solubility in aqueous medium of any pH. Carboxy– and amino–substituted phosphines are soluble only in basic or acidic solution, respectively, while the solubility of hydroxyl containing phosphines varies according to parent phosphine and the number of incorporated hydroxyls.[55]

In 1977 Dror and Manassen,[56] reported the biphasic hydrogenation of olefins in an attempt to overcome the separation problems of homogeneous catalysis. A benzene solution of $Rh(PPh_3)_3Cl$ was stirred under hydrogen and an aqueous solution of butene-diol was added, butane-diol was recovered from the aqueous layer. Subsequent removal of

the old aqueous layer, and addition of new aqueous solutions of butene-diol resulted in further reductions of the olefin, with only small decreases in the activity of the catalyst. Clearly water did not deactivate the catalyst, but the utility of this system was limited because of the small number of water soluble olefins. The authors then prepared water soluble rhodium complexes by adding sodium diphenylphosphinobenzene–*m*– sulphonate (dpm) to rhodium (III) chloride trihydrate. The exact structure of the resultant complex was not reported. When aqueous solutions of this complex were stirred with cyclohexane solutions of olefins under hydrogen, little hydrogenated product was recovered from the cyclohexane layer. However, upon adding a water miscible cosolvent (methanol, ethanol, DMA) reasonable rates of hydrogenation were achieved. Analysis of the solutions determined that no olefins were lost by side reactions. From separate kinetic experiments the authors concluded that the rate of hydrogenation is dependent on the solubility of the olefins and the reaction does not occur at the water-cyclohexane interface.

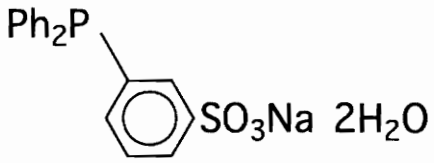

sodium diphenylphosphinobenzene±*m*±sulphonate
(dpm)

Borowski, Cole–Hamilton, and Wilkinson[54] prepared water soluble complexes of Ru, Rh, Pd, and Pt by exchanging sodium diphenylphosphinobenzene–*m*– sulphonate (dpm) for triphenylphosphine in known catalytically active molecules. The exchange was performed in one of two manners. A methylene chloride solution of the PPh_3 complex is mixed with an aqueous solution of dpm; then the exchanged complex is extracted into the

aqueous layer and precipitated with THF; Alternately both the original complex and dpm were dissolved and refluxed in an organic solvent, followed by recrystallization by cooling or addition of a non–polar solvent. The latter procedure was deemed more useful because of higher yields and easier purifications. $RhCl(dpm)_3 \cdot 4H_2O$ and $RuHCl(dpm)_3 \cdot 2H_2O$ were active hydrogenation catalysts. Olefins were stirred directly with aqueous solutions of the catalysts, without cosolvents and $RhCl(dpm)_3 \cdot 4H_2O$ was determined to be the more active of the two, with hydrogenation yields of 73 % at 25 °C vs. 55 % at 80 °C for $RuHCl(dpm)_3 \cdot 2H_2O$ with 1–hexene, although both catalysts resulted in olefin isomerization to 2-hexene (22% vs. 13%, respectively). $RuHCl(dpm)_3 \cdot 2H_2O$ was also an active catalyst for the hydroformylation of 1–hexene to the aldehyde in 30% yields at 90 °C, 60 atm for 24 hours. Isomerization of the olefins was again a competing side reaction.

Joo and Toth[55] synthesized the complexes $RuCl_2(dpm)_2$, $RuHCl(dpm)_3$, and $RuH(OAc)(dpm)_3$. The first two complexes were active catalysts in the hydrogenation of unsaturated carboxylic acids (maleic, fumaric, crotonic, cinnamic, itaconic), while the last two hydrogenated 2–oxo–acids. The rates at 60 °C, 1 atm H_2 were about 100–700 mol H_2/mol catalyst. Kinetic studies indicated the complexes with only two phosphines per metal atom were much more active catalysts for hydrogenation, than those compounds with three phosphines per metal atom. Only those with three phosphines per metal atom were active for the hydrogenation of 2–oxo–acids.

In a later study, Benyei and Toth[57] reported the synthesis of the new complexes, $RuHCl(CO)(dpm)_3$, $RuCl_2(CO)_2(dpm)_2$ and $IrCl(CO)(dpm)_2$. The new complexes $IrCl(CO)(dpm)_2$, $RuHCl(CO)(dpm)_3$, as well as $RuCl_2(dpm)_2$ and $RhCl(dpm)_3$ catalyzed the transfer hydrogenation of aldehydes to alcohols under biphasic conditions, but did not hydrogenate olefinic double bonds or aromatic ring substituents. $RuCl_2(CO)_2(dpm)_2$ showed no activity. $RuCl_2(dpm)_2$ was the most active of the complexes achieving nearly

100 % conversion and > 90% yields for many aldehydes. A comparative summary of all the complexes is included in Table 2.1.

Table 2.1 Reduction of Benzaldehyde by Formate in the Presence of Different Catalysts[a]

Catalyst	r_0 (mM/min)	Time (min)	Conv (%)
$RuCl_2(dpm)_2$	90	20	100
$RuHCl(CO)(dpm)_3$	29	60	80
$RuCl_2(CO)_2(dpm)_2$	0	60	0
$IrCl(CO)(dpm)_2$	16	130	11
$RhCl(dpm)_3$	1.3	72	22

[a]Conditions: 0.01 mmol catalyst, 0.1 mmol dpm, 5 mL of 0.5 M benzaldehyde in chlorobenzene, 3ml 5M sodium formate in water, 80 °C.

This reduction did not require phase transfer agents. The use of quarternary ammonium salts transferred the catalyst to the organic phase, as judged by color change, but decreased the rate of transfer hydrogenation. Further kinetic studies on $RuCl_2(dpm)_2$ and benzaldehyde indicated excess dpm was crucial to achieving high rates. In the absence of dpm, the initial rate is slow and conversion is also limited to 20%. The addition of one equivalent of dpm gives only a slightly higher rate, but 90% conversion. Continued addition of dpm increased the rate up to the solubility limit of the aldehyde. This leads to the assumption that the catalytically active species contains at least three dpm ligands. The excess dpm is thought to inhibit the formation of the catalytically inactive species. A reaction mechanism is presented in Figure 2.10.

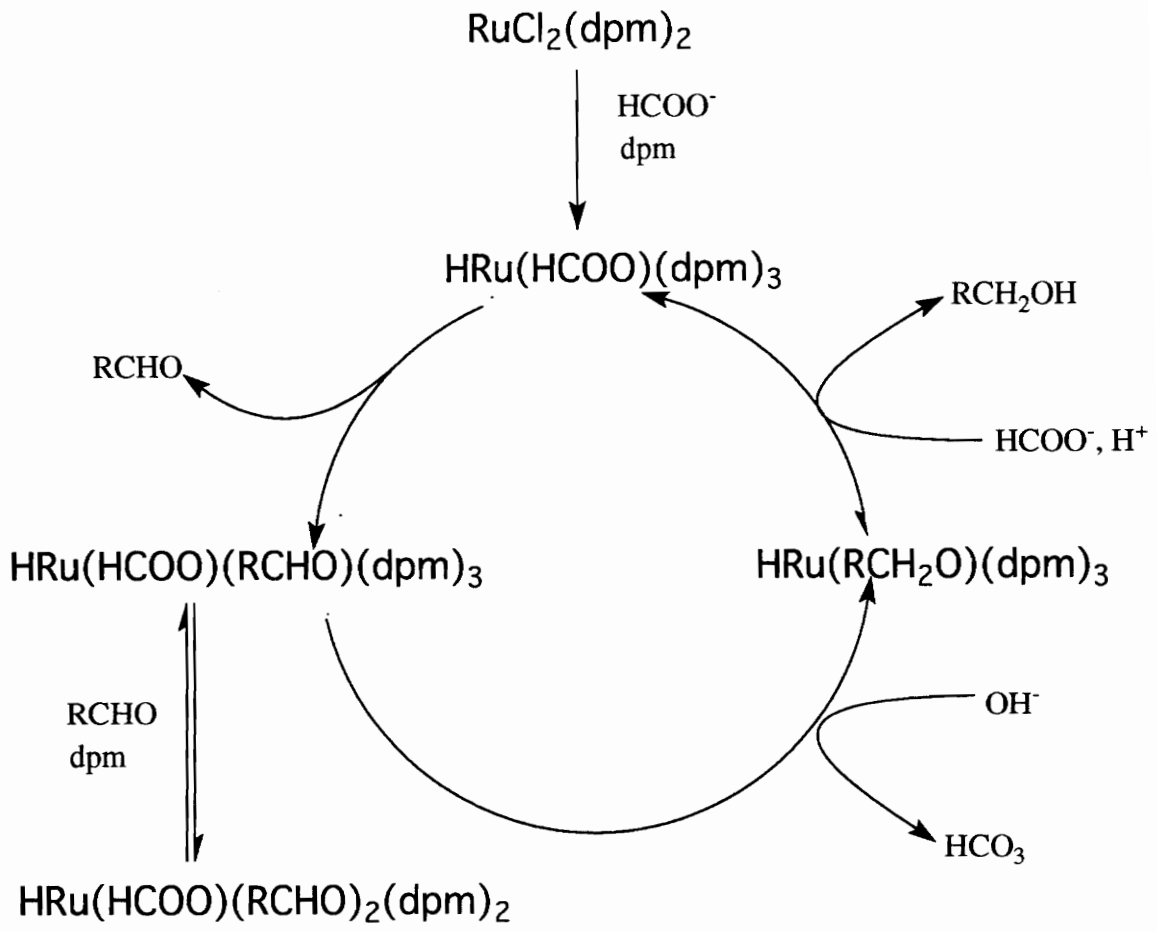

Figure 2.10 Proposed Mechanism of Aldehyde Reduction by Catalyzed Hydrogen Transfer from Formate

In 1987, the complex $RhH_2Cl(TPPTS)_3$ was generated by oxidative addition of hydrogen to the water soluble $RhCl(TPPTS)_3$ (TPPTS = P(*m* $-C_6H_4SO_3Na)_3$) in both the novel *cis –fac* dihydride and the expected *cis –mer* dihydride.[58] The *cis– mer* dihydride would appear to be the thermodynamic product. When an aqueous solution of the two isomers under hydrogen is allowed to sit, the proportion of the *cis– mer* dihydride increases without decomposition of total product. NMR studies in water indicate the dissociation of a phosphine ligand, although the ionic strength must be closely controlled. Although this dissociation should have provided an open coordination site for

hydrogenation of olefins, very low reactivities were observed for either water soluble substrates or under biphasic conditions. Studies with cycloheptene indicated significant decomposition of the dihydride complexes over time.

Sinou[59] reported the preparation of catalyst precursors for transfer hydrogenation from formate by the addition of tppts or the chiral CBD (CBD = cyclobutanediop) to $[Rh(COD)Cl]_2$. Use of the TPPTS–catalyst gave yields of up to 100 % for itaconic acid and mesaconic acid. Hydrogenation with the CBD–catalyst resulted in yields typically around 50% and enantiomeric excesses of from 10 % (itaconic acid) to 43% (acetamidocinnamic acid). The 43% *e.e.* surpasses that achieved with hydrogen in water or in a two-phase system (34% *e.e.*) and is only slightly lower than that obtained in homogeneous transfer hydrogenation using diop as the ligand (50 %).

Sinou, *et.al.*,[60] also prepared *in situ* a Pd(0)–$(TPPTS)_n$ complex that catalyzed the nucleophilic substitution of allylic substrates in a two–phase aqueous–organic medium as shown in Eq. 2.24. The total yields were typically 95–100%.

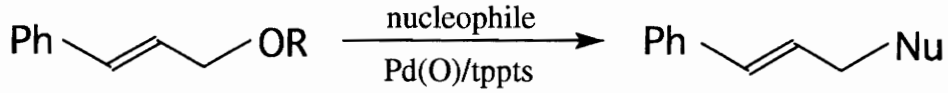

(2.24)

Other water soluble metal complexes were prepared from the monodentate phosphine ligands; phophos,[61] $[Ph_2P(CH_2)_n PMe_3]X$ (n = 2, 3, 6, 10; X = NO_3^-, Cl^-, PF_6^-), and amphos,[62] $Ph_2PCH_2CH_2NMe_3^+$. The complex $[Rh(NBD)(n - phophos)_2]X$ (NBD = norbornadiene) was a very active olefin hydrogenation catalyst for 1–hexene in aqueous and biphasic systems. The chain length was definitely a factor affecting activity (6>10≥3>2), although no rationale for the order was determined. Aqueous solutions of $[Rh(NBD)(amphos)_2]^{3+}$ catalyzed the hydrogenation of water soluble olefins in single phase systems (water and methanol), and the hydrogenation and hydroformylation of water

insoluble olefins dissolved in organic solvents. Hydrogenation yields of maleic acid and styrene were 80% (single phase) and 45% (two phase), respectively.

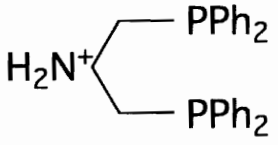

bis[2±(diphenylphosphino)ethyl]amine

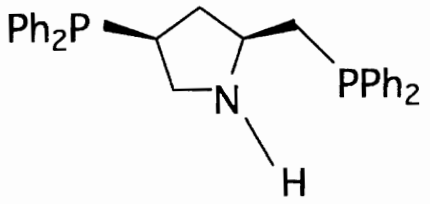

2±[(diphenylphosphinomethyl]±4± (diphenylphsophino)pyrrolidine

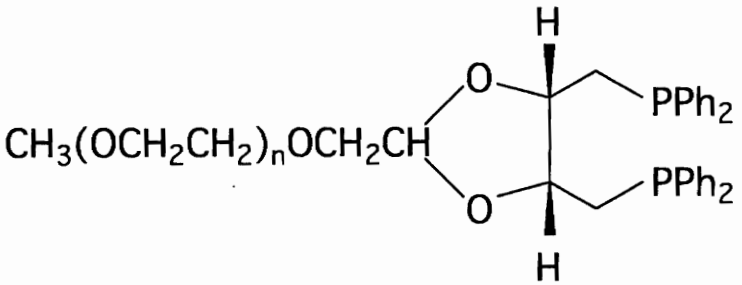

(R,R) (-) PGE n-DIOP

Whitesides, *et. al.*,[63] synthesized a variety of water soluble bichelating diphosphine ligands from bis[2–(diphenylphosphino)ethyl]amine which were complexed to rhodium (I) systems. The authors observed, generally, catalyst activity followed the water solubility of the complex.

Sinou, *et. al.*,[64], made several asymmetric water soluble diphosphine complexes of the type $[Rh(COD)(ligand)]^+ClO_4^-$ by preparing chiral derivatives of 2–[(diphenylphosphino)methyl]–4–(diphenylphosphino)pyrrolidine. Catalytic hydrogenation at 25 °C, 1 atm H_2 in aqueous solutions of α–acetamido acrylic acid, α–acetamido cinnamic acid, and itaconic acid, resulted in optical yields of 34%, 60%, and

59%, the highest enantioselective yields achieved in water. Comparative studies in ethanol found selectivities and rates to be slightly higher, although the results were not explained. Amrani and Sinou[65,66] also synthesized four asymmetric polyoxa–1,4–diphosphines ((R,R) (-) PGE n-DIOP (n=6,16,17,42)). These DIOP derivatives, when complexed to form [Rh(COD)(ligand)]$^{+}ClO_4^{-}$, did not result in as high enantioselectivies.

Hanson, *et. al.* prepared the water-soluble tetra-amine functionalized derivatives of the chiral phosphine ligands BDPP (2,4-bis(diphenylphosphino)pentane), DIOP (2,3-O-isopropylidene-2,3-dihydroxy-1,4-bis(diphenylphosphino)butane), Prophos (1,2-bis(diphenylphosphino)propane, Chiraphos (2,3-bis(diphenylphosphino)butane, and CyclobutaneDIOP (1,2-bis((diphenylphosphino)methyl)cyclobutane).[67,68] After complexation to the corresponding rhodium diene, the ligands were quarternized with $(CH_3)_3OBF_4$, to give systems that were extremely water soluble, but very insoluble in organic solvents, making complexes of this type ideal for two-phase reaction systems. This procedure for making ligands water-soluble does not attack sensitive functional groups within the target ligands, as has been observed with direct sulfonation methods.

Transition Metal Complexes Containing Water as a Ligand

Transition metal solvento complexes, which contain weakly coordinated solvent molecules as ligands, are considered to be intermediates in many homogeneous catalytic systems[69] and are of great importance.[70] Many of the mechanisms presented for catalytic systems hinge around the creation of an open coordination site around the various metal centers so the substrate can bind to the metal and undergoactivation. In many of these systems, the solvent ligands in metal solvento complexes are believed to be sufficiently labile as to lead to the catalytically active coordinatively unsaturated species by either dissociation or displacement. Even though water has been proposed to be a coordinated ligand in many homogeneous systems, few examples of transition metal aquo complexes have been isolated and unequivocally characterized. Halpern deduced from mechanistic studies of the rhodium catalyzed homogeneous hydrogenation of olefins[71] that when a catalytic reaction is under way, the species which accumulate in sufficient concentration to be characterized are often not directly involved in catalysis. Simple extension of these findings leads one to expect reactive species or species directly involved in catalysis will not accumulate in sufficient quantities to be characterized, let alone isolated. This concept goes a long way towards explaining the small number of aquo complexes found in the literature.

Boniface, *et. al.*,[108] synthesized $RuH(H_2O)(CO)(PPh_3)_3$ from the reaction of $RuH_2(CO)(PPh_3)_3$ with tetrafluoroboric acid and water.[1] Carbonylation of the former gives $RuH(H_2O)(CO)_2(PPh_3)_3$. IR spectra of this isolated dicarbonyl complex suggested the tetrafluoroborate anion might be coordinated to the metal, but X-ray crystallography indicated it was instead hydrogen bonded with the coordinated water molecule and the

ethanol molecule of crystallization. The coordination around the ruthenium center was determined to be distorted octahedral. The geometry around the oxygen of the water molecule was planar (all the bonds of the water molecule and the Ru–O bond were in the same plane). The Ru-CO distances were significantly different (1.83 and 1.97(2) Å), with the longer bond *trans* to the hydrido ligand. This difference can be attributed to the high *trans* influence of the hydride ligand.[72] The hydride ligand, a strong σ–donor, is said to have a high *trans* influence because of its polarizability, allowing it to form strong σ–bonds with the metal center. Because of the geometries of the metal *d* and *p* orbitals involved in the bonding, the strong bond of the hydride ligand usually leads to the relative weakening of the ligand–metal bond *trans* to the hydride–metal bond. Hence hydrides are considered to have a strong *trans* influence. Ligands which are not very polarizable, such as water and methanol, to name a few, exhibit weak *trans* influences and do not lead to appreciable lengthening of the *trans* metal–ligand bond. Ligands, such as tertiary phosphines, exhibit intermediate *trans* influence. The Ru–H bond length of 1.7(2) Å was comparable to values seen in other ruthenium hydrides. The Ru–OH_2 bond length of 2.15(1) Å was considerably longer than predicted by the sum of the covalent radii (1.99 Å)[73] or from the expected M–ligand distance of 2.05 Å compiled by Shustorovich.[72] This could possibly be due to slight weakening of the bonds through hydrogen bonding.

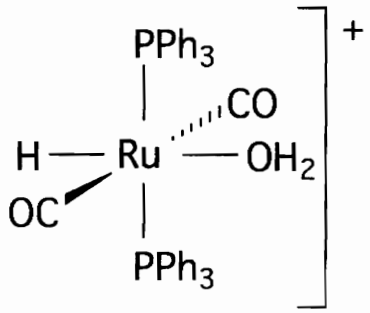

It might be beneficial at this point to introduce the key concepts of Hard–Soft Acid–Base theory (HSAB),[74] symbiosis,[75] and the antisymbiotic effect.[76] HSAB applies to the polarizability of atoms and molecules. Those which are not very polarizable, like F^- and OH_2, are considered to be "hard", while polarizable molecules or atoms, like H^- and Br^-, are "soft." One of the implications of HSAB is soft donors, or bases, will bond more strongly with soft acceptors, or acids, than with hard bases and *vice versa* . Third–row and, to a lesser extent, second–row transition metals in low oxidation states are generally soft while more electropositive transition metals and metals in high oxidation states are generally hard. Most organometallic catalysts (mostly second– or third–row transition metal complexes in low oxidation states) are, by definition considered, to be soft. Thus HSAB favors the stronger bonding of H^- over OH_2 to most catalytic metal centers. *Symbiosis* refers to the tendency of soft ligands to congregate in metal complexes, because the complexation of the initial soft ligands generally makes a metal center more polarizable, and thereby more likely to bind with other soft ligands. Another general trend was observed by Chatt and Heaton[77] — soft ligands generally encourage hard ligands to bind in the *trans* position, also known as the *antisymbiotic effect.* Pearson,[76] and Chatt and Heaton[77] postulated that two soft ligands bound *trans* to each other will have a mutually destabilizing effect, while a soft ligand *trans* to a hard ligand will be more stable. This effect holds true for $RuH(H_2O)(CO)_2(PPh_3)_3$ as mentioned above, in which the softest ligand, H^-, is *trans* to OH_2, the hardest ligand. It is not difficult to see the relationships between these concepts and that of *trans* influence. One last clarification should be made—*trans* influence deals with the effect of a ligand X on the equilibrium properties of the M–L_{trans} bond, while the term *trans* –effect deals with the effect of ligand X on the rate of L_{trans} ligand substitution by some nucleophile.[72]

In 1985 Bauer, Nagel, and Beck[78] reacted $[IrH(CO)(PPh_3)_2(Cl)]BF_4$ with water and isolated the aquo compound $[IrH(CO)(PPh_3)_2(Cl)(OH_2)]BF_4$. (Eq. 2. 25)X-ray

crystallography determined the Ru–O bond length to be 2.25 Å. The aquo ligand was hydrogen bonded to the tetrafluoroborate anion, and the geometry around the aquo oxygen appeared to be planar. Again this bond length is significantly longer than either of the expected values of 1.99 or 2.05 Å. These authors also explained this phenomenon as being caused by the *trans* influence of the hydride ligand.

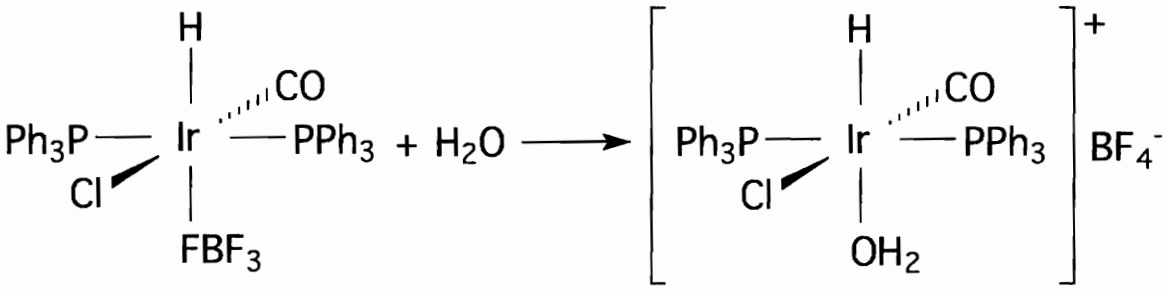

(2.25)

While studying the hydrolysis of acetonitrile to acetamide catalyzed by *trans* -$PtHCl(PR_3)_2$ (R=Me, Et) and 1 equivalent of NaOH in 1:1 water/acetonitrile solutions, Jensen and Trogler,[79] intercepted and spectrally characterized one of the catalytic intermediates $[PtH(H_2O)(PR_3)_2]^+$. Rates for this reaction at 80 °C were 178 and 70 mol/(mol of catalyst•hr) with turnovers greater than 6000 for the Me and Et derivatives, respectively. The proposed mechanism is shown in Figure 2.11. From this can be seen the importance of a labile ligand, such as water, which is easily displaced from the complex to form the open coordination site for binding of the substrate.

Garlaschelli, *et. al.*,[80] found IR evidence for the presence and participation of the *cis* –$Rh(CO)_2(H_2O)I$ tight ion pair in the catalyzed hydrocarboxylation of isoprene. When dried under vacuum and then THF was added, the complex *cis* –$Rh(CO)_2(THF)I$ is reversibly formed.

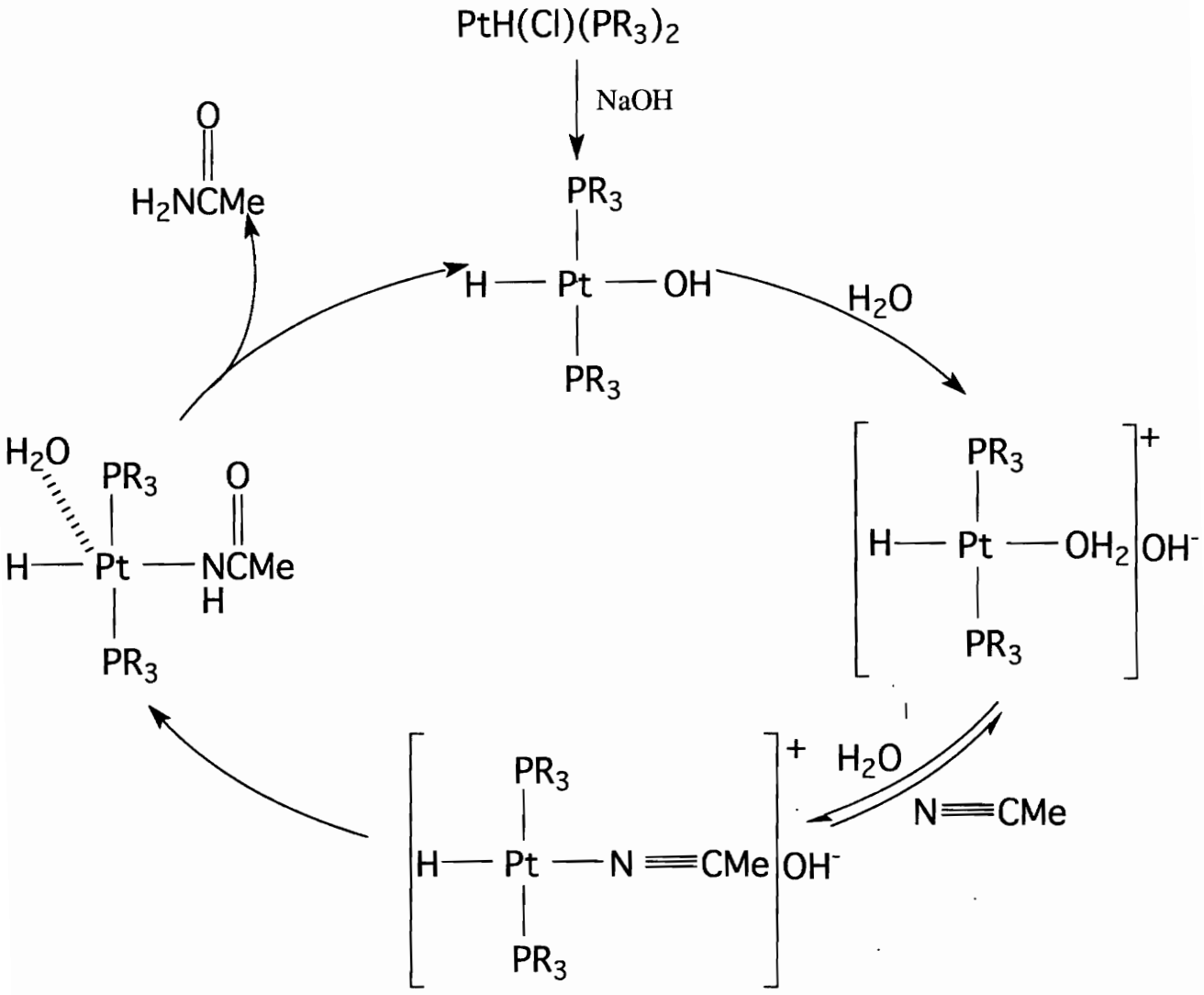

Figure 2.11 Catalytic Cycle for the Hydrolysis of Acetonitrile to Acetamide

Leoni, *et. al.*,[81] reported the crystal structure of the hydrido aquo palladium complex, *trans* –$[(Cy_3P)_2Pd(H)(H_2O)]BF_4$. The Pd–O bond length was 2.206(5) Å. This is again longer than the bond length of 2.00 Å predicted by Shustorovich.[72] The water ligand was *trans* to the hydride and assumed a pyramidal geometry about the oxygen.

The crystal structure for the cationic square planar complex *trans* –$[(PPh_3)_2Rh(CO)(H_2O)]^+[CF_3SO_3]^-$ was also determined.[82] The Rh–O bond length was 2.316 Å, slightly longer than the range 2.20–2.28 Å found in other Rh-water complexes.[83-85] The geometry about the water, nor hydrogen bonding, if any, were reported.

In 1986 the complexes $M(O_3SR)_2(H_2O)(CO)(PPh_3)_2$ (M=Ru, Os; R=CH_3, CF_3, $CH_3C_6H_4$, or d-camphor) were prepared by Harding, *et. al.*, and isolated as air-stable yellow crystalline solids from refluxing $MH_2(CO)(PPh_3)_3$ with RSO_3H in moist benzene.[107] The complexes were characterized by ^{31}P and ^1H NMR. The X–ray crystal structure of $Ru(O_3SC_6H_4CH_3)_2(H_2O)(CO)(PPh_3)_2$ showed the Ru–O(H_2O) bond length to be 2.202(6) Å . The water molecule was hydrogen bonded to the non–coordinated oxygens of the anionic ligand, and the geometry around the aquo oxygen was trigonal instead of planar, as in the previous complex. This bond length was also longer than expected from the covalent radii, but unlike the earlier two examples, does not have a high *trans* –influence ligand, like a hydride, *trans* to it.

Clark and Reimer [86] prepared the aquo complexes $[MCl_2(H_2O)(PMe_2Ph)_3]PF_6$ (M=Rh, Ir) by treating *mer* –$[MCl_3(PMe_2Ph)_3]$ with $AgPF_6$ in moist acetone. Deeming, *et. al*,[87] prepared the perchlorate analogs from $AgClO_4$ and obtained a crystal structure of $[IrCl_2(H_2O)(PMe_2Ph)_3]ClO_4$. The three phosphines and the water ligands were in a meridonal arrangement, with the two chlorines *trans* to each other. The hydrogens of the water molecule were hydrogen bonded to two perchlorate anions in the crystal. The geometry around the oxygen in the water molecule is planar with respect to the Ir–O bond, which has a length of 2.189(6) Å. The Ir–P bond *trans* to the water ligand was 2.249(3) Å, 0.13 Å shorter than the average of the other two Ir–P bonds. Variable temperature ^1H and ^{31}P NMR indicated rate-determining dissociation of the aquo ligand led to the five–

coordinate intermediates $[MCl_2(PMe_2Ph)_3]^+$, which were probably square-pyramidal species undergoing rapid pseudo–rotation.

In 1990, Bergmeister, Hanson, and Merola[88], obtained crystals of $Ru(CO)_3Cl_2H_2O$·diglyme while investigating reactions of ruthenium carbonyl chlorides adsorbed on metal oxide surfaces. The water ligand was bound *trans* – to one of the carbonyls, with a bond length of 2.105 Å and in a pyramidal geometry. The hydrogens of the water were hydrogen bonded to the diglyme. The bond length of the Ru–CO bond *trans* to the water ligand is 1.889(5) Å, essentially the same as the Ru–CO bond length *trans* to one of the chlorines (1.905(5) Å).

The crystal structure of $[Co(4\text{-pmpe})_2(H_2O)_2][ClO_4]_2$ (4-pmpe = diethyl 4-pyridylmethylphosphonate) was determined.[89] The two water molecules occupied the fifth and sixth coordination sites *trans* to each other, with Co–O bond lengths of 2.101(2) Å, and each in planar geometries.

Perhaps, some of the more involved work in this area has been performed by Crabtree and coworkers on complexes of the type, $[MH_2(S)_2(L)_2]X$ (where M =Ir, Rh;S is a weakly coordinating solvent, L is typically PPh_3, and X is BF_4^- or SbF_6^-). Complexes of the type $[MH_2(cod)_2(L)_2]X$ are active hydrogenation catalysts for olefins. When the complexes were rhodium based, their activity did not show a great deal of dependence on the solvent system, while the corresponding iridium systems showed a significant dependence — much higher activity in non-coordinating solvents, such as CH_2Cl_2 versus EtOH. The rates (catalytic cycles per hour) for the hydrogenation of 1-hexene for the following systems listed as (metal/solvent) were: (Ir, CH_2Cl_2), 5000 > (Rh,CH_2Cl_2), 4000 > (Rh, EtOH), 600 > (Ir, EtOH), 5.[90] While attempting to elucidate the mechanism of hydrogenation for these solvent systems by ^1H NMR, Crabtree, *et. al.*,[91] observed that similar complexes in which a weakly coordinating solvent had replaced the olefin, appeared

to act as dehydrogenation catalysts for olefins. (Fig. 2.12) The first example followed by NMR was the displacement of acetone from $[IrH_2(acetone)_2(PPh_3)_2]BF_4$ with cyclooctene at -60°C yielding $[IrH_2(coe)_2(PPh_3)_2]BF_4$, as the colorless solution was heated to -10°C, it turned red and NMR indicated the formation of $[Ir(coe)_2(PPh_3)_2]^+$. Upon sitting for several hours, the unusual occurred, new peaks in the spectra appeared corresponding to the formation of $[Ir(cod)_2(PPh_3)_2]^+$. This type of reaction was reported for a host of other

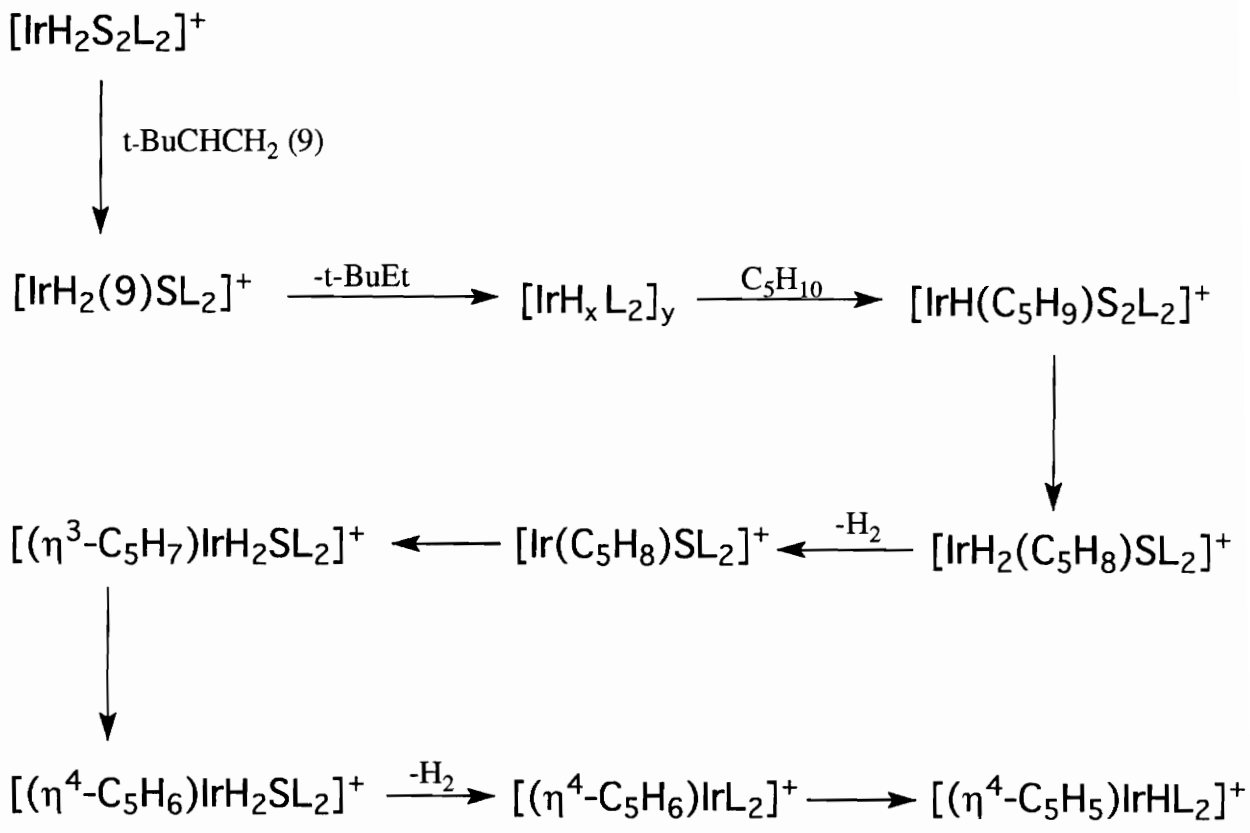

Figure 2.12 Dehydrogenation Using $[IrH_2(H_2O)_2(PPh_3)_2]BF_4$

monoolefins as well. Thus the complexes $[MH_2(S)_2(L)_2]X$, were active as hydrogenation, as well as, dehydrogenation catalysts, as would be expected by microscopic reversibility.[92]

A later paper reported the synthesis of $[IrH_2(H_2O)_2(PPh_3)_2]BF_4$ and its utility in developing the following reaction mechanism for dehydrogenation.[93]

Later papers[94,95] reported the homogeneous catalysis of silane alcoholysis by $[IrH_2S_2(PPh_3)_2]SbF_6$ (S = H_2O, THF, CH_3OH, and dmso). A X-ray crystal structure of the mixed solvent complex $[IrH_2(THF)(H_2O)(PPh_3)_2]SbF_6$ was obtained. The two phosphine ligands were mutually *trans* , and the solvent molecules were each *trans* to a hydride. The Ir–O bond lengths were comparable to those in other complexes in which solvent molecules were *trans* to hydride ligands.

Chapter 3 - Previous Work on $IrH_2(PMe_3)_3Cl$

Synthesis and Characterization of $IrH_2(PMe_3)_3Cl$

Integral to this thesis is a review of the work done by Dr. T. X. Le. It is her original synthesis of $IrH_2(PMe_3)_3Cl$ (**1**) and $IrH_2(PMe_3)_3(O_2CPh)$ (**2**), and the findings that both were soluble and functioned as active hydrogenation catalysts in water that led directly to the research presented in this thesis.

As mentioned earlier in the literature review, Le synthesized the pale yellow iridium (III) dihydride, $IrH_2(PMe_3)_3Cl$ (**1**), by hydrogenating $[Ir(COD)(PMe_3)_3]Cl$ in mesitylene as shown below in Equation 3.1.

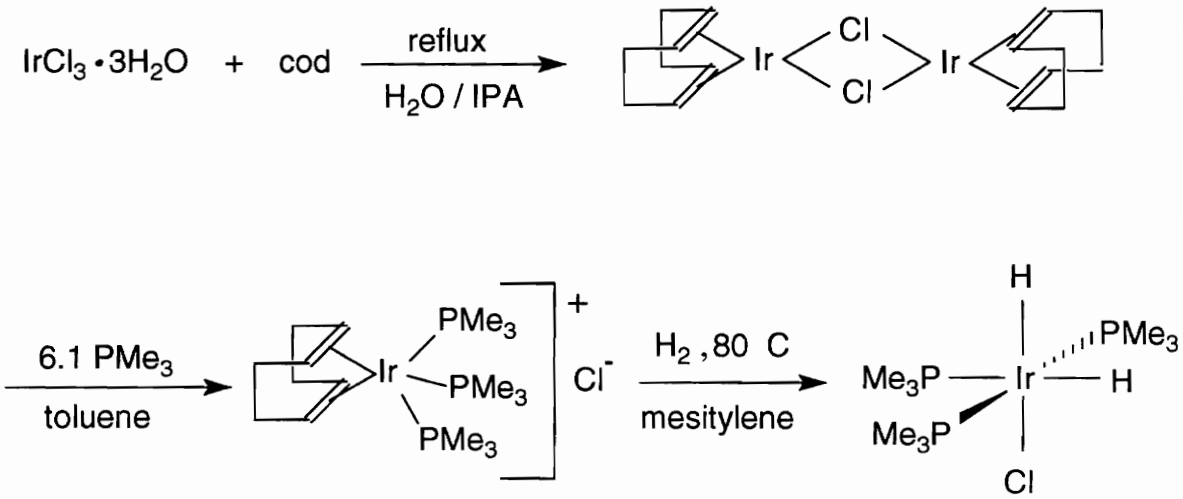

(3.1)

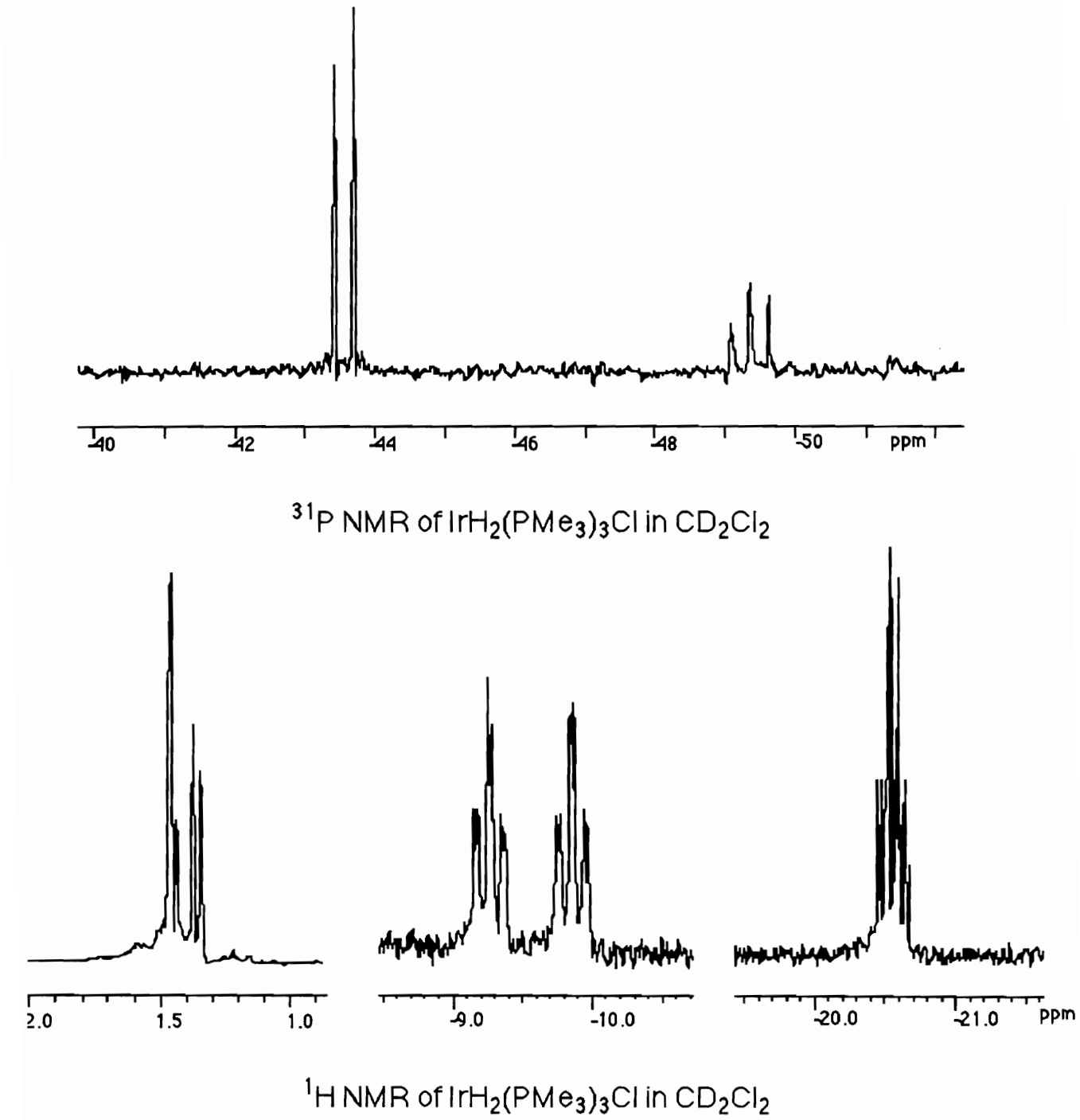

Figure 3.1 NMR Spectra of $IrH_2(PMe_3)_3Cl$ in CD_2Cl_2

X-ray crystallography, ^1H NMR and ^{31}P NMR in CD_2Cl_2 indicated the complex had an octahedral structure with meridonal phosphines, mutually *cis* hydrides, and a chloride ligand occupying the sixth coordination site *trans* to one of the hydrides.[11] The ^1H NMR and ^{31}P NMR spectra in CD_2Cl_2 are shown in Figure 3.1.

Reactivity of $IrH_2(PMe_3)_3Cl$

Since it is common knowledge that nucleophilic substrates often add to dihydrido complexes similar to (**1**), as revealed in the earlier reviews of dihydride chemistry, the reactivity of (**1**) was explored. Le found that (**1**) would not react with either alkynes or triphenylphosphine in methylene chloride, even upon heating. (Eq. 3.2) In fact, Le determined that $TlPF_6$, a common agent for activating stubborn coordinatively saturated complexes by removing chloride ions, was required to get any reactivity at all when methylene chloride was the solvent. (Eq. 3.3)

After this discovery, the previous mentioned reactions with trimethylphosphine and alkynes were performed again using distilled water, instead of dichloromethane, as the solvent. Addition of alkynes (1 equiv.) to (**1**) resulted in the clean formation of iridium-alkene coordination complexes (Eq. 3.4), while the iridum-tetrakisphosphino complex could be synthesized without using the "chloride scavenger", $TlPF_6$. (Eq. 3.5)

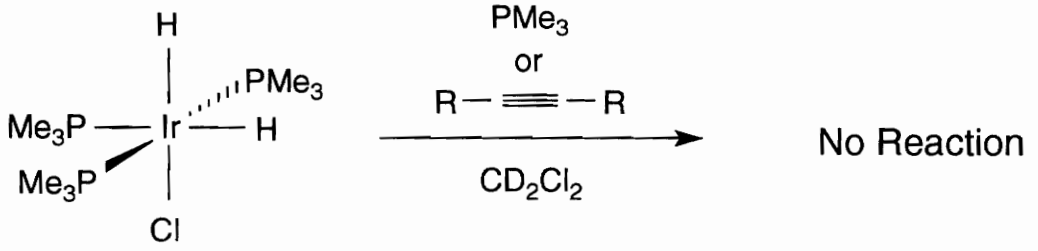

(3.2)

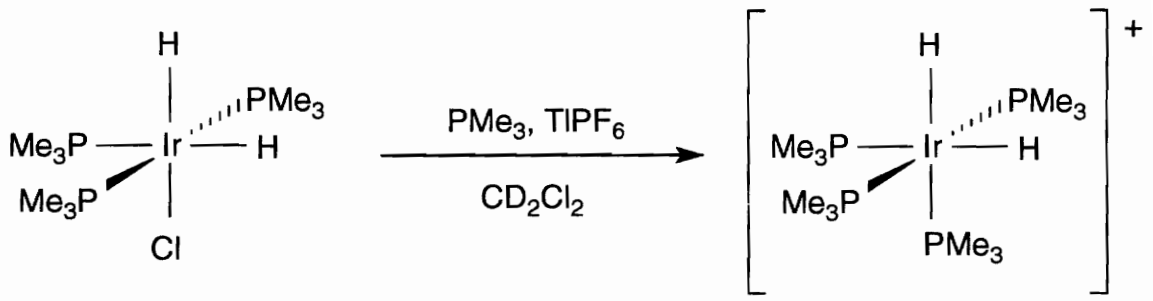

(3.3)

During the course of these reactivity studies, Le determined that (**1**) was moderately soluble in water (approximately 0.04g/mL at ambient temperature). Thus, (**1**) is a rare example of a transition metal dihydrido complex without ligands specifically functionalized to import water solubility that is water soluble. Even, for example, those dihydride complexes containing water as one of the coordinating ligands are not water soluble.[93]

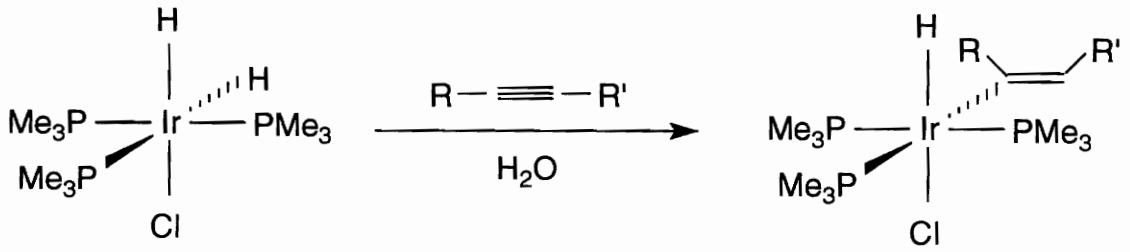

(3.4)

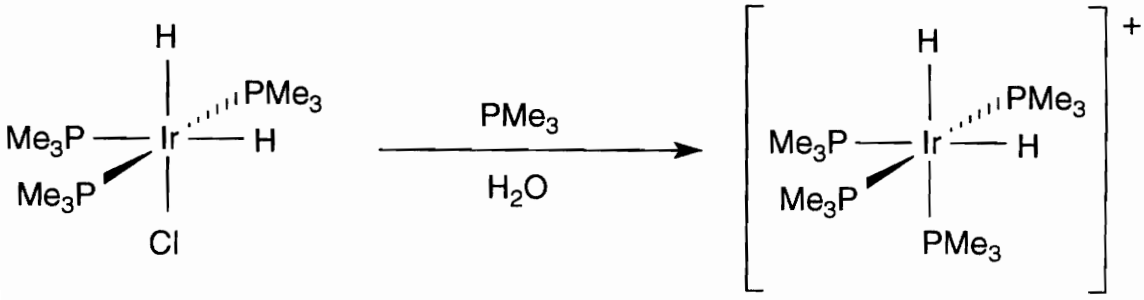

(3.5)

The alkyne addition reactions were then repeated, only under hydrogen atmosphere with excess alkyne. The product mixtures were found to contain alkanes, alkenes, and the starting iridium complex (**1**). Not only was (**1**) soluble in water, but these results suggested, even more surprisingly, that (**1**) was also acting as a hydrogenation catalyst in water. Specific hydrogenation studies are outlined in Table 3.1.

When the catalytic hydrogenation of phenylacetylene at 200 psi H_2 with (**1**) as the catalyst was carried out in toluene, no reduction was observed. However, when the hydrogenation was attempted under similar pressure/temperature conditions *in an aqueous solution* of (**1**) the reduction of phenylacetylene to the products styrene, ethyl benzene, and what was determined to be a "dimeric" phenylacetylene compound, depending upon the conditions, was observed.

It is not unheard of that water participates in and accelerates reactions. Grubbs, *et. al.* [96] demonstrated that the water soluble complex $RuCl_3$, although not a hydride complex, will catalyze ring opening methathesis polymerizations (ROMP) in organic solvents, however, the reaction proceeded faster and to higher molecular weight products in water. What makes this iridium dihydrido catalyst system unusual is that water is the solvent, not an additive. Le performed several experiments in an attempt to determine what factors made (**1**), not only soluble in water, but also an effective hydrogenation catalyst only in water.

Table 3.1 Catalytic Hydrogenation of Phenylacetylene

Run	Catalyst	Starting Material	Conditions	Product(s)
1	none	20 eq phenyl acetylene in **water**	T=60°C, P=200 psi H_2, t=48h, glass pressure tube	**no reaction**
2	(1)	20 eq phenyl acetylene in **water**	T=60°C, P=400 psi H_2, t=24h, stainless steel pressure tube	**100% yield** 100% ethyl benzene
3			T=RT, P=400 psi H_2, t=24h, stainless steel pressure tube	**49% yield** 24% ethyl benzene 25% styrene
4			T=60°C, P=200 psi H_2, t=24h, glass pressure tube	**81% yield** 47% ethyl benzene, 28% styrene, 6% phenyl acetylene dimer
5			T=RT, P=200 psi H_2, t=24h, glass pressure tube	**75% yield** 43% ethyl benzene, 27% styrene, 15% phenyl acetylene dimer
6			T=60°C t=24h, glass pressure tube	**65% yield** 65% phenylacetylene dimer
7	(1)	20 eq phenyl acetylene in **toluene**	T=60°C, P=200 psi H_2, t=24h, glass pressure tube	**no reaction**

The Aqueous Equilibrium of $IrH_2(PMe_3)_3Cl$

^1H NMR and ^{31}P NMR spectra of (**1**) in D_2O, instead of CD_2Cl_2, indicated the presence of not one, but two separate, although similar, dihydrido complexes in solution. (Figure 3.2) Analysis of the hydride region of the ^1H NMR in D_2O spectrum revealed a major species, which will be called complex **Y** for simplicity, (represented by the doublet of triplets at δ -9 and the multiplet at -22 ppm) and a minor species, complex **Z**, (the peaks at δ -8 and -25 ppm) with similar peak splitting. It can be inferred from the ^1H NMR of (**1**) that these two sets of hydride peak patterns are both representative of *cis* hydrides. Analysis of the ^{31}P NMR in D_2O also indicates a major (the large doublet at δ -45 ppm and the triplet at -50 ppm) and a minor (peaks at δ -40 and -44 ppm) species with similar peak shapes. Similar correlation between the NMR spectrum in CD_2Cl_2 and X-Ray structure of (**1**), leads to the inference that both the major and minor products contain a meridonal arrangement of phosphines. Thus for the two species in water, five of the six coordinating groups, and their respective spatial arrangements, are identical. Hence, the basis for stating that the two species are similar.

At this point, one of the first suppositions made was that the catalytically active species derived from (**1**) might be a cationic intermediate in which the chloride had been displaced by a water molecule. This seems reasonable in light of the many solvent coordinated intermediates that have been proposed in catalytic mechanistic schemes, *e.g.* Wilkinson's catalyst.[97] The catalytic process might occur as illustrated in Figure 3.3. First, chloride dissociates from complex (**1**) in water and is replaced by a water molecule to form the cationic "iridium-aquo complex". This iridium-aquo complex coexists in solution with another octahedral iridium complex with meridional phosphines and *cis* hydrides. The alkyne then replaces the water molecule in the sixth coordination site forming an iridium-

alkynyl complex. The alkyne inserts into the *cis* iridium-hydride bond, while the chloride reoccupies the sixth coordination site forming an iridium-vinyl complex. The vinyl group then reductively eliminates, and the original (**1**) is formed by the oxidative addition of molecular hydrogen.

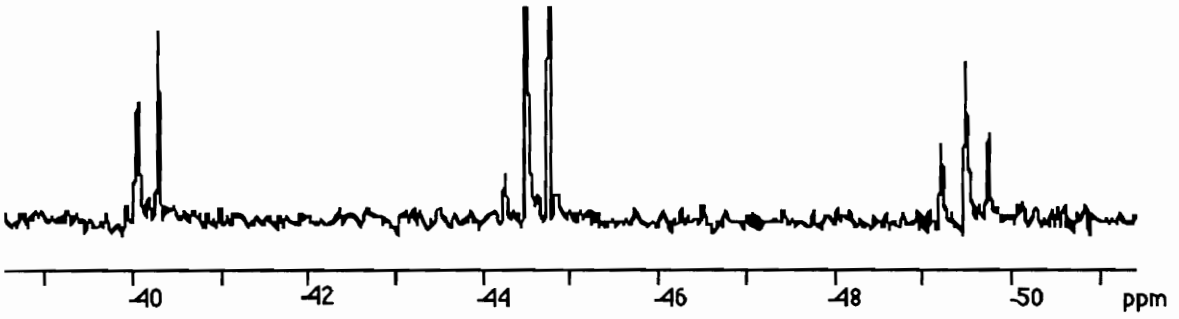

^{31}P NMR of $IrH_2(PMe_3)_3Cl$ (**1**) in D_2O

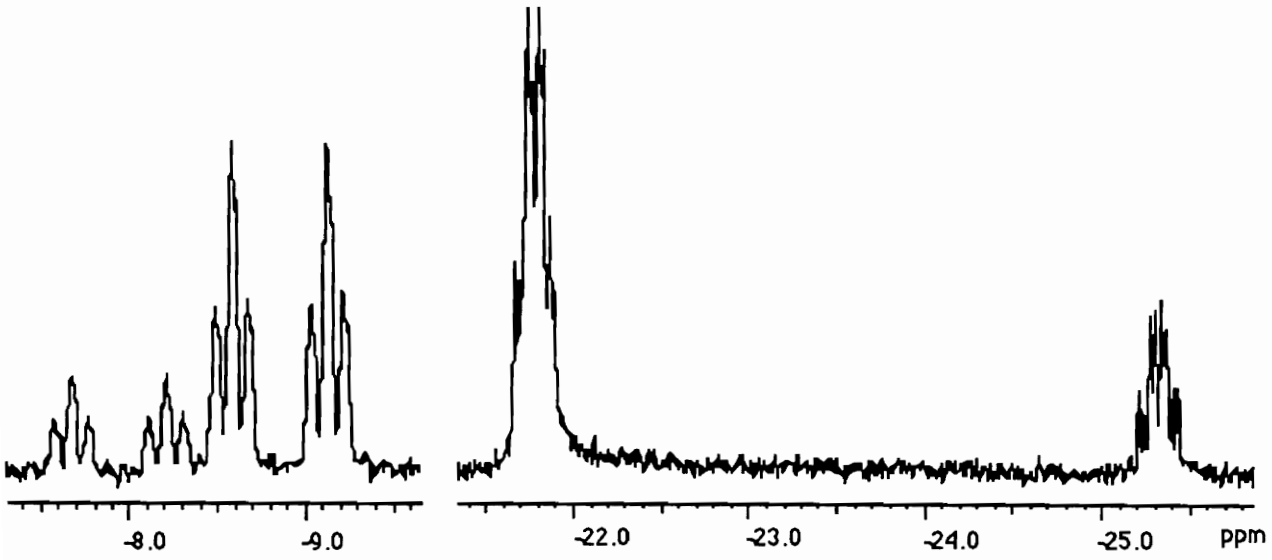

^{1}H NMR of $IrH_2(PMe_3)_3Cl$ (**1**) in D_2O

Figure 3.2 NMR Spectra of $IrH_2(PMe_3)_3Cl$ in D_2O

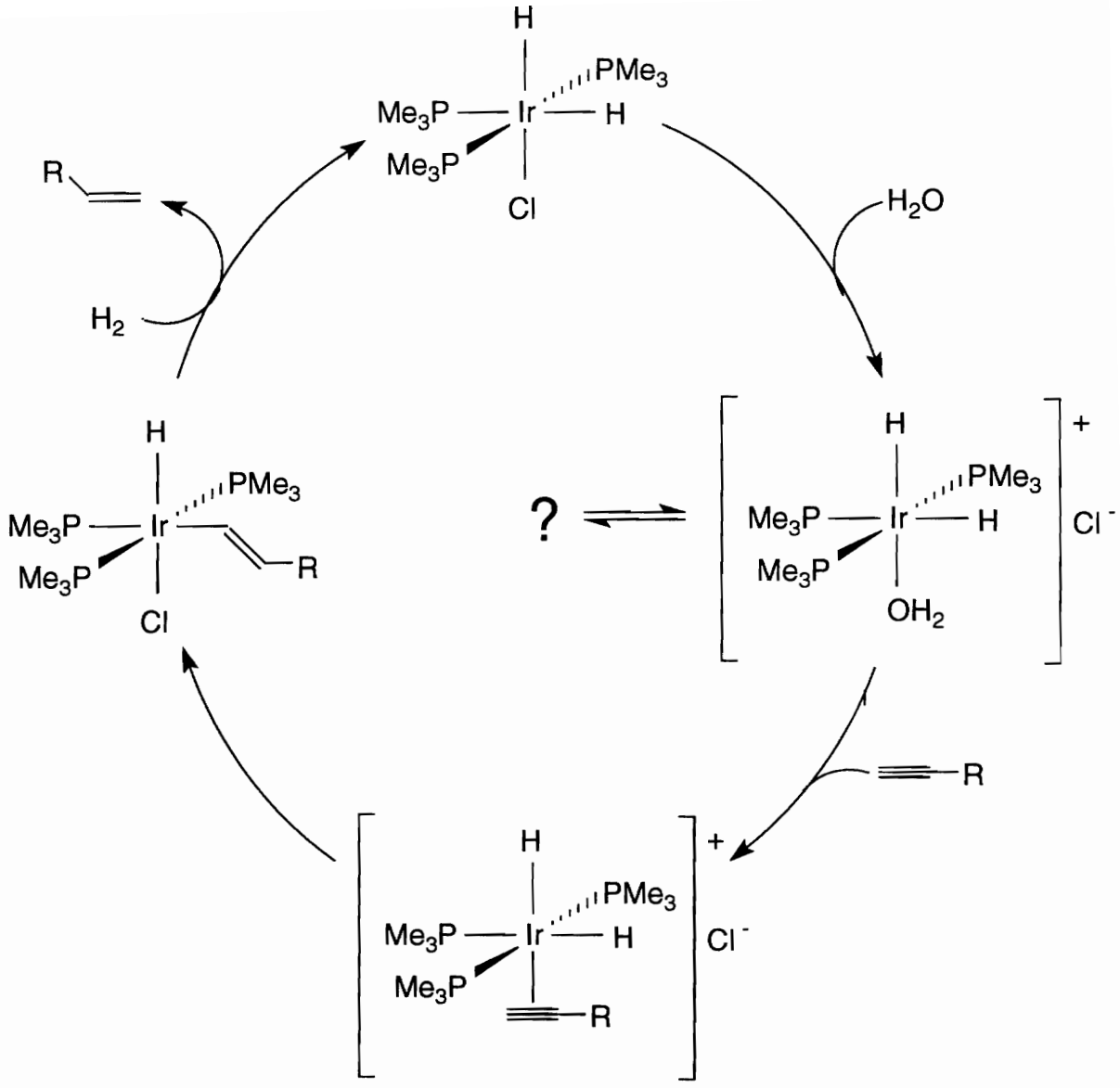

Figure 3.3 Proposed Catalytic Mechanism for the Hydrogenation of Alkynes Using (**1**) in H_2O

While attempting to trap the cationic iridium-aquo complex from aqueous solution using KPF_6 as the counter ion, Le isolated the dimeric μ-chloro bridged complex (**2**) as a white precipitate. (Fig. 3.4) The structure of (**2**) was verified by single crystal X-ray crystallography. ^1H NMR of the supernatant liquid indicated both sets of hydride peaks

had decreased in intensity. ^{1}H NMR of (**2**) redissolved in excess D_2O showed peaks identical to that of the original (**1**). Several experiments were then performed to determine if, indeed, (**2**) was the missing complex "**?**", in the catalytic scheme in Figure 3.3.

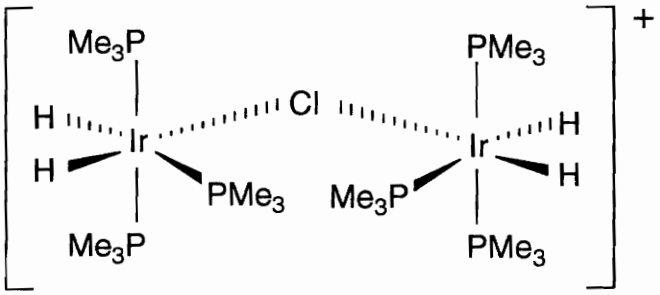

(**2**)

Figure 3.4 Structure of Chloro-bridged Dinuclear Iridium Complex

When excess NaCl was added to a D_2O solution of (**1**) and examined by ^{1}H NMR it was found that the relative intensity of the hydride peaks of **Z** (the so-called minor product) had decreased with respect to those of **Y**. More quantitative equilibrium ^{1}H NMR experiments were attempted by varying the concentration of (**1**) in D_2O and using variable temperature NMR. In general, the results indicated the relative concentration of **Y**, the major product, increased as the concentration of (**1**) increased, but decreased with increasing temperature. The general results are illustrated in Figure 3.5.

Attempts to fit the concentration data, derived from the integration of the hydride regions, to various equilibria expressions, however, gave unsatisfactory results. So although general equilibrium trends were observed, no consistent quantitative equilibrium expressions, and therefore no specific complexes were identified.

It is at this point that the transition from the review of Le's work to the crux of this thesis - Chapter Four "Elucidation of the Aqueous Equilibrium System of $IrH_2(PMe_3)_3Cl$ and "Chapter Five " Related Iridium Dihydride Complexes," is made.

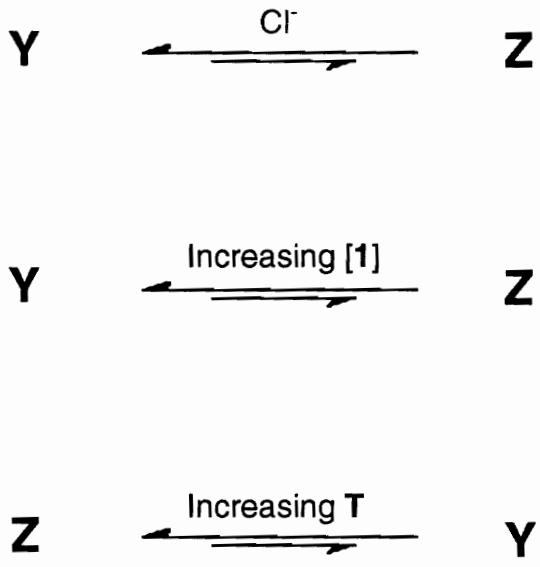

Figure 3.5 Results of Crude Equilibrium Tests on $IrH_2(PMe_3)_3Cl$

Chapter 4 - Elucidation of the Aqueous Equilibrium System of $IrH_2(PMe_3)_3Cl$

Introduction

Chapter Three of this thesis summarized the work of T. X. Le related to $IrH_2(PMe_3)_3Cl$ (**1**) and its unique solubility and reactivity in water, as well as the subsequent discovery of the two species system when (**1**) is dissolved in H_2O. Qualitative analysis of the aqueous system revealed the relative concentrations of the two species were sensitive to the overall concentration of (**1**), to added chloride ion, and to temperature.[98] These observations would naturally lead to the conclusion that the two species in solution are in equilibrium. Attempts to quantify the equilibrium by determining the concentrations of the two species by manipulation of the NMR integration data of the hydride region gave results that, although following general trends, were not consistent enough to determine the exact nature of the equilibrium system. This lack of consistency might have been caused by two factors. Firstly, there is considerable difficulty associated with obtaining accurate and precise integration values in the hydride region of the proton spectrum, mainly due to the poor signal to noise ratio. Secondly, deuterium exchange occured at both hydride positions in (**1**), although slowly on the NMT time scale. Deuterated product would not appear in the hydride region and thus skew the integration data. It is possible that either of these two factors was enough to prevent the quantification of the equilibrium expression.

To ascertain the specific equilibrium system involved in the aqueous chemistry of $IrH_2(PMe_3)_3Cl$ (**1**) two requirements had first to be met: Precise and accurate concentration

data had to be acquired, and suitable equilibrium equations had to be developed to which the data could be applied. This chapter will outline the NMR experiments and the analysis of their data leading to the elucidation of the aqueous equilibrium system of (**1**).

Probable Equilibria Systems

The development of suitable equilibrium equations is not a trivial affair. If done carelessly, the mathematical fitting of concentration data will lead to meaningless results. Le's previous work and the restrictions of the system offered several guidelines from which to build possible equilibrium expressions.

1) There are only two species in equilibrium.
2) All iridium species contain three meridonal phosphines and two *cis* - hydrides in an octahedral arrangement.
3) The species are related by the loss/gain of chloride ion.
4) The chloro-bridged complex $[H_2(Me_3P)_3Ir\text{-}Cl\text{-}Ir(PMe_3)_3H_2]$, (**2**), might be one of the species.
5) Other than the original components of (**1**), only water is available as a ligand

Four plausible expressions were developed that satisfied these guidelines and are outlined in Figure 4.1.

Case 1

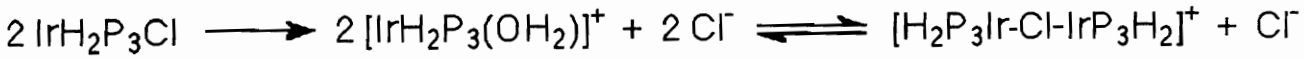

Case 2

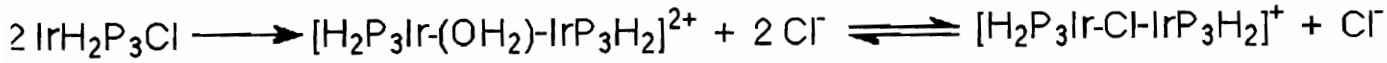

Case 3

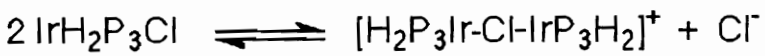

Case 4

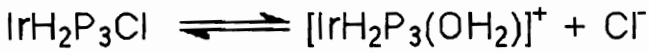

Figure 4.1 Possible Cases for the Aqueous Equilibrium of (**1**)

In Case 1, it is proposed that as (**1**) is dissolved in water it dissociates completely to give a cationic water coordinated "monoiridium-aquo" complex, which is in equilibrium with the cationic chloro-bridged diiridium complex, (**2**), formed by the displacement of water ligands from two iridium-aquo complexes and then bridged coordination by chloride. In Case 2, (**1**) dissolves and dissociates completely, but this time first forms an aquo-bridged diiridium dication, which then is in equilibrium with (**2**). In Case 3, dissolved (**1**)

is in equilibrium with (**2**). In Case 4, (**1**) is in equilibrium with the monoiridium-aquo complex.

These four cases seem to be the only reasonable possibilities. Any iridium species other than mono- or diiridium complexes can be ruled out because of the required octahedral environment with five of the six coordination sites already accounted for by the phosphines and the hydrides. Phosphine bridged diiridium complexes are not expected because they would require one iridium center to release a phosphine ligand prior to bridged coordination to uphold the coordination guidelines imposed by the NMR data, but no free phosphines are observed in the NMR spectra. It is possible, as in Case 2, the order of development of the species is backwards (i.e. (**2**) is formed first, then equilibrates with the aquo bridged diiridium cation), but this does nothing other than inverting the K_{eq} expression derived from this equation, which will make no difference when the K_{eq} values are analyzed for constancy.

Variable Concentration ^{31}P NMR Experiments

The purpose of variable concentration experiments is quite simple: If equilibrium concentration values can be determined for the proposed equilibrium species in each of the variable concentration trials and K_{eq} values then calculated, comparison of these K_{eq} values within each Case will give evidence as to whether or not that specific proposed equilibrium Case might accurately describe the actual system. If the K_{eq} values for the various concentration trials within a specific case are not experimentally constant, it can generally be assumed that specific Case does not well represent the actual system. However, if the K_{eq} values are constant, that Case *might* describe the actual system. Hence, it was attempted to obtain reliable equilibrium concentration data from integration of NMR

signals, apply this data to each of the four proposed equilibrium cases, and then determine the constancy of the K_{eq} values derived from this data.

Because of the poor signal/noise ratio in the hydride region, it was decided to determine the relative concentrations of the two equilibrium species by ^{31}P NMR integration. The rationale behind this decision is as follows. The phosphines do not undergo any type of mechanism similar to deuterium exchange, as do the hydrides, thus the integration values obtained from the ^{31}P NMR spectra should be more reproducible. Likewise the integration of the phosphine signals will be unaffected by the deuterium exchange of the hydrides. Repeated measurement of a standard sample's phosphine signals integrations yielded a range of precision of approximately 10%. Complete experiments were not repeated, although some trials within experiments were repeated to insure self-consistency. The results of two variable concentration experiments at 300 K with H_2O (km181) and D_2O (km184) as the solvents are tabulated in Table 4.1. Sample ^{31}P NMR spectra of (**1**) in H_2O are included in Figure 4.2

Table 4.1 Integration Data for the Variable Concentration ^{31}P NMR of (**1**)

Solvent = H_2O			Solvent = D_2O		
[Ir]	Int (-39 ppm)	Int (-49 ppm)	[Ir]	Int (-39 ppm)	Int (-49 ppm)
0.005	6.439	3.072	- - -	- - -	- - -
0.015	4.627	3.805	.015	4.766	4.223
0.024	3.847	3.991	.025	3.578	3.917
0.036	3.103	3.828	.035	2.837	4.231
0.046	2.777	4.147	.046	2.546	4.217
0.053	2.422	4.013	.053	2.412	4.282
0.060	2.357	4.221	.060	1.908	4.024
0.065	1.845	3.356	.071	2.005	3.997

[Ir] = The total molarity of iridium species in the solution.
Int(-39 ppm) = The integration of the ^{31}P NMR signal at -39 ppm.
Int(-49 ppm) = The integration of the ^{31}P NMR signal at -49 ppm.

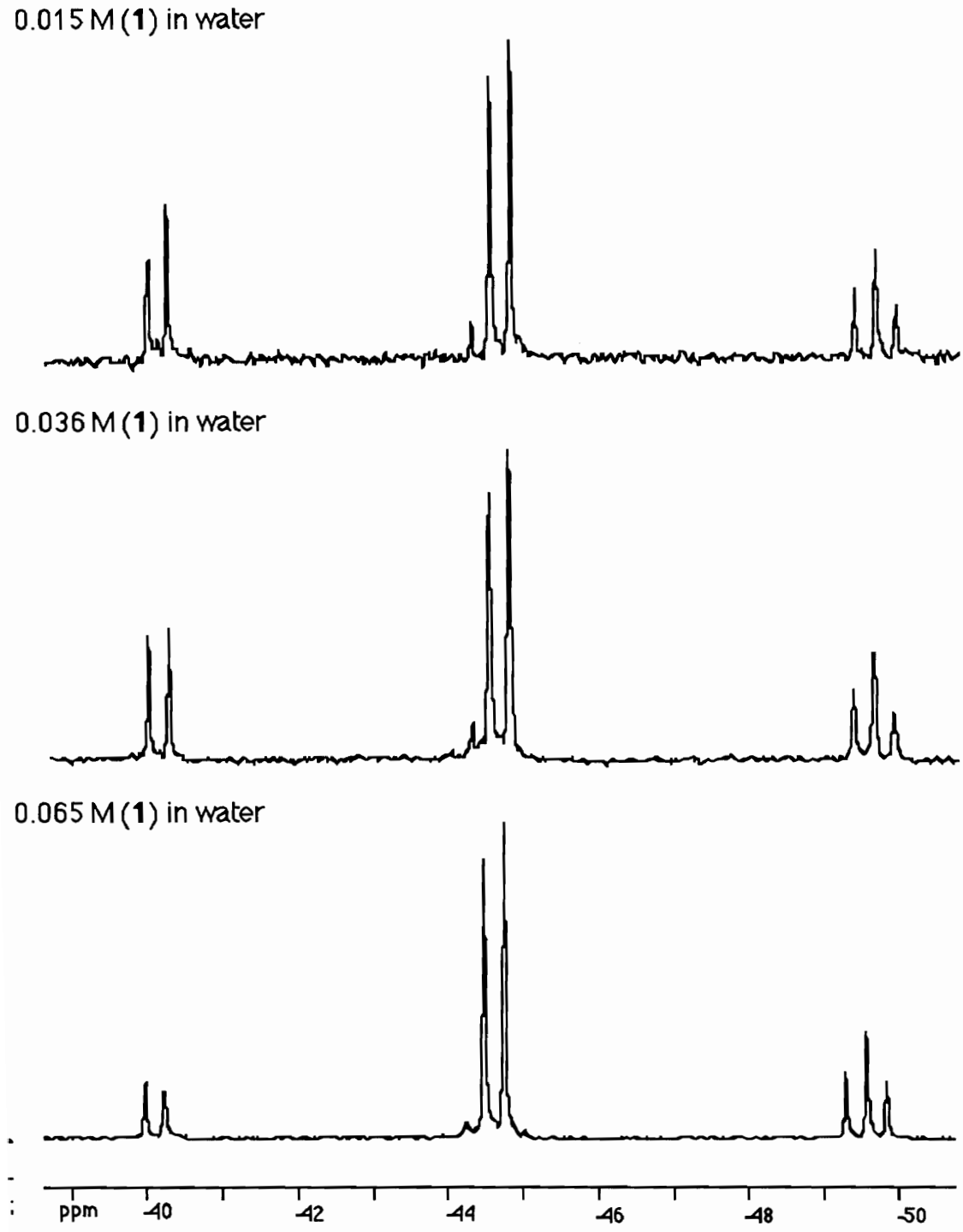

Figure 4.2 ^{31}P NMR of (**1**) in H_2O - Sample Spectra

Viewing the sample ^{31}P NMR spectra, especially at the higher concentrations, it appears questionable that there are two similar sets of peaks, each consisting of a doublet and a triplet. However if the 0.015 M spectrum is viewed, evidence can be seen in the -44 ppm region of the triplet from the upfield set "growing in" underneath the doublet from the downfield set. The relative increase in peak size of the upfield set (doublet at -44 ppm and triplet at -49 ppm) versus the downfield set (doublet -40 ppm and triplet -44 ppm) as the concentration of (**1**) increases can also be seen. Integration data was collected for the peak at -40 ppm and the peak at -49 ppm, as each of these two peaks represent one of the two separate species in solution, while the two peaks at -44 ppm were too close together to obtain accurate integration data from them. The integration data from each spectra was converted to concentration values for the relevant equilibrium species and these concentration data were then used to calculate a value for the K_{eq} for each concentration of (**1**) in that specific solvent. The experiments in water and deuterium oxide were treated separately. An example of this procedure is outlined below for the calculation of a K_{eq} value from the spectrum of 0.065 M (**1**) in H_2O utilizing the Case 4 equilibrium equation.

The Case 4 equilibrium expression is . . . .

$$\underset{\textbf{A}}{IrH_2P_3Cl} \rightleftharpoons \underset{\textbf{B}}{[IrH_2P_3(OH_2)]^+} + Cl^-$$

Because it is known from Le's previous work, that the addition of chloride ion to the equilibrium system favors the species represented by the upfield set of peaks (the doublet at -44 ppm and the triplet at -49 ppm), simple application of Le Chetalier's principle to the

Case 4 equilibrium system implies the addition of chloride ion shifts the equilibrium to the left, increasing the concentration of species **A**. By extrapolation, in Case 4, species **A** is represented by the upfield peak set, and species **B** by the downfield peak set. However, the concentration of species **A** cannot be found by simply taking the ratio of the integration of the -49 ppm multiplet over the total integration of the -39 ppm multiplet and the -49 ppm multiplet, and multiplying by the total concentration of iridium in solution (0.065 M). The triplet at -49 ppm is due to the splitting of the central phosphine in the meridonal arrangement by the two other equivalent phosphines. Therefore the integration value of the -49 ppm multiplet is directly proportional to the concentration of species **A** in solution. But the doublet peak at -39 ppm arises from the splitting of the two equivalent phosphines by the central phosphine. Therefore, the concentration of species **B** in solution is actually going to be related to one-half of the value of the integration of the -39 ppm multiplet. Thus specifically for Case 4, the relationships between the integrals of the two species and their concentrations are as follows.

$$[\mathbf{A}] \propto \text{Integration of -49 ppm peak}$$

$$[\mathbf{B}] \propto 1/2 \text{ x Integration of -40 ppm peak}$$

For the Case 4 equilibrium, the equilibrium constant is given by the following equation.

$$K_{eq} = \frac{[\mathbf{B}][Cl^-]}{[\mathbf{A}]} = \frac{(x)(x)}{[Ir]_{total} - x}$$

Manipulating this equation gives

$$\frac{[B]}{[A]} = \frac{(x)}{[Ir]_{total} - x}$$

If the variable, z, is then defined as,

$$z = \frac{1/2(\text{integral of -40 ppm peak})}{(\text{integral of -49 ppm peak})} = \frac{[B]}{[A]}$$

it follows that

$$z = \frac{(x)}{[Ir]_{total} - x}$$

which is solved for **x**.

$$x = \left(\frac{z}{1 + z}\right)[Ir]_{total}$$

x is then plugged into the original K_{eq} equation, and the equation solved for K_{eq}.

A similar procedure was used to arrive at K_{eq} values for the other three cases, and the derivations of equations and subsequent K_{eq} values for four cases are outlined in the Appendix. The calculated values for the concentrations of the equilibrium species and the K_{eq} for each of the four proposed equilibrium cases are collated in Tables 4.2 - 4.5.

Table 4.2 Concentration and K_{eq} data for Equilibrium Case 1 in H_2O

Z	x	$[IrH_2P_3H_2O]^+$	$[Cl]^-$	$[Ir\text{-}Cl\text{-}Ir]^+$	Keq
0.4771	0.0012	0.0026	0.0038	0.0012	49339
0.8223	0.0047	0.0057	0.0103	0.0047	14028
1.0374	0.0081	0.0078	0.0159	0.0081	8358
1.2336	0.0128	0.0104	0.0232	0.0128	5123
1.4933	0.0172	0.0115	0.0288	0.0172	4499
1.6569	0.0204	0.0123	0.0326	0.0204	4131
1.7908	0.0235	0.0131	0.0365	0.0235	3742
1.8190	0.0255	0.0140	0.0395	0.0255	3285

Table 4.3 Concentration and K_{eq} Data for Equilibrium Case 2 in H_2O

Z	x	$[Ir\text{-}O\text{-}Ir]^{2+}$	$[Cl]^-$	$[Ir\text{-}Cl\text{-}Ir]^+$	Keq
0.9542	0.0012	0.0013	0.0038	0.0012	252.5
1.6447	0.0047	0.0028	0.0103	0.0047	159.1
2.0749	0.0081	0.0039	0.0159	0.0081	130.5
2.4673	0.0128	0.0052	0.0232	0.0128	106.4
2.9867	0.0172	0.0058	0.0288	0.0172	103.8
3.3138	0.0204	0.0061	0.0326	0.0204	101.5
3.5817	0.0235	0.0065	0.0365	0.0235	98.0
3.6379	0.0255	0.0070	0.0395	0.0255	92.1

Table 4.4 Concentration and K_{eq} Data for Equilibrium Case 3 in H_2O

Z	x	$[IrH_2P_3Cl]$	$[Ir\text{-}Cl\text{-}Ir]^+$	$[Cl]^-$	Keq
0.5240	0.0013	0.0024	0.0013	0.0013	0.2746
0.3040	0.0028	0.0093	0.0028	0.0028	0.0924
0.2410	0.0039	0.0162	0.0039	0.0039	0.0581
0.2027	0.0052	0.0256	0.0052	0.0052	0.0411
0.1674	0.0058	0.0345	0.0058	0.0058	0.0280
0.1509	0.0061	0.0407	0.0061	0.0061	0.0228
0.1396	0.0065	0.0469	0.0065	0.0065	0.0195
0.1374	0.0070	0.0510	0.0070	0.0070	0.0189

Table 4.5 Concentration and K_{eq} Data for Equilibrium Case 4 in H_2O

Z	x	$[IrH_2P_3Cl]$	$[IrH_2P_3H_2O]^+$	$[Cl]^-$	Keq
1.048	0.0026	0.0024	0.0026	0.0026	**0.0027**
0.608	0.0057	0.0093	0.0057	0.0057	**0.0034**
0.482	0.0078	0.0162	0.0078	0.0078	**0.0038**
0.405	0.0104	0.0256	0.0104	0.0104	**0.0042**
0.335	0.0115	0.0345	0.0115	0.0115	**0.0039**
0.302	0.0123	0.0407	0.0123	0.0123	**0.0037**
0.279	0.0131	0.0469	0.0131	0.0131	**0.0037**
0.275	0.0140	0.0510	0.0140	0.0140	**0.0039**

It can easily be seen that only for Case 4 do the derived values of K_{eq} achieve any sort of constancy ($K_{eq} = 0.0037 \pm 0.0003$). Indicating, of the four proposed equilibrium cases equilibrium cases, only Case 4 comes close to describing the actual equilibrium system occurring in water. The equilibrium concentration values and K_{eq} values calculated of (**1**) in D_2O are presented in Table 4.6.

Table 4.6 Concentration and K_{eq} Data for Equilibrium Case 4 in D_2O

Z	x	$[IrH_2P_3Cl]$	$[IrH_2P_3H_2O]^+$	$[Cl]^-$	Keq
0.563	0.0054	0.0096	0.0054	0.0054	**0.0030**
0.457	0.0078	0.0172	0.0078	0.0078	**0.0036**
0.335	0.0088	0.0262	0.0088	0.0088	**0.0029**
0.302	0.0107	0.0353	0.0107	0.0107	**0.0032**
0.282	0.0116	0.0414	0.0116	0.0116	**0.0033**
0.237	0.0115	0.0485	0.0115	0.0115	**0.0027**
0.251	0.0142	0.0568	0.0142	0.0142	**0.0036**

The calculated K_{eq} values for the D_2O experiment are also experimentally constant ($K_{eq} = 0.0032 \pm 0.0003$) when applied to Case 4. The K_{eq} values and their respective standard deviations are well in line with the approximate 10% error possible from the original integration data. These results indicate two things: The equilibrium in D_2O is also consistent or similar to that proposed by the Case 4 equilibrium expression. And, by inference, the equilibrium systems in water and D_2O are similar, but not necessarily the

same, as judged by the average K_{eq} values for the two experiments. Analysis of the average K_{eq} vales and their respective standard deviations, give, at best, inconclusive interpretations. The two average K_{eq} values are experimentally equal, but just barely.

A particular note should be made at this point. Of the four proposed equilibrium systems, case 4 is unique in one major way - it is the only case in which both of the equilibrium species are mononuclear. In the other three cases, at least one of the proposed equilibrium species is a dinuclear iridium complex. Even if the exact composition of the equilibrium species is temporarily ignored, it can be generalized the equilibrium of (**1**) in aqueous solutions involves two mononuclear species. Remembering from interpretation of the NMR data that the two equilibrium species must both contain meridonal phosphines and cis - hydrides in five of the six coordination sites, and the sixth coordination site must be occupied by some component of the original complex, (**1**), or the solvent, but not a phosphine or hydride ligand, the mononuclear-to-mononuclear equilibrium system proposed in Case 4 seems to be the only consistent choice.

Variable Temperature Studies

Next variable temperature ^{31}P NMR studies on constant concentration samples of $IrH_2(PMe_3)_3Cl$ in both H_2O (km188) and D_2O (km189). From which, as before, K_{eq} values were calculated by applying the integration data to the Case 4 equilibrium system. Then by plotting the relevant data on Van't Hoff coordinates, the relative changes in the enthalpy, the entropy, and Gibb's free energy values for the system were derived.

Sample spectra of the experiment in H_2O are shown in Figure 4.3. The data collected and calculated values for both experiments is tabulated below in Table 4.7 (H_2O) and Table 4.8 (D_2O). The Van't Hoff plots are presented in Figure 4.4.

Table 4.7 Data and Calculation Results for ^{31}P VTNMR in H_2O

T (K)	[Ir]tot	Int (-39)	Int (-49)	Keq	ln Keq	1/T
280	0.0650	1.3680	4.9170	0.0011	-6.8086	0.00357
285	" "	1.6540	4.4050	0.0019	-6.2508	0.00351
290	" "	1.8310	4.3190	0.0024	-6.0282	0.00345
295	" "	1.9420	4.3790	0.0026	-5.9461	0.00339
300	" "	2.2350	4.1870	0.0037	-5.6117	0.00333
305	" "	2.4190	3.9990	0.0046	-5.3893	0.00328
310	" "	2.4800	3.9180	0.0049	-5.3093	0.00323

Table 4.8 Data and Calculation Results for ^{31}P VTNMR in D_2O

T (K)	[Ir]tot	Int (-39)	Int (-49)	Keq	ln Keq	1/T
280	0.0706	1.317	4.535	0.0013	-6.6455	0.00357
285	" "	1.433	4.389	0.0016	-6.4269	0.00351
290	" "	1.603	4.322	0.0020	-6.1908	0.00345
295	" "	1.838	4.279	0.0027	-5.9217	0.00339
300	" "	1.997	4.310	0.0031	-5.7840	0.00333
305	" "	2.204	4.172	0.0039	-5.5477	0.00328
310	" "	2.272	4.322	0.0039	-5.5565	0.00323

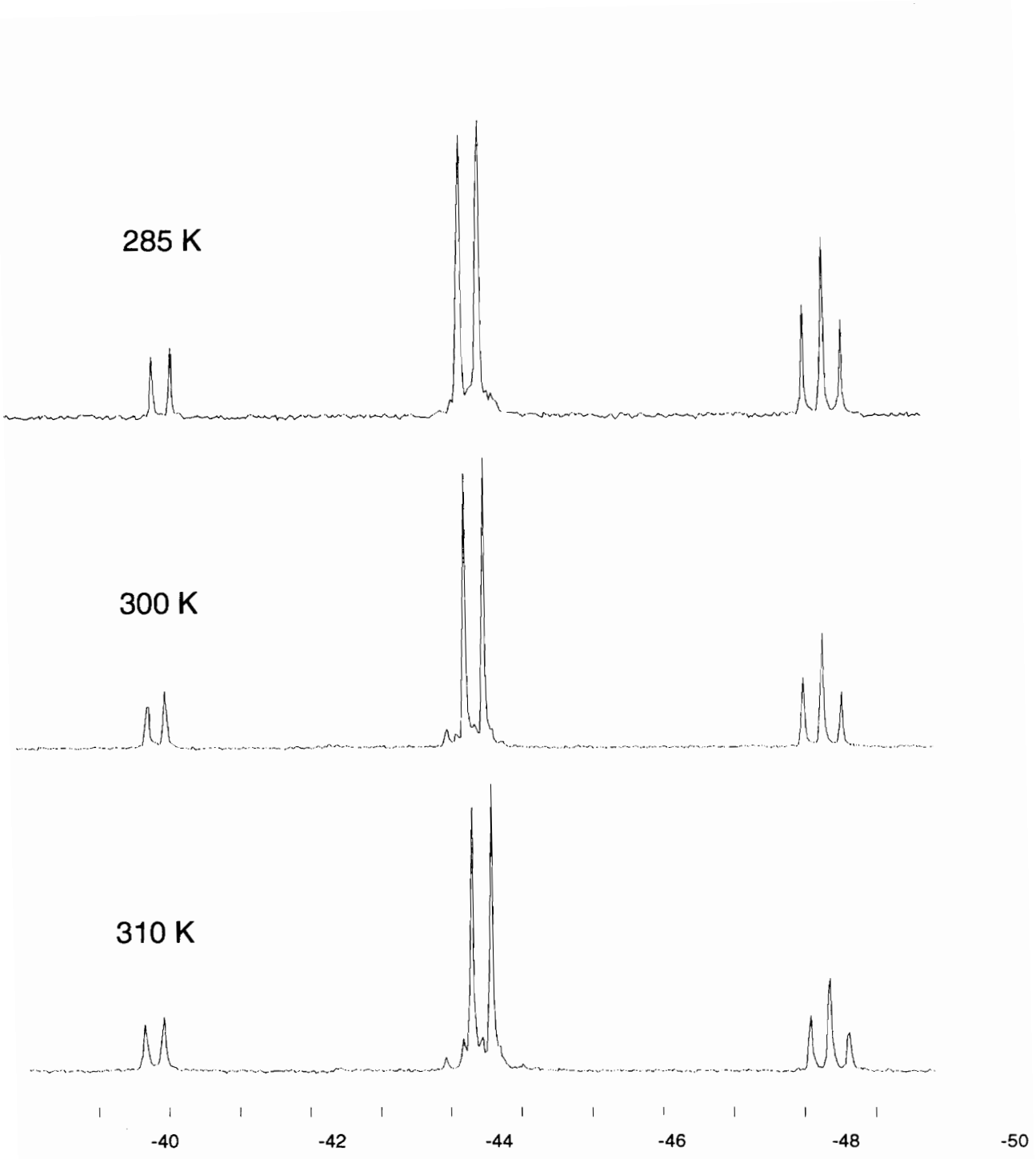

Figure 4.3 Representative ^{31}P VTNMR spectra of $IrH_2(PMe_3)_3Cl$ in H_2O

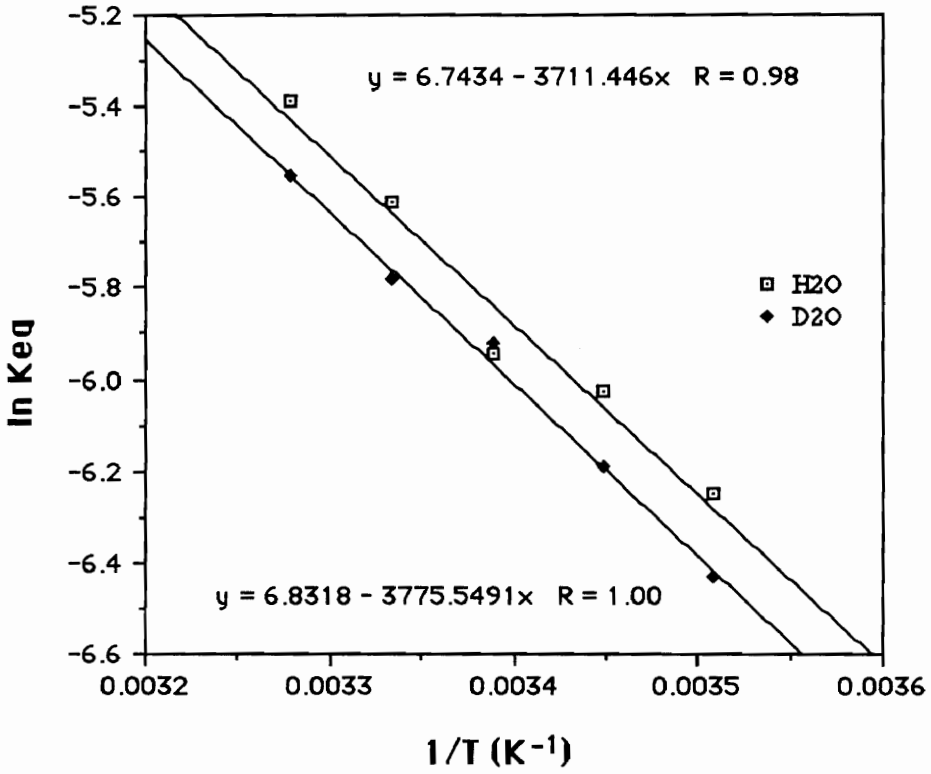

Figure 4.4 Van't Hoff Plots of ^{31}P VTNMR Data for H_2O and D_2O

Linear regression analysis of the plots of the H_2O and the D_2O data resulted in the respective best-fit equations, y = -3711.446x + 6.7434 (r = 0.98) and y = -3775.5491x + 6.8318 (r = 1.00) By applying the Van't Hoff Equation to the regression equation's slope

$$\ln K = \frac{-\Delta H}{RT} + \frac{\Delta S}{R}$$

and y-intercept, the values for ΔH, ΔS, and, consequently, ΔG can be determined for the equilibrium systems. The results of these calculations for the equilibrium of (**1**) in both H_2O and D_2O are contained in Table 4.9.

Table 4.9 Thermodynamic Results of the Van't Hoff Plots

	H_2O	D_2O
ΔH (kJ/mol)	30.8	31.2
ΔS (J/Kmol)	56.0	56.1
ΔG (kJ/mol)	14.1	14.5

As can be seen, the thermodynamic values for the equilibrium of (**1**)in both H_2O and D_2O are quite similar, and consistent with both the Case 4 equilibrium and physical evidence. In our equilibrium model, a stronger Ir-Cl bond is broken to form a weaker Ir-O bond (by Hard-Soft/Acid-Base theory; the "soft" iridium center will bond more strongly with the "softer" ligand, in this case the chloride.[99,100]) The positive, or unfavorable, change in enthalpy correlates well with the experimentally obtained values of 30.8 and 31.2 kJ/mol.

The highly positive, or favorable, entropy value is slightly more difficult to account for. Going from a single neutral complex to two charged species is entropically favorable, or positive. Often in cases such as this, extensive solvent ordering around the charged species occurs and this would contribute a negative entropy component, resulting in either a small negative or small positive overall net change in entropy .

However, if a simple and almost necessary assumption is invoked, the positive entropy value makes more sense. If the ^{31}P NMR results and the conclusions derived from them are correct, and the aqueous equilibrium is described by Case 4, what makes $IrH_2(PMe_3)_3Cl$ soluble in water? As stated before, there is no real reason, as deduced from its overall structure or the innate solubility of its components to expect (**1**) to be soluble in water, but it is. Therefore the assumption that extensive hydrogen bonding is involved in the solvation of (**1**) is almost required. This would imply that all three of the species in aqueous solution ($IrH_2(PMe_3)_3Cl$ (**1**), $[IrH_2(PMe_3)_3(H_2O)]^+$, and Cl^-) are each surrounded by highly ordered hydrogen-bonded solvent molecules. In this case, the large

positive entropy can now be explained as being due to the forming of two charged species from one neutral species, a very favorable entropy process, with the unfavorable component of solvent ordering canceling itself out on both sides of the equilibrium. The favorable entropy gain is the reason why this equilibrium exists at all, since, enthalpically, the breaking of the Ir-Cl bond to form the Ir-O bond is unfavorable.

The Gibbs' free energy term also is in accord with physical evidence. Applying the average of the two ΔG values (14.1 and 14.5 kJ/mol) to the equation, $\Delta G = -RT\ln K_{eq}$, results in the calculation of a K_{eq} value equal to 0.0032, which is quite close to the experimentally derived K_{eq} values of 0.0033 and 0.0037 for (**1**) in H_2O and D_2O, respectively.

Adding Chloride Ion to $IrH_2(PMe_3)_3Cl$

One last experiment was performed to test the integrity of the proposed Case 4 equilibrium system. To a series of NMR samples containing aqueous solutions of (**1**) of

Case 4 Equilibrium System

$$IrH_2P_3Cl \rightleftharpoons [IrH_2P_3(OH_2)]^+ + Cl^-$$

known molarity and volume, were added incremental equivalents of aqueous NaCl. ^{31}P NMR spectra were then recorded, the integrals of the relevant peaks determined and K_{eq}s were calculated in the manner explained previously in this chapter. The results of that experiment are tabulated below.

Table 4.10 Calculated K_{eq}'s for Adding Cl^- to (**1**) (km196)

$[IrH_2(PMe_3)_3Cl]_{init}$	Equiv's of Cl^- added	K_{eq}
0.0498	0.00	.00555
" "	0.10	.00538
" "	0.25	.00526
" "	0.50	.00626

As is obvious from the table, the K_{eq} values for this experiment do not match those from the previous experiments. However, this may be a result of the inherent uncertainities in the preparation of the solution, since the high K_{eq} value for the trial where no Cl^- was added cannot be an artifact of added chloride ion, yet it is consistent with the values of the other three trials. A more detailed discussion of experimental uncertainties is included later in thsi chapter. This aside, what is important is the self-consistency of these results. The average of the K_{eq} values is 0.0056 ± 0.0004. Again, the constancy of the four K_{eq} values adds further evidence to support the proposed aqueous Case 4 equilibrium between $IrH_2(PMe_3)_3Cl$ and $IrH_2(PMe_3)_3(H_2O)^+$.

The Role of $IrH_2(PMe_3)_3(O_2CPh)$

$IrH_2(PMe_3)_3(O_2CPh)$ (**3**) was first synthesized by Le[11] and was also found to be a water soluble iridium dihydride with the ability to catalytically hydrogenate alkynes when H_2O was the solvent. ^1H NMR of (**3**) in D_2O indicated that the hydrides underwent more rapid deuterium exchange than did the hydrides of (**1**). NMR spectroscopy indicated the material synthesized by Le's synthetic procedure was not obtained in high purity. ^{31}P NMR of (**3**) in D_2O showed a confusing multitude of peaks at δ–39 ppm, d; -44 ppm, d; -49 ppm , m; -55 ppm, t; and -61 ppm, t. (A copy of this spectrum can be found on page

152, reference 11.) When (**3**) was prepared by the method outlined in the experimental section of this chapter, the ^{1}H NMR and ^{31}P NMR of (**3**) in CD_2Cl_2 clearly indicated a pure product with the familiar *cis* -hydrides and meridonal phosphines had been obtained. (Fig. 4.6) ^{1}H NMR and ^{31}P NMR of (**3**) in D_2O indicated only a single product was present in aqueous solution, unlike the spectra of

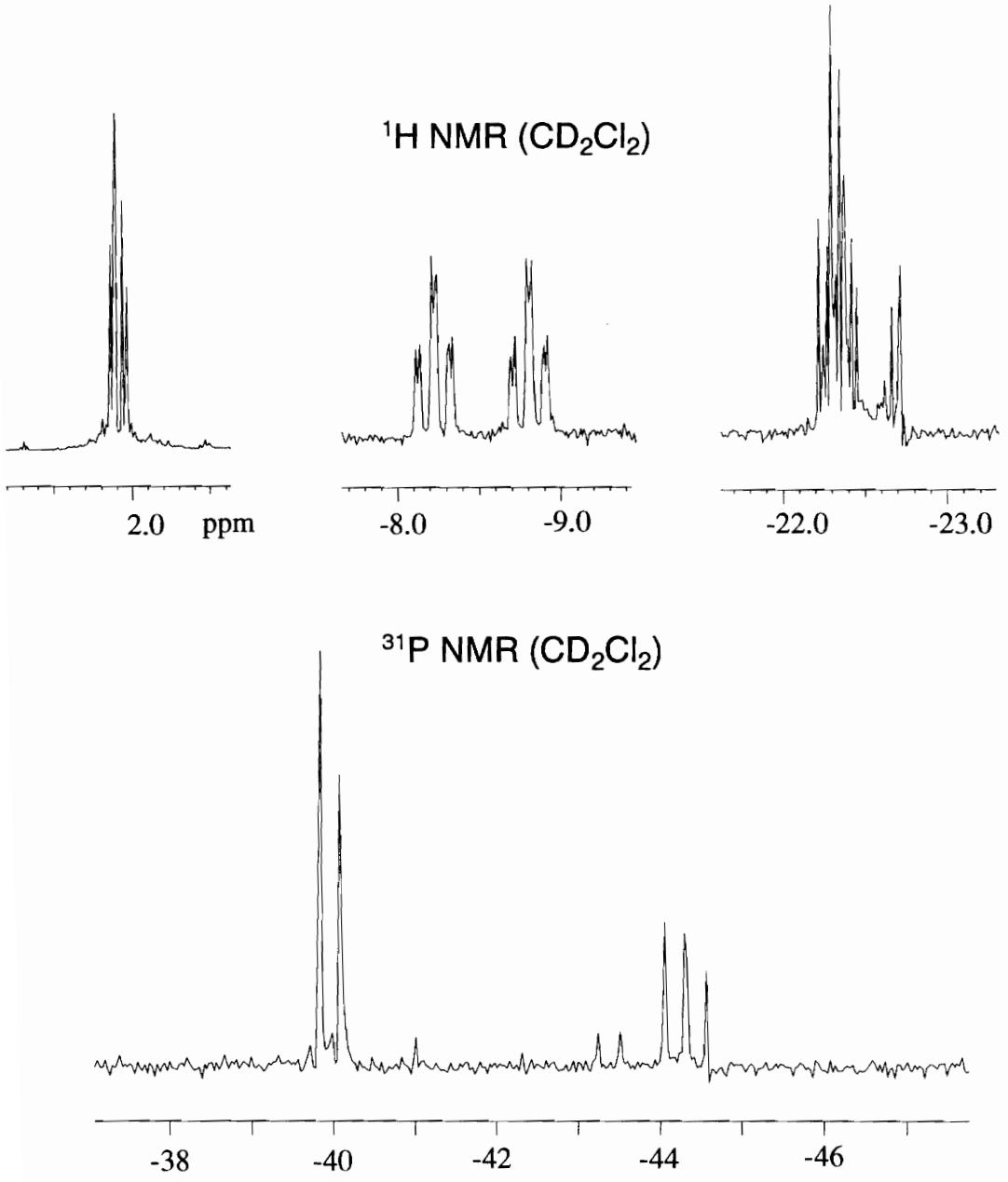

Figure 4.5 ^{1}H NMR and ^{31}P NMR of $IrH_2(PMe_3)_3(O_2CPh)$ (**3**) in CD_2Cl_2 (Note: The aromatic region is not shown in the ^{1}H NMR)

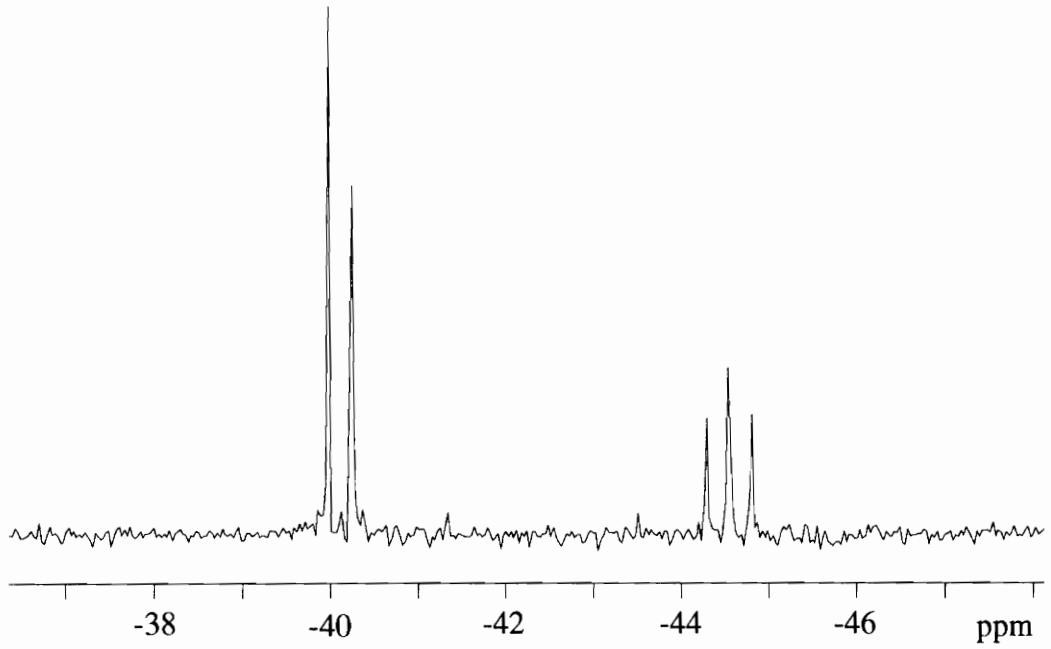

Figure 4.6 ^{31}P NMR of $IrH_2(PMe_3)_3(O_2CPh)$ (**3**) in H_2O

$IrH_2(PMe_3)_3Cl$ (**1**) in D_2O, which indicated the presence of two species. The ^{31}P NMR of (**3**) in D_2O is illustrated in Figure 4.6. Comparison of the ^{31}P NMR of (**3**) to that of (**1**) revealed the chemical shifts of (**3**) very closely matched the chemical shifts of what had been previously determined to be the "iridium-aquo" species, as can be seen in Figure 4.7. A simple, but rough ^{31}P NMR experiment (km194) was conceived to test whether (**3**) was dissociating fully in water to give 100% of what has been circumstantially identified as the "iridium-aquo" complex, or whether the similar shifts are an artifact of both (**3**) and the aquo complex having very similar Ir-O bonded structures leading to nearly identical chemical shifts of the phosphines. Two NMR tubes were prepared. One tube contained (**1**) in D_2O, the other (**3**) in D_2O in roughly equimolar quantities. ^{31}P NMR spectra were acquired for each sample and then the contents of one the tube containing (**3**) were removed and syringed into the tube containing (**1**) and a ^{31}P NMR spectrum immediately acquired.

Analysis of the spectrum resulting from the mixing of the two tubes' samples concluded that no obvious broadening of the lines had occurred. If (**3**) was not fully dissociating in

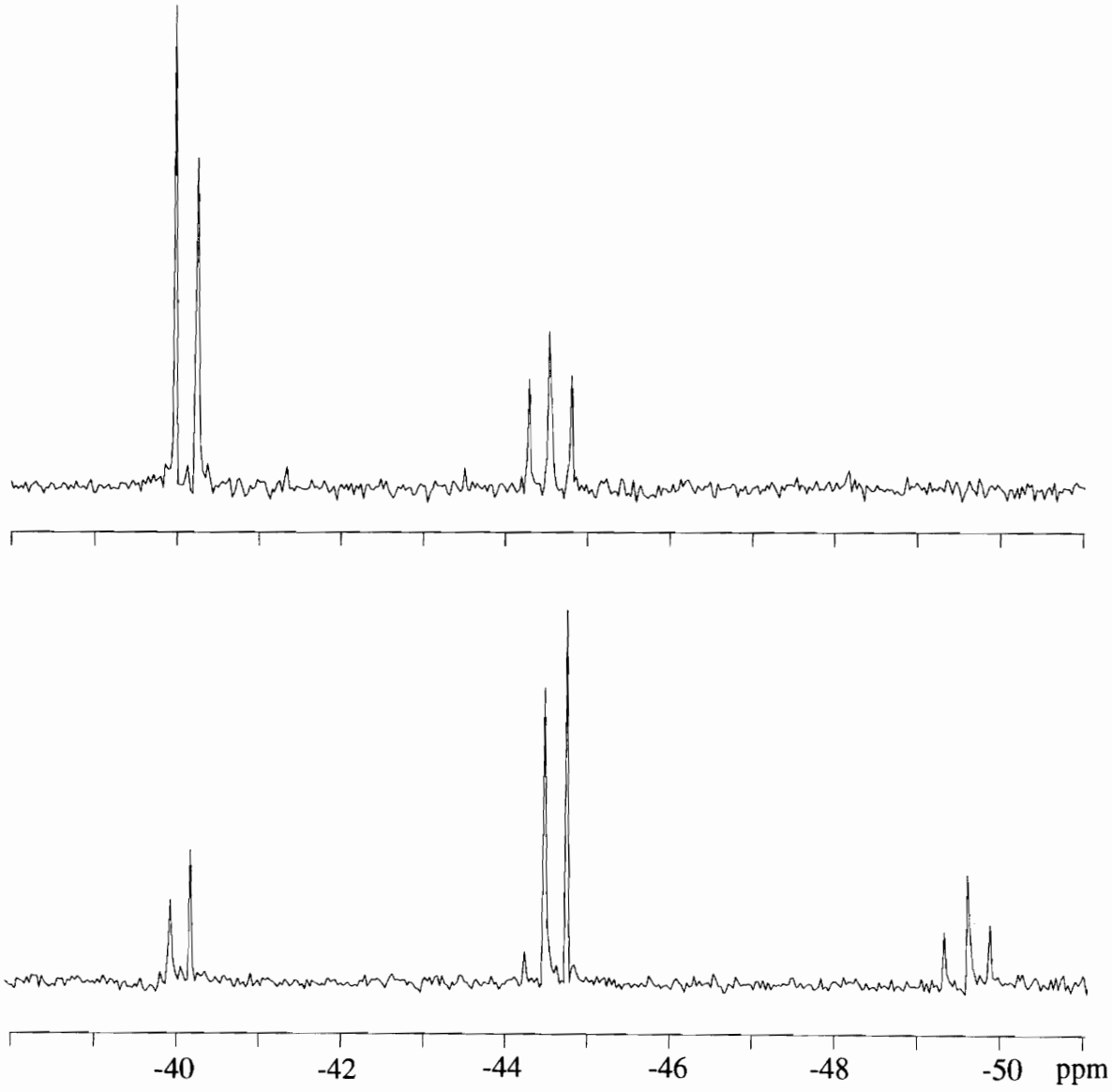

Figure 4.7 ^{31}P NMR of $IrH_2(PMe_3)_3Cl$ (**1**) and $IrH_2(PMe_3)_3(O_2CPh)$ (**3**) in H_2O

water to give the aquo complex and the similarity of the chemical shifts in the two spectra was only coincidental, a broadening of the peaks where the signals from the two different complexes overlapped would be expected, as it would be very improbable that two different complexes would exhibit identical chemical shifts and their signals overlap perfectly. If on the other hand, (**3**) was dissociating completely in H_2O to give the aquo complex, upon mixing of the two samples, no broadening of the peaks would be expected. The latter would then seem to be the case for (**3**) in aqueous solution based upon the results of km(194). Also obvious in this experiment was that the equilibrium had shifted in favor of the -39 ppm set of peaks after the tubes containing (**1**) and (**3**) had been mixed, but this was consistent with the above arguments. After mixing, there was approximately one-half the "normal" total concentration of chloride in the solution relative the total concentration of iridium species. By LeChetalier's Principle, this would shift the equilibrium system to liberate more chloride ion, and consequently relatively more of the "iridium-aquo" species would be present.

If (**3**) does indeed dissociate fully in water to give the aquo complex, then if chloride ion is added to this solution, an equilibrium situation similar to that of (**1**) in aqueous solution should arise. This hypothesis was tested experimentally (km191). 0.5, 1.0, and 1.5 equivalents of chloride ion were added to three NMR tubes containing aqueous solutions of (**3**). ^{31}P NMR spectra were acquired, the integrations of the peaks determined, and the equilibrium constants calculated using the Case 4 equilibrium equations. The data and results are presented in Table 4.11. The results, to say the

Table 4.11 Data and Results of 0.5, 1.0, and 1.5 Equiv's of Cl^- Added to (**3**)

[$IrH_2(PMe_3)_3(O_2CPh)$]	Equiv's NaCl	Int (-39 ppm)	Int(-49 ppm)	Keq
0.054	0.5	6.501	2.833	0.0021
0.054	1.0	2.781	4.435	0.0040
0.054	1.5	1.611	4.659	0.0060

least, are interesting. When 1.0 equivalent of NaCl was added, the calculated K_{eq} just falls within the range of the average K_{eq} value (0.0037 ± 0.0003) determined in experiment km181. However, the results of the other two trials are not that consistent, although a distinct trend is obvious. As more equivalents of chloride are added the K_{eq} seems to systematically increase. It is quite possible the benzoate counter ion is not a perfect spectator ion in this system, and is in some way interfering with the ideal equilibrium system necessary to achieve constant K_{eq} values. Perhaps what is seen in this case is an equilibrium pH effect as the benzoate ion is "liberated" from close interaction with the iridium center by introduction of the chloride ion, though at this point that idea is pure conjecture.

A Discussion of Error

The purpose of this section is not to claim that a specific error(s) has been committed in either the experimental procedures or the manipulations of the data presented in this chapter, but rather to specifically address the *possibility* of errors and their subsequent ramifications with respect to this research. This discussion is intended to be predominately qualitative in nature, not rigorously quantitative.

That the calculations utilized in this chapter are themselves beyond suspect is a assumption that must necessarily be made, without it the following discussion is useless. The numerical results of the calculations, and the calculations, have been checked and rechecked for accuracy. In leiu of this assumption there would appear to be three major areas where sources of error might have been introduced; in the preparation of the stock solutions, in the preparation of the NMR samples, and in the actual accumulation and integration of the data.

The preparation of the stock solutions was accomplished by the method outlined in the Experimental section of of this chapter. A small quantity of (**1**) (0.089 g for the variable concentration experiment km181) was weighed on an electronic balance, by first zeroing the weight of a piece of weighing paper, then weighing out the required amount of (**1**), and finally transferring the sample to a septa bottle, which was sealed under nitrogen in a glove box, then adding 3.00 mL of solvent via syringe. Under normal circumstances balances of the type used are considered accurate in single measurements to ± 0.002 g. Using a typical error calculation from General Chemistry Lab, (error for 2 measurements each with ± 0.002 g = $[2(0.002)^2]^{1/2}$ = 0.0028) the uncertainty in the measurement of the weight of (**1**) was ± 0.003 g. Or in other words, errors of approximately 3 % can be reasonably expected to occur solely from the weighing of the sample. Add to this the difficulty of weighing materials in the glove box, versus *normal conditions*, and an uncertainty due to weighing of ± 0.005 g is not unreasonable. The addition of 3.00 mL of solvent was accomplished by the addition of three 1.00 mL samples using a 1000 μL syringe. A reasonable single measurement error might be ± 20 μL (This number was chosen arbitrarily). This results in an uncertainty of volume measurment of ± 0.04 mL. By utilizing the uncertainties of these two measurements, the total uncertainty in the concentration of the stock solution is calculated to have been (0.065 ± 0.004) M, or approximately a 6 % uncertainty.

Using this value and similar uncertainty calculations, typical uncertainties for the preparation of the NMR samples from the stock solutions range from ± 0.006 M (for 0.060 M) to ± 0.002 M (for 0.015 M). Thus, since the calculated K_{eq} values are directly related to the original concentration of (**1**), the calculated K_{eq} values have an uncertainty of approximately ± 10 - 13 %, due solely to the preparation of the NMR sample.

As stated earlier in thsi chapter, repeated measurements of the integrations of ^{31}P NMR peaks yielded ranges of ± 5 % of the average value. By again applying uncertainty

calculations, typical uncertainties of ± 12 % for the K_{eq} values are obtained just from the uncertainty of the integration measurements.

The total combined quantitative effect of these uncertainties upon the calculated K_{eq} values is difficult to determine, although their qualitative effects might be described. Uncertainties due to preparation of the stock solution will result in all K_{eq} values calculated for NMR samples derived from that stock solution to be either all higher or all lower than expected. Or in other terms such an error will affect the accuracy of the K_{eq} values. Uncertainties in the preparation of the individual NMR samples or in the determination of the integration values will, in all probability, be random, resulting in neither consistently high nor low values throughout a series. These last two errors will then predominately affect the precision of the K_{eq} values.

The relevance of this discussion becomes evident upon comparing the data from Tables 4.5, 4.6, and 4.10. Tables 4.5 and 4.6 list the K_{eq} values obtained from the variable concentration studies of (**1**) in D_2O and H_2O, respectively. The average K_{eq} values derived from these two experiements are different [(0.0037 ± 0.0003) and (0.0032 ± 0.0003), respectively], but when judged in light of the possible experimental uncertainties, the difference is negligible. Thus, no definite conclusions can at this point, nor should, be drawn from the difference of their values. However, as noted previously in this chapter, it is not as much the actual value of the K_{eq} derived for each experiment that is relevant when comparing results between experiments, but the evident consistency of values within these experiments. This constancy strongly supports the mononuclear-mononuclear system proposed as the equilibrium system of (**1**) in water.

Experimental

$[Ir(COD)(PMe_3)_3]Cl$[101] and $Ir(COD)(PMe_3)_3O_2CPh$[11] were prepared as per the literature. All solvents were dried by common methods and freshly distilled. The NMR samples used in the following experiments were prepared from stock solutions of $IrH_2(PMe_3)_3Cl$ in either D_2O (km184) or HPLC grade H_2O (km181) freshly distilled under argon. Prior to introduction of the samples, NMR tubes were pre-rinsed with distilled water and dried at 373 K overnight. These precautions were deemed necessary to insure elimination of trace impurities interfering with the equilibrium systems, especially at the lower concentrations. NMR samples were prepared under argon or nitrogen atmospheres. ^{31}P and ^{1}H NMR spectra were obtained on a Bruker WP 200MHz spectrometer. Signals were referenced to 85% H_3PO_4 (δ 0 ppm) in a sealed capillary tube contained in the sample NMR tube. The probe temperature was 300 K, unless otherwise noted. The samples were allowed to equilibrate at the probe temperature for 10 minutes before starting acquisitions. Acquisitions were run for 512 scans to achieve reasonable S/N ratios.

Synthesis of $Ir(H)_2(PMe_3)_3Cl$ (**1**) (km158)

A 50.0 mL two-necked flask, equipped with a magnetic stir bar and septa, was charged with 1.00 g (1.77 mmol) of $[Ir(COD)(PMe_3)_3]Cl$ under nitrogen. The flask was fitted with a reflux condenser with nitrogen inlet and connected to a double manifold Schlenk line. 20.0 mL of mesitylene was added by syringe and the suspension was stirred magnetically. H_2 was bubbled through the solution at a slow rate via a glass pipette inserted through one of the septa, then the mixture was immersed in a 353 K oil bath.

Upon heating the clear solution turned yellow and the majority of solids dissolved. After three hours the solution was cooled to ambient temperature and filtered to give a grey/white precipitate and a clear yellow solution. The grey/white precipitate was identified by ^{31}P and ^{1}H NMR to be $[Ir(H)_2(PMe_3)_4]Cl$. The solvent was removed from the filtrate under reduced pressure to give a pale yellow solid. The solid was dissolved in 0.5 mL of methylene chloride and then 10.0 mL of ether was added. The solution was again filtered and the solvent removed from the filtrate under reduced pressure yielding 0.59 g (1.29 mmol, 73 % yield) of pure (**1**).

^{1}H NMR (CD_2Cl_2): δ -24.0 ppm (m, J_{HP} = 12.0 Hz, J_{HH} = 4.8 Hz, 1H), −11.4 ppm (dtd, $J_{HPtrans}$ = 136.0 Hz, J_{HPcis} = 22.3 Hz, J_{HH} = 5.2 Hz, 1H), 1.55 (d, J_{HP} = 11.1 Hz, 9H of cis PMe_3), 1.63 (t, J_{HP} = 4.8 Hz, 18H of trans PMe_3).

^{31}P NMR (CD_2Cl_2): δ -49.3 ppm (t, J_{PP} = 54.2 Hz,2 P of cis PMe_3), -43.6 ppm (d, J_{PP} = 55.0 Hz, 1 P of trans PMe_3).

Synthesis of $Ir(H)_2(PMe_3)_3(CO_2Ph)$ (**3**)

A 50.0 mL two-necked flask equipped with a magnetic stir bar and septa, was charged with 1.00 g (1.62 mmol) of $[Ir(COD)(PMe_3)_3](O_2CPh)$ under nitrogen. The flask was fitted with a reflux condenser with nitrogen inlet and connected to a double manifold Schlenk line. 20.0 mL of mesitylene was added by syringe and the suspension was stirred magnetically. H_2 was bubbled through the solution at a slow rate via a glass pipette inserted through one of the septa. The mixture was then immersed in a 353 K oil bath. Upon heating the solids dissolved and the solution turned clear yellow. After three

hours the solvent was removed under reduced pressure to giving a pale yellow solid. The solid was dissolved in 0.5 mL of methylene chloride and then 10.0 mL of ether was added. The solution was filtered and the solvent removed from the filtrate under reduced pressure yielding 0.57 g (1.05 mmol, 68 % yield) of pure (**3**).

^{1}H NMR (CD_2Cl_2): δ -26.4 ppm (m, J_{H-P} = 12.1 Hz, J_{H-H} = 5.4 Hz, 1H), δ −10.6 ppm (dtd, $J_{H-Ptrans}$ = 134.2 Hz, J_{H-Pcis} = 22.5 Hz, J_{H-H} = 5.3 Hz, 1H), δ 1.55 (d, J_{H-P} = 8.3 Hz, 9H of cis PMe_3), δ 1.60 (t, J_{H-P} = 4.2 Hz, 18H of trans PMe_3). δ 7.1 -7.3 ppm (m, 3H of phenyl ring), δ 7.85 - 7.9 ppm (m, 2H of phenyl ring).

^{31}P NMR (CD_2Cl_2): δ -44.7 ppm (t, J_{P-P} = 20.9 Hz, 1P of trans PMe_3), δ -40.4 ppm (d, J_{P-P} = 20.6 Hz, 2P of cis PMe_3).

Variable Concentration ^{31}P NMR of $IrH_2(PMe_3)_3Cl$ (**1**) in H_2O (km181)

A 0.065 M aqueous solution of (**1**) was prepared by charging a septum bottle equipped with a magnetic stir bar with 0.089g (0.194 mmol) of $IrH_2(PMe_3)_3Cl$, sealing under nitrogen in a glove box, and adding 3.0 mL of H_2O by syringe. The mixture was stirred until the solution became homogeneous. Sample NMR tubes were flushed and sealed under argon with septa. The samples were prepared by adding reagents by syringe in the quantities listed below. ^{31}P NMR spectra were acquired as per above and integration values determined.

sample	0.065 M (**1**) (μL)	H_2O (μL)	M_{final}
A	400	0	0.071
B	340	60	0.060
C	300	100	0.053
D	260	140	0.046
E	200	200	0.035
F	140	260	0.025
G	85	315	0.015
H	30	370	0.005

sample	0.065 M (**1**) (mL)	H_2O (mL)	M_{final}
A	400	0	0.065
B	30	370	0.005
C	90	310	0.015
D	150	250	0.024
E	220	180	0.036
F	280	120	0.046
G	340	60	0.053
H	370	30	0.060

Variable Concentration ^{31}P NMR of $IrH_2(PMe_3)_3Cl$ (**1**) in D_2O (km184)

A 0.071 M solution of (**1**) was prepared by charging a septum bottle equipped with a magnetic stir bar with 0.097g (0.212 mmol) of $IrH_2(PMe_3)_3Cl$, sealing under nitrogen in a glove box, and adding 3.0 mL of D_2O by syringe. The mixture was stirred until the solution became homogeneous. Sample NMR tubes were flushed and sealed under argon with septa. The samples were prepared by adding reagents by syringe in the quantities listed below. ^{31}P NMR spectra were acquired as per above and integration values determined.

Variable Temperature ^{31}P NMR of $IrH_2(PMe_3)_3Cl$ (**1**) in H_2O (km188)

Sample A prepared from experiment km181 was utilized in this experiment. ^{31}P NMR spectra were acquired as per above at the temperatures indicated and integration values determined. 310 K was not exceeded to avoid decomposition. The first spectrum was acquired at 300 K and used as a reference spectrum. The temperature was incrementally lowered by 5 K, the temperature of the sample allowed to equilibrate, and then data was acquired, and the whole process repeated down 280 K. The probe was then slowly warmed to 300 K, the sample allowed to equilibrate, and then data acquired. This spectrum was checked against the reference spectrum to insure that no decomposition had occurred. The temperature was then incrementally increased by 5 K, the temperature of the sample allowed to equilibrate, and then data was acquired, and the whole process repeated until 310 K. The probe was slowly cooled to 300 K, the sample allowed to equilibrate, and then data acquired. This spectrum was again checked against the reference spectrum to insure that no decomposition had occurred.

Trial	Temperature (K)
1	280
2	285
3	290
4	295
5	300
6	305
7	310

Variable Temperature ^{31}P NMR of $IrH_2(PMe_3)_3Cl$ (**1**) in D_2O (km189)

Sample A prepared from experiment km184 was used in this experiment. ^{31}P NMR spectra were acquired as per above at the temperatures indicated and integration values determined. A temperature of 310 K was not exceeded to avoid decomposition. The first spectrum was acquired at 300 K and used as a reference spectrum. The

temperature was incrementally lowered by 5 K, the temperature of the sample allowed to equilibrate, and then data was acquired, and the whole process repeated until 280 K. The probe was then slowly warmed to 300 K, the temperature of the sample allowed to equilibrate, and then data acquired. This spectrum was checked against the reference spectrum to insure that no decomposition had occurred. The temperature was then incrementally increased by 5 K, the temperature of the sample allowed to equilibrate, and then data was acquired, and the whole process repeated until 310 K. The probe was slowly cooled to 300 K, the temperature of the sample allowed to equilibrate, and then data acquired. This spectrum was again checked against the reference spectrum to insure that no decomposition had occurred.

Trial	Temperature (K)
1	280
2	285
3	290
4	295
5	300
6	305
7	310

Variable [Cl^-] Equivalents added to Constant (**1**) Concentration ^{31}P NMR Study (km196)

A 0.050 M solution of (**1**) was prepared by charging a septum bottle equipped with a magnetic stir bar with 0.068 g (0.149 mmol) of $IrH_2(PMe_3)_3Cl$, sealing under nitrogen in a glove box, and adding 3.0 mL of D_2O by syringe. The mixture was stirred until the solution became homogeneous. A 0.93 M solution of KCl was prepared by charging a septum bottle equipped with magnetic stir bar with 0.090 g KCl and adding 1.3 mL of D_2O by syringe under similar conditions. Sample NMR tubes were flushed and sealed under argon with septa. The samples were prepared by adding reagents by syringe in the

quantities listed below. ^{31}P NMR spectra were acquired as per above and integration values determined.

Sample	0.050 M (**1**) (μL)	0.93 M KCl (μL)	Equivalents of Cl^-
A	400	0	0
B	400	2.2	0.10
C	400	5.3	0.25
D	400	10.7	0.50

Variable Concentration ^{31}P NMR of $IrH_2(PMe_3)_3(O_2CPh)$ (**3**) and Chloride ion in H_2O (km191)

A 0.054 M solution of (**3**) was prepared by charging a septum bottle equipped with a magnetic stir bar with 0.088g (0.162 mmol) of $IrH_2(PMe_3)_3(O_2CPh)$, sealing under nitrogen in a glove box, and adding 3.0 mL of H_2O by syringe. The mixture was stirred until the solution became homogeneous to give a. Sample NMR tubes were flushed and sealed under argon with a septum. A 0.486 M NaCl aqueous was prepared by dissolving 0.0852 g of NaCl in 3.0 mL of H_2O under similar conditions. The samples were prepared by adding reagents by syringe in the quantities listed below. ^{31}P NMR spectra were acquired as per above and integration values determined.

Trial	0.054 M (**3**) (μL)	0.486 M NaCl (μL)	Equivalents of Cl^-
A	400	22.2	0.5
B	400	44.4	1.0
C	400	66.7	1.5

Chapter 5 - Related Iridium Dihydride Complexes

Introduction

Having determined that $IrH_2(PMe_3)_3Cl$ (**1**) and $IrH_2(PMe_3)_3O_2CPh$ (**3**) were both water soluble, active catalysts for the hydrogenation of unsaturates, it was decided to synthesize other iridium dihydrides of the general type, $IrH_2(PMe_3)_3X$, to see if water solubility and catalytic capabilities extended to the whole class of iridium (III) dihydrido tristrimethylphosphine complexes. Le had previously synthesized $IrH_2(PMe_3)_3I$ (**4**) and $[IrH_2(PMe_3)_3(py)]PF_6$ (**5**)[11] and found that (**4**) and (**5**) were only very slightly soluble in water. (**5**) was found to be catalytically active in CH_2Cl_2.

This chapter contains the synthesis, isolation, and characterization of $IrH_2(PMe_3)_3Br$ (**6**), the attempted synthesis and isolation of $IrH_2(PMe3)_3F$, the attempted trapping of $[IrH_2(PMe_3)_3(OH_2)]^+$, various new reactions with (**1**) and (**3**), and a discussion of the NMR chemical shift trends of the iridium dihydride complexes.

$IrH_2(PMe_3)_3I$

As mentioned earlier, Le synthesized $IrH_2(PMe_3)_3I$ (**4**) by adding KI to an aqueous solution of $IrH_2(PMe_3)_3Cl$ (**1**). Sample spectra of this complex in CD_2Cl_2 are presented in Figure 5.1. The resulting pure $IrH_2(PMe_3)_3I$ is almost totally insoluble in water and hence was completely useless as a water soluble hydrogenation catalyst. However, the fact that

(**4**) is not water soluble does start to define some of the limitations of these iridium dihydride systems. Solubility of these complexes will be based primarily upon two factors — metal–halide bond strength and the solubilities of the ions formed by breaking of the metal–halide bond. The first issue can be addressed by applying the tenets of Pearson's hard-soft/acid-base theory[99] that was introduced earlier. The appreciable lower solubility of $IrH_2(PMe_3)_3I$ (**4**) versus $IrH_2(PMe_3)_3Cl$ (**1**) is quite easily explained by assuming the "softer" iodide ligand will form a stronger bond with the relatively "soft" iridium metal center than will the "harder" chloride ion. The stronger Ir–I bond will be less likely to dissociate than an Ir–Cl bond.

Secondly, since an equilibrium between the original iridium halide and an "aquated" complex has been indicated by the research presented in Chapter 4 of this thesis, the relative solubilities of the ions in aqueous solution are also important. For complexes **1** and **4**, the cationic complex formed, in both cases, by dissolution will be $IrH_2(PMe_3)_3^+$, the anions Cl^- and I^-, respectively. Obviously there is no cationic solubility difference, but

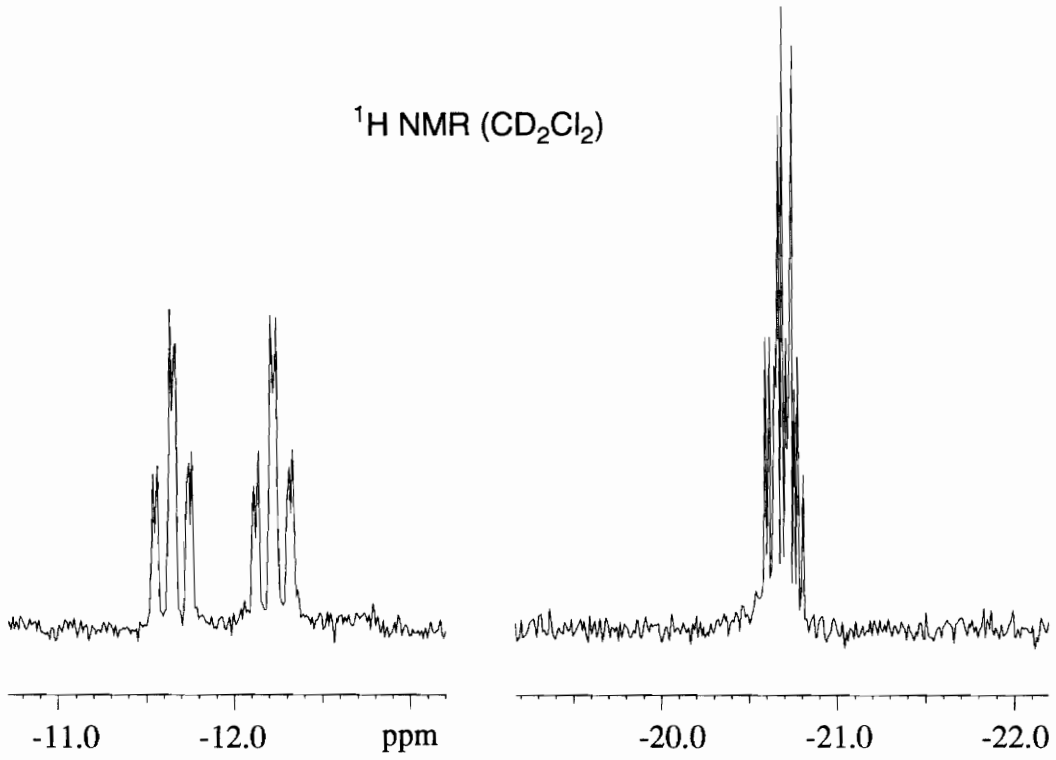

Figure 5.1 ^{1}H NMR (CD_2Cl_2) of $IrH_2(PMe_3)_3I$ (**4**)

Cl^- is more soluble than I^- (the standard molar ion hydration energies (kJ/mol) for F^-, Cl^-, Br^-, and I^- are -506, -364, -337, and -296, respectively)[106]. Thus the two factors would appear to be working in concert with each other. As the halide ligand is changed from I^- to Cl^-, not only should the Ir–X bond become weaker, allowing more dissolution, but the resulting anions should become more soluble. If these assumptions are correct, "harder" ligands should result in weaker Ir–ligand bonds and more water-soluble complexes. In this vein, syntheses of the complexes $IrH_2(PMe_3)_3Br$, with a ligand of intermediate "softness", and $IrH_2(PMe_3)_3F$, with a very "hard" ligand were attempted.

$IrH_2(PMe_3)_3Br$

$IrH_2(PMe_3)_3Br$ (**6**) was synthesized in the same manner as $IrH_2(PMe_3)_3I$ (**4**). $IrH_2(PMe_3)_3Cl$ (**1**) was dissolved in water and excess KBr was added to the aqueous solution. The solvent was evaporated and the residue extracted with CH_2Cl_2 to give pure (**6**) in quantitative yields (km241). This complex was determined to be only very slightly soluble in water. ^1H NMR and ^{31}P NMR of (**6**) in CD_2Cl_2 are illustrated in Figure 5.2. ^1H NMR of (**6**) in D_2O showed only the familiar methyl region peaks. It must be assumed the limited solubility of the complex prevented the viewing of the inherently faint hydride peaks. ^{31}P NMR of (**6**) in D_2O was only slightly more revealing. The signal-to-noise ratio was very poor, preventing any quantitative measurements, but major and minor sets of doublet and triplet peaks were evident. The chemical shifts of the minor product in the ^{31}P NMR spectrum again corresponded to the chemical shifts of the minor product in the spectrum of $IrH_2(PMe_3)_3Cl$ in H_2O and to the chemical shifts of the only product of $IrH_2(PMe_3)_3O_2CPh$ in H_2O.

It is quite obvious by the signal/noise ratio of the spectrum of $IrH_2(PMe_3)_3Br$ in H_2O, the overall concentration of the $IrH_2(PMe_3)_3Br$ species in aqueous solution is lower

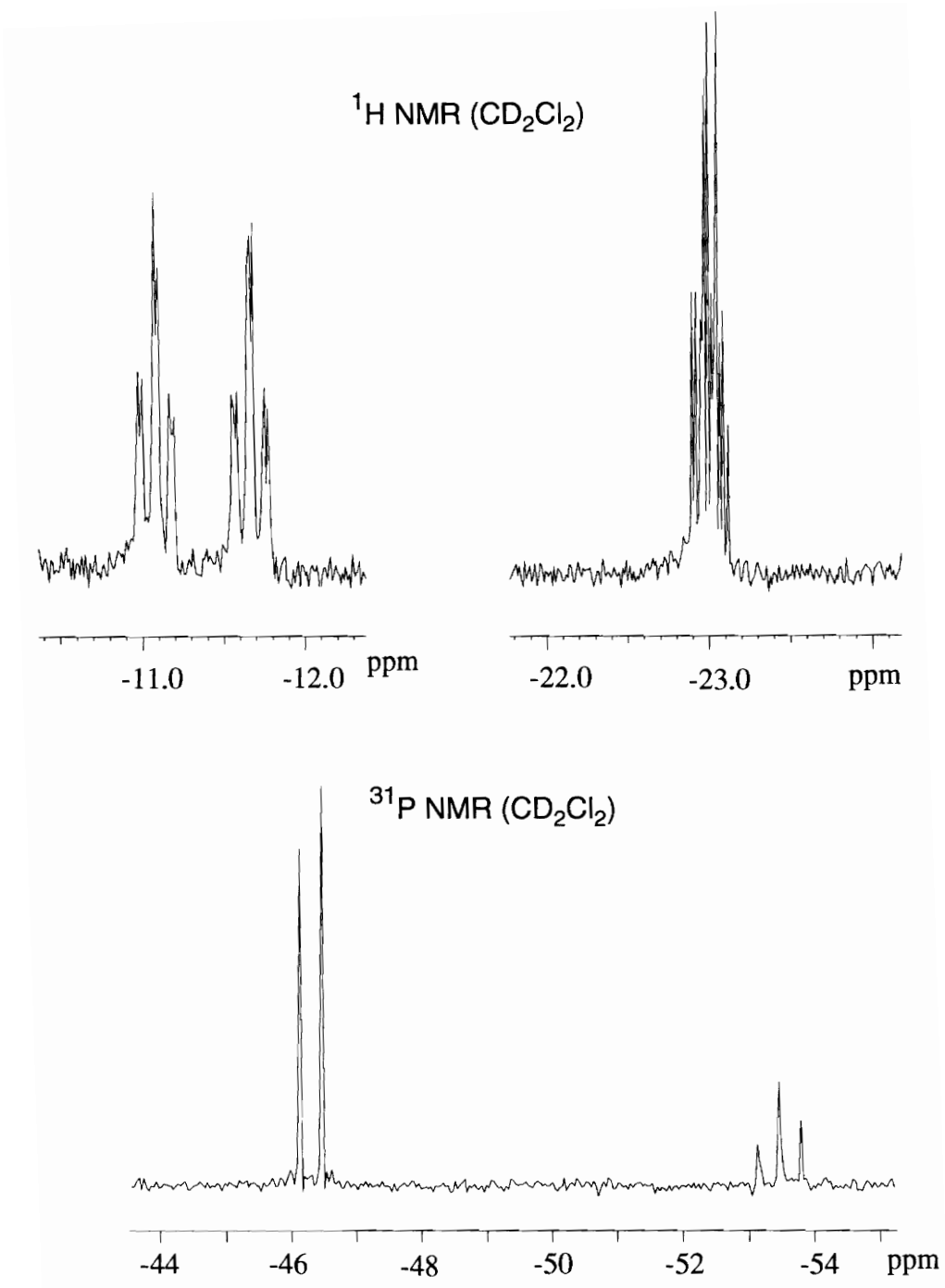

Figure 5.2 ^{1}H NMR and ^{31}P NMR (CD_2Cl_2) of $IrH_2(PMe_3)_3Br$ (**6**)

than that obtained with $IrH_2(PMe_3)_3Cl$. This result corresponds to the earlier assumption that the solubility of these iridium dihydride complexes is very likely controlled by the strength of the Ir-X bond. Theoretically, bromide is a "softer" ligand than chloride, but "harder" than iodide, thus the strength of the Ir-Br bond should be intermediate between that of Ir-Cl and Ir-I, ultimately leading to intermediate water solubility of the $IrH_2(PMe_3)_3Br$ complex, as appears to be the case. Given the encouraging support of the operating assumption, the synthesis of $IrH_2(PMe_3)_3F$, an iridium dihydride with a "hard" ligand, was attempted.

Attempts to Synthesize $IrH_2(PMe_3)_3F$

Multiple synthetic strategies were used in the attempted synthesis of $IrH_2(PMe_3)_3F$. Unfortunately, none was successful. The strategy of adding a soluble potassium fluoride salt to an aqueous solution $IrH_2(PMe_3)_3Cl$ (**1**), similar to the strategy used to synthesize $IrH_2(PMe_3)_3Br$ and $IrH_2(PMe_3)_3I$, would not work in this instance because of the greater strength of the Ir-Cl bond versus Ir-F. The strategies involved utilizing thallium and silver fluoride salts in various solvents systems, in which the thallium or silver ions would hopefully act as chloride scavengers by forming insoluble metal-chloride salts, leaving excess fluoride ion in solution. In all cases, either there was no obvious change

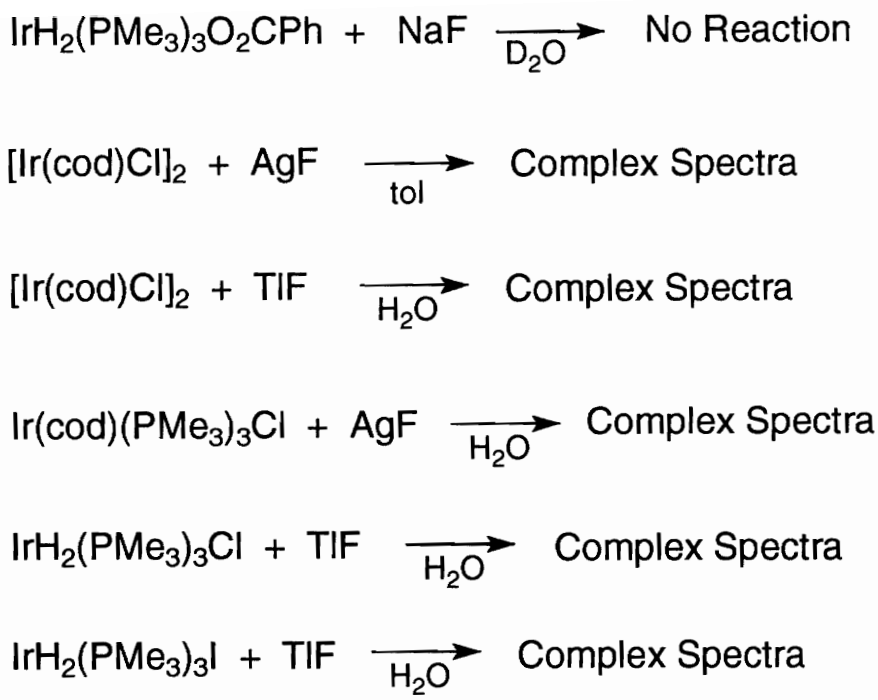

Figure 5.3 Attempts to Synthesize $IrH_2(PMe_3)_3F$

in the spectra of the product versus the starting materials or the spectra were so ambiguous or complex as to make analysis impossible. In all cases, attempts to isolate single, pure products were unsuccessful. A review of these attempts is presented in Figure 5.3. It is quite possible, at least for those attempts when silver salts were used, some of the ambiguity of the spectra may be due to the formation of silver(I) diiridium polyhydride complexes similar to those described by Caulton.[102] In the other syntheses it can only be assumed the fluoride ion is so "hard" as to prevent formation of a stable complex with the iridium metal center.

Attempts to Isolate $[IrH_2(PMe_3)_3(H_2O)]^+$

The isolation of $[IrH_2(PMe_3)_3(H_2O)]^+$ was attempted to further substantiate the hypothesis that $[IrH_2(PMe_3)_3(H_2O)]^+$ is the second species involved in the aqueous equilibrium of $IrH_2(PMe_3)_3Cl$. The isolation attempts fell into two categories: One, the addition of water soluble counterions to aqueous solutions of $IrH_2(PMe_3)_3O_2CPh$ (Figure 5.4) , or two, the addition of counterions to aqueous solutions of iridium dihydride halides in the presence of halide scavengers (Figure 5.5). In all cases a reaction took place, but characterization of the specific products was impossible.

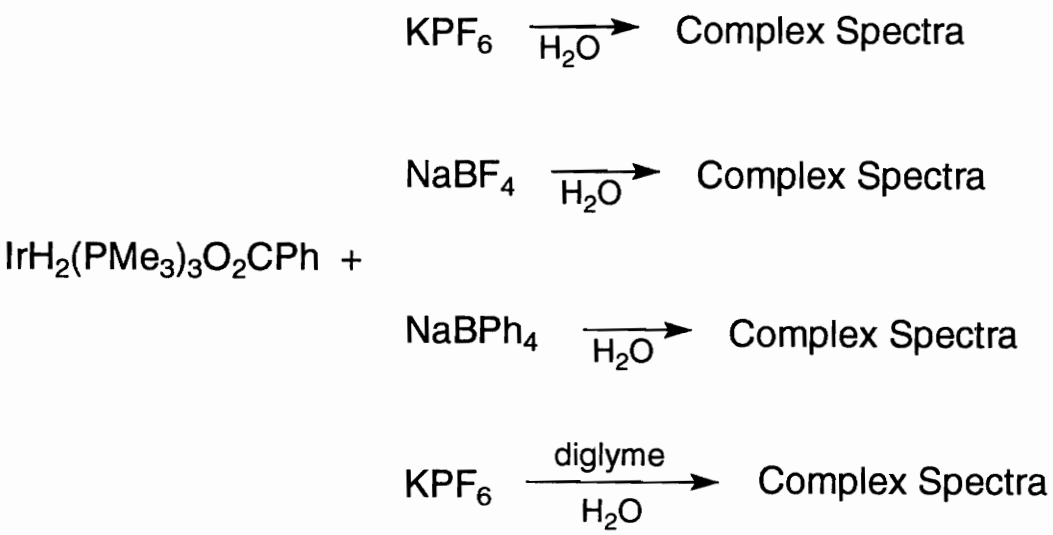

Figure 5.4 Attempted Isolation of $[IrH_2(PMe_3)_3(H_2O)]^+$ with Counterions

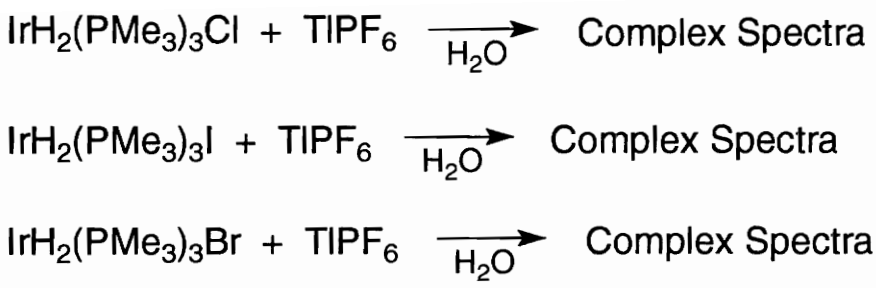

Figure 5.5 Attempted Isolation of $[IrH_2(PMe_3)_3(H_2O)]^+$ with Counterions in the resence of Halide Scavengers

NMR Trends of the Iridium Dihydrides

While reviewing ^1H NMR data a trend was noticed in the chemical shifts of the hydrides. The doublet of triplet of doublets due to the hydride trans to the phosphine group shifted downfield as the ligand in the sixth coordination site was changed from I^- to Br^- to Cl^-. Manipulation of the data found plotting of the chemical shift of the trans hydride versus electronegativity of the ligand atom bonded to the iridium center yielded a linear relationship. Upon this discovery, the chemical shifts of the cis hydride and the phosphines were also plotted against electronegativity. The data for this are in Table 5.1 and Figure 5.6..

Analysis of the plot reveals some interesting trends. As the ligand, **X**, becomes more electronegative the chemical shifts of the hydride cis to the ligand **X** and the phosphines all shift downfield, corresponding to a greater withdrawal of electron density from the metal center onto the more electronegative ligand, thus deshielding these ligands. However, the chemical shift of the hydride trans to **X** displays an opposite effect. This cannot be explained in terms of electronegativity, otherwise a downfield shift similar to the cis hydride and the phosphines would be expected. The chemical shift behaviour of the

trans hydride can be rationalized as some sort of "trans effect", although the specific mechanism of the effect is not clear.

In 1971 Birnbaum[105] described similar results in a study of the hydride shifts of monohydrido halo transition metal complexes. He observed that the chemical shift of a hydride *trans* to the halide decreased in the order $Cl^- > Br > I^-$, while the chemical shifts of the hydride *cis* to the halide increased in the order $Cl^- < Br^- < I^-$. These experimental results were exactly the opposite of the trends theoretically predicted by Buckingham and Stevens in 1964. Birnbaum attributed this to an increase in the covalent character of the complexes in the order $Cl^- < Br^- < I^-$.

Interestingly enough, the one ligand that shows fairly poor correlation of its chemical shifts versus electronegativity is also the only ligand to be bonded to the iridium through an aromatic system. Analysis of the hydride shifts of $[IrH_2(PMe_3)_3(py)]PF_6$ would indicate the nitrogen of pyridine is a poorer σ–donor, than say alkylated amines, but at the same time it is also a poorer π-donor. This follows if the lone pair of nitrogen in pyridine is tied up in the aromaticity of the ring. It will be less available for σ–donation and there will be less π-donation from the aromatic p orbitals.

Table 5.1 Ligand Chemical Shifts of $IrH_2(PMe_3)_3X$ in CD_2Cl_2

X	∈	H_{cis}	H_{trans}	$P_{downfield}$	$P_{upfield}$
O_2CPh	3.4	-10.6	-26.4	-40.4	-44.7
Cl	3.2	-11.4	-24.0	-43.6	-49.3
Br	3.0	-11.3	-23.0	-45.8	-52.8
NC_5H_5	3.0	-10.7	-23.6	-	-
I	2.7	-12.1	-20.8	-51.6	-60.9

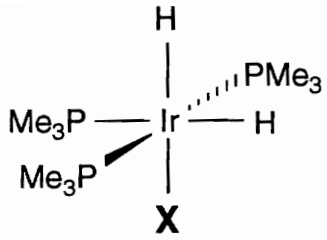

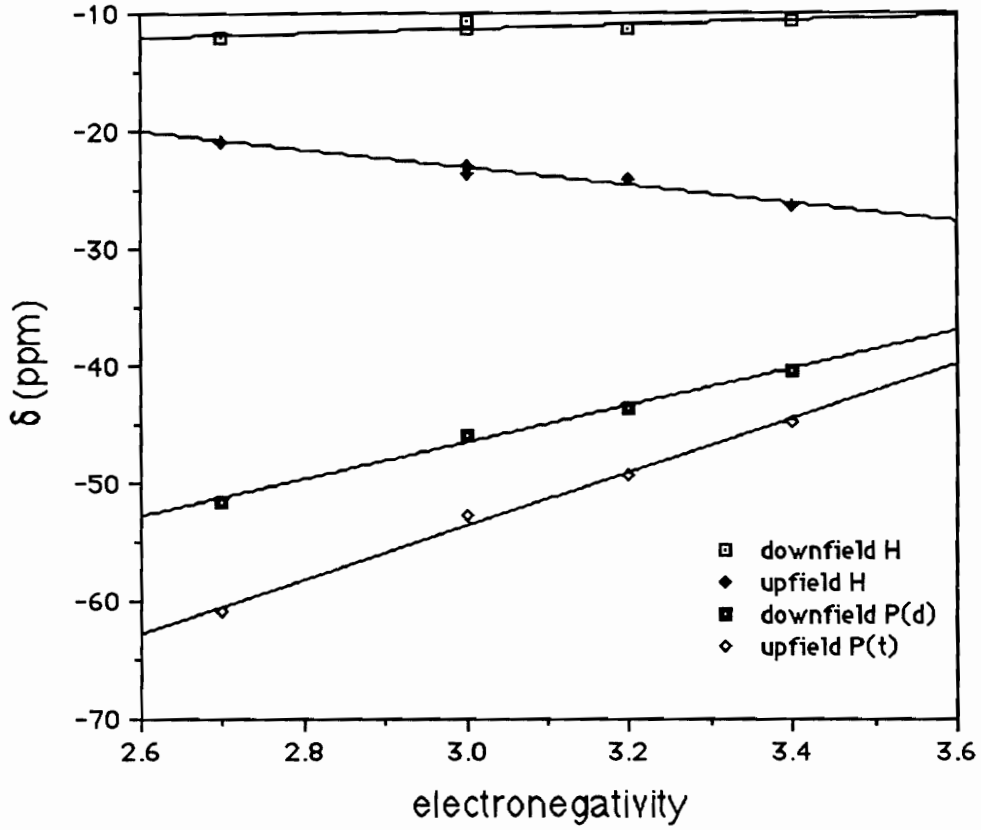

Figure 5.6 Plot of Chemical Shifts vs Electronegativity of $IrH_2(PMe_3)_3\mathbf{X}$ in CD_2Cl_2

A plot of chemical shifts of $IrH_2(PMe_3)_3\mathbf{X}$ versus electronegativity in D_2O shows similar behavior (Figure 5.8 and Table 5.2).

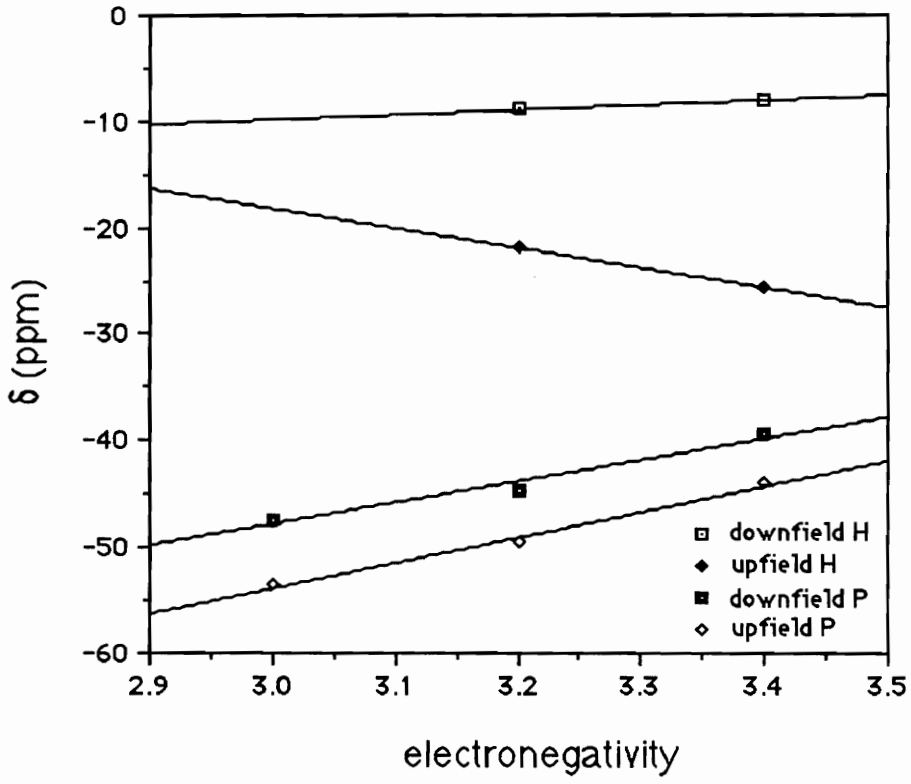

Figure 5.7 Plot of Chemical Shifts vs Electronegativity of $IrH_2(PMe_3)_3X$ in D_2O

Table 5.2 Ligand Chemical Shifts of $IrH_2(PMe_3)_3X$ in D_2O

X	∈	H_{cis}	H_{trans}	$P_{downfield}$	$P_{upfield}$
O_2CPh	3.4	-8.0	-25.5	-39.5	-44.0
Cl	3.2	-8.9	-21.8	-44.7	-49.5
Br	3.0	-	-	-47.4	-53.5

Specific chemical shift data on a similar complex was found in the research of Eisenberg, *et. al.*, [103,104] on iridium dihydrides formed by hydrogenation of Ir(CO)(dppe)X (X = Cl, Br, I).

It is obvious from the plot of chemical shifts versus electronegativity of ligand X in Eisenberg's complexes, and from Birnbaum's studies that this is not an isolated phenomenon.

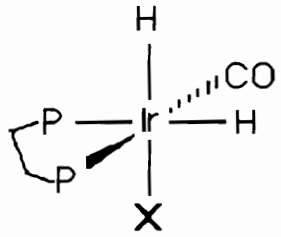

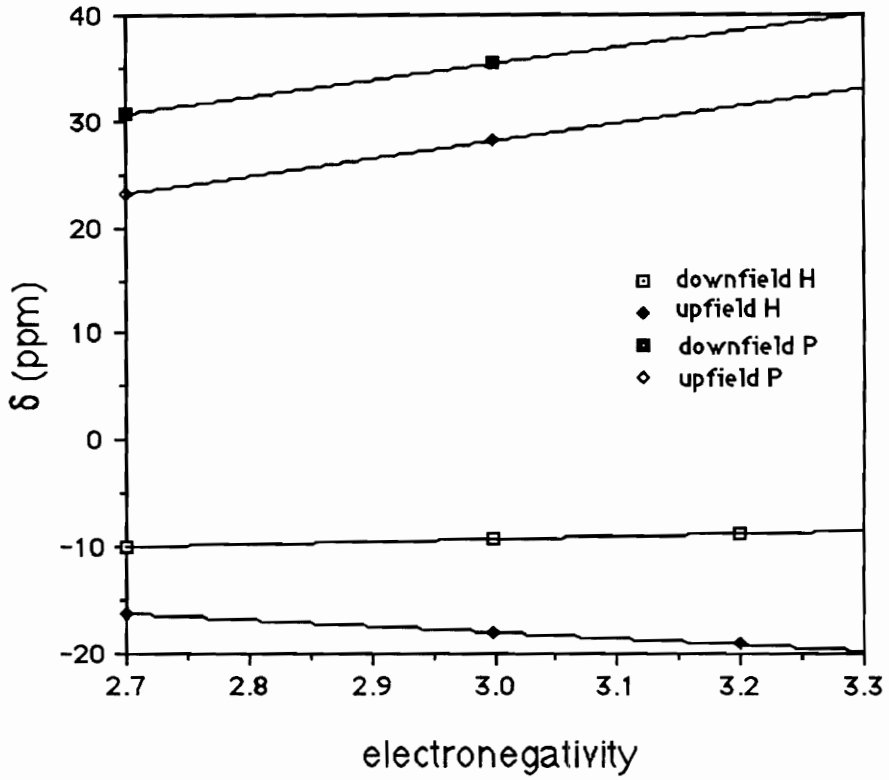

Figure 5.8 Plot of Chemical Shifts vs Electronegativity of $IrH_2(CO)(P\text{-}P)\mathbf{X}$

Experimental

Standard Schlenk techniques were employed. All solvents were dried and distilled by common methods under either nitrogen or argon. All NMR spectra were acquired on a Bruker WP200 spectrometer. ^{1}H NMR chemical shifts were referenced versus TMS (δ 0.0 ppm) and ^{31}P NMR chemical shifts were referenced versus 85% H_3PO_4 (δ 0.0 ppm). All spectral data were accumulated at 300 K, unless otherwise noted. KBr, KI, $TlPF_6$, KPF_6, HBF_4, and diglyme were obtained from Aldrich and used as received without further purification. $IrH_2(PMe_3)_3I$ (**4**) was prepared according to the literature.[11]

Synthesis of $IrH_2(PMe_3)_3I$ (**4**)

A sidearm flask equipped with septa and stirrer was charged with (**1**) (0.25 g, 0.55 mmol) under nitrogen. 10.0 mL of water was added by syringe and the solution stirred until homogeneous. Excess KI (0.91 g, 5.5 mmol) was added and a white precipitate immediately formed, while the solution was stirred for 1 h. The solvent was removed under reduced pressure and the residue extracted with 2 x 5 mL of CH_2Cl_2 to give pure (**4**) as a white powder.

^{1}H NMR (CD_2Cl_2): δ –20.8 ppm (m, 1 H), -11.3 (dtd, $J_{HPtrans}$ = 132.2 Hz, J_{HPcis} = 21.9 Hz, J_{HHcis} = 5.2 Hz, 1 H), 1.6 (d, J_{HP} = 7.8 Hz, 9 H of cis PMe_3), 1.72 (t, J_{HP} = 3.4 Hz, 18 H of trans PMe_3).

^{31}P NMR (CD_2Cl_2): δ -60.9 ppm (t, J_{PP} = 53.0 Hz, cis PMe_3), –51.5 (d, J_{PP} = 54.0 Hz, trans PMe_3).

Synthesis of $IrH_2(PMe_3)_3Br$ (**6**) (km241)

A sidearm flask equipped with septa and stirrer was charged with (**1**) (0.25 g, 0.55 mmol) under nitrogen. 10.0 mL of H_2O was added by syringe and the solution stirred until homogeneous. Excess KBr (0.65 g, 5.5 mmol) was added and a white precipitate immediately formed, while the solution was stirred for 1 h. The solvent was removed under reduced pressure and the residue extracted with 2 x 5 mL of CH_2Cl_2 to give pure (**6**), (0.23 g, 85%), as a white powder. Analysis - found (calc'd): C, 21.80 (21.5); H, 5.81 (5.87).

^{1}H NMR (CD_2Cl_2): δ –23.0 ppm (m, 1 H), -11.3 (dtd, $J_{HPtrans}$ = 134 Hz, J_{HPcis} = 22.3 Hz, J_{HHcis} = 5.1 Hz, 1 H), 1.50 (d, J_{HP} = 7.3 Hz, 9 H of cis PMe_3), 1.65 (t, J_{HP} = 5.7 Hz, 18 H of trans PMe_3).

^{31}P NMR (CD_2Cl_2): δ -53.7 ppm (t, J_{PP} = 62.1 Hz, cis PMe_3), –46.7 (d, J_{PP} = 54.1 Hz, trans PMe_3).

^{31}P NMR (H_2O): major product δ –53.4 ppm (t, J_{pp} = 48.1 Hz, cis PMe_3), -47.3 (d, J_{PP} = 55.0 Hz, trans PMe_3); minor product δ –44.0 ppm (t, cis PMe_3), -39.5 (d, J_{pp} = 54.4 Hz, trans PMe_3)

Reaction of $IrH_2(PMe_3)_3O_2CPh$ and NaF (km213)

A screwtop NMR tube equipped with septa was charged with (**3**) (0.013 g, 0.024 mmol) and NaF (0.001 g, 0.024 mmol) under nitrogen. 1.0 mL of D_2O was added by syringe and the tube shaken until homogeneous.

^{31}P NMR spectra of the solution was identical to that of starting material,

(**3**).Reaction of $[Ir(cod)Cl]_2$ and AgF (km207)

A sidearm flask equipped with septa and stirrer was charged with $[Ir(cod)Cl]_2$ (0.134 g, 0.20 mmol) and AgF (0.10 g, 0.80 mmol) under nitrogen. 10 mL of toluene was added and the solution stirred for 36 h in the absence of light, resulting in a black solution and a red precipitate. ^1H NMR (CD_2Cl_2) of the red ppt indicated it was $[Ir(cod)Cl]_2$. The solvent was removed from the black solution to yield a light green powder.

^1H NMR and ^{31}P NMR (CD_2Cl_2) of the green powder were inconclusive.

Reaction of $Ir(cod)(PMe_3)_3Cl$ and AgF (km211)

A sidearm flask equipped with septa and stirrer was charged with $Ir(cod)(PMe_3)_3Cl$ (0.10 g, 0.18 mmol) and AgF (0.025 g, 0.20 mmol) under nitrogen. 10 mL of H_2O was added by syringe. The solution stirred for 24 h in the absence of light, and changed from a black to grey solution. The solvent was evaporated and the residue extracted with CD_2Cl_2.

^1H NMR and ^{31}P NMR (CD_2Cl_2) were inconclusive, but did indicate a reaction had taken place, eliminating all $Ir(cod)(PMe_3)_3Cl$.

Reaction of (km211) and H_2 (km215)

A 50.0 mL two-necked flask, equipped with a magnetic stir bar and septa, was charged with 0.2 g of the CH_2Cl_2 extract from km211 under nitrogen in a dry box. The flask was fitted with a reflux condenser with nitrogen inlet then connected to a double manifold Schlenk line. 20.0 mL of mesitylene was added by syringe and the suspension was stirred magnetically. H_2 was bubbled through the solution at a slow rate via a glass pipette inserted through one of the septa, then the mixture was immersed in a 80 C oil bath. After three hours the solution was cooled and filtered. The solvent was removed under reduced pressure and the residue analyzed by ^1H NMR and ^{31}P NMR (CD_2Cl_2).

The spectra were inconclusive. Some starting material remained but new peaks were evident. Attempts to purify this material were unsuccessful.

Reaction of Ir(cod)$(PMe_3)_3$Cl and TlF (km218)

A sidearm flask equipped with septa and stirrer was charged with Ir(cod)$(PMe_3)_3$Cl (1.04 g, 1.85 mmol) and TlF (0.45 g, 2.03 mmol) under nitrogen. 20 mL of H_2O was added by syringe. A fine cream colored precipitate formed immediately as the solution stirred for 24 h. The solution was filtered and the solvent evaporated yielding 0.92 g of a dark brown precipitate.

^1H NMR and ^{31}P NMR (CD_2Cl_2) were inconclusive, but did indicate a reaction had taken place, eliminating all Ir(cod)$(PMe_3)_3$Cl.

Reaction of $IrH_2(PMe_3)_3$Cl and TlF (km219)

A sidearm flask equipped with septa and stirrer was charged with $IrH_2(PMe_3)_3$Cl (0.10 g, 0.22 mmol) and TlF (0.0250 g, 0.24 mmol) under nitrogen. 10 mL of H_2O was

added by syringe and the solution was stirred for 24 h. The solution was filtered and the solvent was evaporated under reduced pressure.

^{1}H NMR and ^{31}P NMR (CD_2Cl_2) spectra of the residue were inconclusive, but did indicate a reaction had taken place.

Reaction of $IrH_2(PMe_3)_3I$ and TlF (km247)

A screwtop NMR tube equipped with septa was charged with a small amount of $IrH_2(PMe_3)_3I$ under nitrogen. 1.0 mL of d^6-acetone was added by syringe and the solution shaken until homogeneous. A solution of TlF in D_2O was added by syringe and the tube shaken. A precipitate formed immediately. The mixture was centrifuged and the solution analyzed by NMR.

^{31}P NMR (CD_2Cl_2) spectra was inconclusive.

Reaction of $IrH_2(PMe_3)_3Cl$ and $TlPF_6$ (km244)

An aqueous solution of $IrH_2(PMe_3)_3Cl$ was prepared and slowly added to a saturated aqueous solution of $TlPF_6$, until a precipitate formed. The solution was filtered and the precipitate dried.

^{31}P NMR (CD_2Cl_2) spectra of the precipitate was inconclusive.

Reaction of $IrH_2(PMe_3)_3I$ and $TlPF_6$ (km245)

A screwtop NMR tube equipped with septa was charged with a small amount of $IrH_2(PMe_3)_3I$ under nitrogen. 0.5 mL of d^6-acetone was added by syringe and the solution shaken until homogeneous. A solution of $TlPF_6$ in D_2O was added by syringe

and the tube shaken. A precipitate formed immediately. The mixture was centrifuged and the solution and precipitate separated and analyzed by NMR.

^{31}P NMR spectra of the solution was inconclusive. And ^{31}P NMR (CD_2Cl_2) of the precipitate showed no peaks, and ^{1}H NMR showed no hydride peaks.

Reaction of $IrH_2(PMe_3)_3Br$ and $TlPF_6$ (km246)

A screwtop NMR tube equipped with septa was charged with a small amount of $IrH_2(PMe_3)_3Br$ under nitrogen. 0.5 mL of d^6-acetone was added by syringe and the solution shaken until homogeneous. A solution of $TlPF_6$ in D_2O was added by syringe and the tube shaken. A precipitate formed immediately. The mixture was centrifuged and the solution and precipitate separated and analyzed by NMR.

^{31}P NMR spectra of the solution was inconclusive. And ^{31}P NMR (CD_2Cl_2) of the precipitate showed no peaks, and ^{1}H NMR showed no hydride peak

Reaction of $IrH_2(PMe_3)_3Cl$ and $SnCl_2$ (km166)

A sidearm flask equipped with septa and stirrer was charged with $IrH_2(PMe_3)_3Cl$ (0.212 g, 0.46 mmol) under nitrogen. An excess of a saturated aqueous solution of $SnCl_2$ 10 mL was added by syringe and the solution was stirred for 1 h, during which time a floculent, white precipitate formed The solution was filtered and the solvent was evaporated under reduced pressure.

^{1}H NMR and ^{31}P NMR (CD_2Cl_2) spectra of the residue were inconclusive, but did indicate a reaction had taken place.

Reaction of $IrH_2(PMe_3)_3O_2CPh$ and KPF_6 (km266)

0.4 mL of 0.050 M solution of $IrH_2(PMe_3)_3O_2CPh$ in D_2O was added by syringe to a screwtop NMR tube equipped with septa under nitrogen. 0.1 mL of a 0.050 M solution of KPF_6 in D_2O was added by syringe and the solution shaken forming a yellow precipitate. The mixture was centrifuged and the solution and precipitate separated and analyzed by NMR.

^{31}P NMR spectra of the solution was identical to that of $IrH_2(PMe_3)_3O_2CPh$. ^{31}P NMR (d^6-acetone) of the precipitate indicated only PF_6^- ion, and ^1H NMR showed no hydride peaks.

Reaction of $IrH_2(PMe_3)_3O_2CPh$ and KPF_6 with diglyme (km266a)

0.4 mL of 0.050 M solution of $IrH_2(PMe_3)_3O_2CPh$ in D_2O was added by syringe to a screwtop NMR tube equipped with septa under nitrogen. 10 μL of diglyme and then 0.1 mL of a 0.050 M solution of KPF_6 in D_2O were added by syringe and the solution shaken forming a yellow precipitate. The mixture was centrifuged and the solution and precipitate separated and analyzed by NMR.

^{31}P NMR spectra of the solution was identical to that of $IrH_2(PMe_3)_3O_2CPh$. ^{31}P NMR (d^6-acetone) of the precipitate indicated only PF_6^- ion, and ^1H NMR showed no hydride peaks. There was no obvious difference between the spectra of km166 and km166a.

Reaction of $IrH_2(PMe_3)_3O_2CPh$ and $NaBF_4$ with diglyme (km267)

A sidearm flask equipped with septa and stirrer was charged with $IrH_2(PMe_3)_3O_2CPh$ (0.077 g, 0.14 mmol). 3.0 mL of H_2O was added by syringe and the

solution stirred until homogeneous. Diglyme (0.10 mL, 0.71 mmol) and then $NaBF_4$ (0.13 g, 1.2 mmol) were added and the solution allowed to stir for 1h. The solvent was evaporated and the residue analyzed by NMR.

^1H NMR and ^{31}P NMR (D_2O) spectra of the residue were inconclusive, but did indicate a reaction had taken place, although no hydrides were detected.

Reaction of $IrH_2(PMe_3)_3O_2CPh$ and $NaBPh_4$ with diglyme (km268)

A sidearm flask equipped with septa and stirrer was charged with $IrH_2(PMe_3)_3O_2CPh$ (0.077 g, 0.14 mmol). 3.0 mL of H_2O was added by syringe and the solution stirred until homogeneous. Diglyme (0.10 mL, 0.71 mmol) and then $NaBF_4$ (0.33 g, 0.96 mmol) were added forming an immediate cream colored precipitate. The solution was stirred for 24 h and then filtered to give 0.1 g of a pale precipitate.

^{31}P NMR (CD_2Cl_2) spectra of the precipitate was inconclusive.

Reaction of $IrH_2(PMe_3)_3O_2CPh$ and HBF_4 with diglyme (km269)

A sidearm flask equipped with septa and stirrer was charged with $IrH_2(PMe_3)_3O_2CPh$ (0.077 g, 0.14 mmol). 3.0 mL of H_2O was added by syringe and the solution stirred until homogeneous. Diglyme (0.10 mL, 0.71 mmol) and then $NaBF_4$ (0.33 g, 0.96 mmol) were added forming an immediate cream colored precipitate in a yellow solution. The solution was stirred for 24 h and then filtered to give a pale precipitate.

^{31}P NMR (CD_2Cl_2) spectra of the precipitate was inconclusive.

Chapter 6 - Conclusions and Future Work

$\underline{IrH_2(PMe_3)_3Cl}$

The results of ^{31}P NMR variable concentration studies of $IrH_2(PMe_3)_3Cl$ (**1**) in H_2O and D_2O indicate the aqueous system of (**1**) is an equilibrium system composed of two octahedral mono-iridium species. Both species contain three phosphines in a meridonal arrangement and two hydrides, one of which is trans to the central phosphine, the other is cis to all three phosphines. The arrangements of the two species differ only in the ligand occupying the sixth coordination site. The ligand restrictions of the system dictate that one of these equilibrium species is the original $IrH_2(PMe_3)_3Cl$, while the other is $[IrH_2(PMe_3)_3(H_2O)]^+$. Evidence for the existence of $[IrH_2(PMe_3)_3(H_2O)]^+$ is all circumstantial as $[IrH_2(PMe_3)_3(H_2O)]^+$ has not actually been isolated. The K_{eq} of this equilibrium is $(3.7 \pm 0.3) \times 10^{-3}$ M in H_2O and $(3.2 \pm 0.3) \times 10^{-3}$ M in D_2O. The proposed equilibrium is illustrated below. This equilibrium system correlates well with the observed experimental data that the relative concentrations of the two iridium species of this system are sensitive to added chloride ion. That $[IrH_2(PMe_3)_3(H_2O)]^+$ is the second species fits nicely with the well known concept of solvento complexes being intimately involved with catalytic mechanistic cycles.

Case 4 Equilibrium System

$$IrH_2P_3Cl \rightleftharpoons [IrH_2P_3(OH_2)]^+ + Cl^-$$

Thermodynamic values derived from Van't Hoff plots of ^{31}P NMR variable temperature experiments on (**1**) suggest the equilibrium is enthalpically unfavorable ($\Delta H \approx 31$ KJ/mol), which fits nicely with the proposed equilibrium of $IrH_2(PMe_3)_3Cl$ dissociating in water to form $[IrH_2(PMe_3)_3(H_2O)]^+$ and Cl^-, as the breaking of the higher energy Ir-Cl bond to form the lower energy Ir-O bond should be unfavorable. The positive entropy of the system ($\Delta S \approx 56$ J/Kmol) suggests that the equilibrium is entropically driven, and results from the formation of two species from one, an entropically favorable process. It is postulated that high orders of hydrogen bonding exist between the solvent and both the iridium species, leading to their unexpected solubility in water and also to the absence of the negative entropy component often associated with solvent cage formation around ionic species. When a value for K_{eq} (3.2×10^{-3}) is derived from the Gibbs' free energy ($\Delta G \approx 14$ KJ/mol) it very nearly matches the experimentally determined average K_{eq} of 3.5×10^{-3}.

$IrH_2(PMe_3)_3O_2CPh$

^{31}P NMR studies of $IrH_2(PMe_3)_3(O_2CPh)$ (**3**) in aqueous solution indicate (**3**) dissociates completely forming $[IrH_2(PMe_3)_3(H_2O)]^+$. While similar ^{31}P NMR variable concentration studies on (**3**) with added chloride ion in H_2O lead to K_{eq} values that are of the same order of magnitude as those (**1**), the values are not constant, although they do follow a trend and are not just random values. It is postulated this inconsistency is due to

the non-ideality of the benzoate counterion. Either it directly interferes with the complexation of Cl^- to the iridium center or it has some effect on the pH of the system and indirectly affects the equilibrium.

$IrH_2(PMe_3)_3Br$

$IrH_2(PMe_3)_3Br$ (**6**) is synthesized quite easily and in high yield by the addition of KBr to aqueous solutions of $IrH_2(PMe_3)_3Cl$. (**6**) is slightly water soluble, more so than the very slightly soluble $IrH_2(PMe_3)_3I$, but less than either $IrH_2(PMe_3)_3Cl$ or $IrH_2(PMe_3)_3O_2CPh$. (**6**) partially dissociates in water to form what has been identified as $[IrH_2(PMe_3)_3(H_2O)]^+$ in this thesis, and most likely is involved in an equilibrium process similar to that of $IrH_2(PMe_3)_3Cl$ in water, although the limited water solubility of (**6**) made quantitative studies impractical.

$IrH_2(PMe_3)_3F$ and $[IrH_2(PMe_3)_3(H_2O)]^+$

All attempts to synthesize $IrH_2(PMe_3)_3F$ and complete the halide series of the $IrH_2(PMe_3)_3X$ complexes were unsuccessful, leading to either no reaction or complicated product mixtures from which isolation of individual products was unlikely. Likewise all attempts to isolate and trap $[IrH_2(PMe_3)_3(H_2O)]^+$ utilizing the common large, bulky counterions also failed.

General Conclusions

The physical properties and reactivities of the series of complexes $IrH_2(PMe_3)_3X$, where X is a halide, seem to follow trends consistent with Pearson's Hard/Soft Acid/Base Theory. The iridium(III) metal center is generally assumed in such schemes to be a "soft" center. It will bind most strongly with ligands that are of similar "softness", and least strongly with ligands that are considered very hard. Added to this, observed results also correspond with the known solublity data of halide anions.

Examination of the halide series finds that iodide, a "soft" ligand, likely forms very strong bonds with the iridium(III) center. The strength of this Ir-I bond prohibits the dissociation of the iodide ligand. Bromide, a slightly "harder" ligand, forms bonds with the iridium(III) center that are just weak enough to allow slight dissociation of the complex. Chloride, a fairly "hard" ligand, forms bonds with the iridium(III) that are weak enough to allow for significant dissociation of the complex in water. Fluoride, a very "hard" ligand forms bonds with the iridium(III) center that are so weak the complexes are, at best, unisolable.

Another very general trend was observed between the electronegativity of the ligand, X, and the NMR chemical shifts of the phosphines and the hydrides of the complexes. As the electronegativity of the ligand increases the chemical shifts of the all the ligands cis to X move upfield. This corresponds to a general decrease in the overall electron density on the metal center as X becomes increasingly more electronegative, thus deshielding the other ligands. However, the chemical shift of the hydride trans to the ligand X exhibits an inverse effect, moving upfield as the electronegativity of X increases. This is probably due to some kind of "trans effect" although the exact nature of this effect is unknown. Examination of the chemical shifts of the complex series Ir(CO)(dppe)X (x =

Cl, Br, I) reveal similar behavior so these effects are not purely an artifact of the $IrH_2(PMe_3)_3X$ system. These trends are consistent with those found by Birnbaum[105] in a 1971 study of hydride chemical shifts of monohydrido halo complexes.

Future Work

In lieu of actually isolating the $[IrH_2(PMe_3)_3(H_2O)]^+$ species and then testing its ability to catalytically hydrogenate unsaturates, two obvious future experiments come to mind. Performing conductivity studies on aqueous solutions to determine the type of species and the extent of ionization of the species in solution, is one of these. At the time the work for this thesis was completed reliable equipment for these studies was unavailable. The second specific experiment is to perform a detailed study of the effect of pH on the equilibrium systems of $IrH_2(PMe_3)_3Cl$ and $IrH_2(PMe_3)_3O_2CPh/Cl^-$.

More generally, it would be interesting to synthesize other complexes similar to $IrH_2(PMe_3)_3X$ to see if other useful water soluble catalysts can be produced.

References

(1) Kaesz, H. D.; Saillant, R. B. *Chemical Reviews* **1972**, *72*, 231.

(2) McCue, J. P. *Coordination Chemistry Reviews* **1973**, 265-333.

(3) Kruck, T. *Angew. Chem. Int. Ed.* **1967**, *6*, 53.

(4) Kruck, T.; Prasch, A. *Z. Anorg. Chem.* **1969**, *371*, 1.

(5) L'Eplattenier, F.; Calderazzo, F. *Inorg. Chem.* **1967**, *6*, 2092.

(6) L'Eplattenier, F.; Calderazzo, F. *Inorg. Chem.* **1968**, *7*, 1290.

(7) Kubas, G. J.; Jarvinen, G. D.; Ryan, R. R. *J. Am. Chem. Soc.* **1983**, *105*, 1883.

(8) Kubas, G. J.; Ryan, R. R.; Swanson, B. I.; Vergamini, P. J.; Wasserman, H. J. *J. Am. Chem. Soc.* **1984**, *106*, 451.

(9) Schubert, U.; Knorr, M. *Inorg. Chem.* **1989**, *28*, 1765-6.

(10) Deutsch, P.; Eisenberg, R. *J. Am. Chem. Soc.* **1990**, *112*, 714-721.

(11) Le, T. X. Doctoral Thesis, Virginia Polytechnic Institute and State University, 1992.

(12) Vaska, L.; Rhodes, R. E. *J. Am. Chem. Soc.* **1965**, *87*, 4970.

(13) Osburn, J. A.; Jardine, F. H.; Young, J. F.; Wilkinson, G. *J. Chem. Soc., A* **1966**, *12*, 1711.

(14) Mague, J. T.; Wilkinson, G. *J. Chem. Soc., A* **1966**, *12*, 1736.

(15) Bennett, M. A.; Milner, D. L. *J. Am. Chem. Soc.* **1969**, *91*, 6983.

(16) Werner, H.; Wolf, J.; Hohn, A. *J. Org. Chem.* **1985**, *287*, 395-407.

(17) Angoletta, M.; Caglio, G. *Gazz. Chim. Ital.* **1969**, *99*, 46.

(18) Freni, M.; Demichelis, R.; Giusto, D. *J. Inorg. Nucl. Chem.* **1967**, *29*, 1433.

(19) Dewhirst, K. C.; Keim, W.; Reilly, C. A. *Inorg, Chem.* **1968**, *7*, 546.

(20) Pearson, R. G.; Walker, H. W.; Mauermann, H.; Ford, P. C. *Inorg. Chem.* **1981**, *20*, 2741-3.

(21) Connor, J. A. *Top. Curr. Chem.* **1977**, *71*, 101.

(22) Chatt, J.; Coffey, R. S.; Shaw, B. L. *J. Chem. Soc.* **1965**, 7391.

(23) Deeming, A. J.; Shaw, B. L. *J. Chem. Soc., A* **1968**, 1887.

(24) Chatt, J.; Johnson, N. P.; Shaw, B. L. *J. Chem. Soc.* **1964**, 1625.

(25) Werner, H.; Stahl, S.; Kohlmann, W. *J. Organomet. Chem.* **1991**, *409*, 285-98.

(26) Harrod, J. F.; Gilson, D. F. R.; Charles, R. *Can. J. Chem.* **1969**, *47*, 2205.

(27) Glockling, F.; Wilbey, M. D. *J. Chem. Soc., A* **1970**, 1675.

(28) Vaska, L. *Chem. Commun.* **1966**, 614.

(29) Fernandez, J. M.; Gladysz, J. A. *Organometallics* **1989**, *8*, 207-19.

(30) Chinn, M. S.; Heinekey, D. M. *J. Am Chem. Soc.* **1990**, *112*, 5166-5175.

(31) Kubas, G. J. *Acc. Chem. Res.* **1988**, *21*, 120 -128.

(32) Vaska, L.; Catone, D. L. *J. Am. Chem. Soc.* **1966**, *88*, 5324.

(33) Sacco, A.; Rossi, M.; Nobile, C. F. *Chem. Commun.* **1966**, 589.

(34) Shapley, J. R.; Schrock, R. R.; Osborn, J. A. *J. Am. Chem. Soc.* **1968**, 2816.

(35) Butter, S. A.; Chatt, J. *J. Chem. Soc. A* **1970**, 1411.

(36) Deeming, A. J.; Shaw, B. L. *J. Chem. Soc. A* **1970**, 3356.

(37) Shapley, J. R.; Schrock, R. R.; Osborn, J. A. *J. Am. Chem. Soc.* **1970**, *91*, 2816.

(38) Bianchini, C.; Mealli, C.; Meli, A.; Peruzzini, M.; Zanobini, F. *J. Am. Chem. Soc.* **1988**, *110*, 8725.

(39) Bianchini, C.; Mealli, A.; Peruzzini, M.; Zanobini, F. *J. Am. Chem. Soc.* **1987**, *109*, 5548.

(40) Bianchini, C.; Peruzzini, M.; Zanobini, F. *J. Organomet. Chem.* **1987**, *326*, C79.

(41) Morris, R. H.; Earl, K. A.; Luck, R. L.; Lazarowych, N. J.; Sella, A. *Inorg. Chem.* **1987**, *26*, 2674-83.

(42) Bianchini, C.; Peruzzini, M.; Zanobini, F. *J. Org. Chem.* **1990**, *390*, C16-C19.

(43) Bianchini, C.; Laschi, F.; Peruzzini, M.; Ottaviani, F. M.; Vacca, A.; Zanello, P. *Inorg. Chem.* **1990**, *29*, 3394-3402.

(44) Mehrotra, R. C.; Bohra, R. *Metal Carboxylates*; Academic Press: 1983, pp 396.

(45) Inglis, T. *Inorg. Chim. Acta, Rev* **1973**, *7*, 35-42.

(46) Kong, P.; Roundhill, D. M. *Inorg. Chem.* **1972**, *2*, 1437.

(47) Commereuc, D.; Douek, I.; Wilkinson, G. *J. Chem. Soc. A* **1970**, 1771.

(48) Komiya, S.; Yamamoto, A. *J. Chem. Soc., Chem. Commun.* **1974**, *13*, 523.

(49) Komiya, S.; Yamamoto, A. *J. Organomet. Chem.* **1975**, *87*, 333-9.

(50) Nagy-Magos, Z.; Vastag, S.; Heil, B.; Marko, L. *J. Organomet. Chem.* **1979**, *171*, 97-102.

(51) Horner, L.; Siegle, H. *Liebigs, Ann. Chem.* **1971**, *751*, 135.

(52) Boyar, E. B.; Higgins, W. G.; Robinson, S. D. *Inorg. Chim. Acta* **1983**, *76*, L293.

(53) Bianchini, C.; Meli, A.; Peruzzini, M.; Zanobini, F. *Organometallics* **1990**, *9*, 1155.

(54) Borowski, A. F.; Cole, H. D. J.; Wilkinson, G. *Nouv. J. Chim.* **1978**, *2*, 137-44.

(55) Joo, F.; Toth, Z. *J. Mol. Catal.* **1980**, *8*, 369-383.

(56) Dror, Y.; Manassen, J. *J. Mol. Catal.* **1977**, *2*, 219.

(57) Benyei, A.; Joo, F. *J. Mol. Catal.* **1990**, *58*, 151-163.

(58) Larpent, C.; Patin, H. *J. Org. Chem.* **1987**, *335*, C13-C16.

(59) Sinou, D.; Safi, M.; Claver, C.; Masdeu, A. *J. Mol. Catal.* **1991**, *68*, L9-L12.

(60) Safi, M.; Sinou, D. *Tetra. Lett.* **1991**, *32*, 2025-2028.

(61) Renaud, E.; Russell, R. B.; Fortier, S.; Brown, S. J.; Baird, M. C. *J. Organomet. Chem.* **1991**, *419*, 403-415.

(62) Smith, R. T.; Ungar, R. K.; Sanderson, L. J.; Baird, M. C. *Organometallics* **1983**, *2*, 1138-1144.

(63) Nuzzo, R. G.; Haynie, S. L.; Wilson, M. E.; Whitesides, G. M. *J. Org. Chem.* **1981**, *46*, 2861-7.

(64) Benhamza, R.; Amrani, Y.; Sinou, D. *J. Organomet. Chem.* **1985**, *288*, C37-C39.

(65) Amrani, D.; Sinou, Y. *J. Mol. Catal.* **1986**, *36*, 319.

(66) Amrani, Y.; Sinou, D. *J. Mol. Catal.* **1984**, *24*, 231-233.

(67) Toth, I.; Hanson, B. E. *Tetrahedron: Asymmetry* **1990**, *1*, 895.

(68) Toth, I.; Hanson, B. E.; Davis, M. E. *Tetrahedron: Asymmetry* **1990**, *1*, 913.

(69) Halpern, J. *Discuss. Faraday Soc., VNo.* **1968**,

(70) Davies, J. A.; Hartley, F. R. *Chem. Rev.* **1981**, *81*, 79.

(71) Collman, J. P.; Hegedus, L. S.; Norton, J. R.; Finke, R. G. *Principles and Applications of Organotransition Metal Chemistry*; University Science Books: Mill Valley, Calif., 1987.

(72) Shustorovich, E. M.; Porai-koshits, M. A.; Buslaev, Y. A. *Coor. Chem. Rev.* **1975**, *17*, 1-98.

(73) Pauling, L. *The Nature of the Chemical Bond;* 3rd ed.; Cornell University Press: Ithaca, New York, 1960.

(74) Pearson, R. G. *Hard and Soft Acids and Bases*; Dowden, Hutchinson, and Ross: Stroudsburg, PA, 1973.

(75) Jorgenson, C. K. *Inorg. Chem.* **1964**, *3*, 1201.

(76) Pearson, R. G. *Inorg. Chem.* **1973**, *12*, 231.

(77) Heaton, I.; Chatt, J. *J. Chem. Soc.* **1955**, 2937.

(78) Bauer, H.; Nagel, U.; Beck, W. *J. Organomet. Chem.* **1985**, *209*, 219.

(79) Jensen, C. M.; Trogler, W. C. *J. Am. Chem. Soc.* **1985**, *108*, 723.

(80) Garlaschelli, L.; Marchionna, M.; Iapalucci, M. C.; Longoni, G. *J. Organomet. Chem.* **1989**, *378*, 457-468.

(81) Leoni, P.; Sommovigo, M.; Pasquali, M.; Midollini, S.; Braga, D.; Sabatino, P. *Organometallics* **1991**, *10*, 1038.

(82) Stang, P. J.; Song, L.; Huang, Y.; Arif, A. M. *J. Organomet. Chem.* **1991**, *405*, 403.

(83) Ahmed, M.; Edwards, A. J.; Jones, C. J.; McCleverty, J. A.; Rothin, A. S.; Tate, J. P. *J. Chem. Soc. Dalton, Trans.* **1988**, 257.

(84) Frisch, P. D.; Khare, G. P. *J. Am. Chem. Soc.* **1978**, *100*, 8267.

(85) Mague, J. T. *Inorg. Chem.* **1973**, *12*, 2649.

(86) Clark, H. C.; Reimer, K. J. *Inorg. Chem.* **1975**, *14*, 2133.

(87) Deeming, A. J.; Proud, G. P.; Dawes, H. M.; Hursthouse, M. B. *J. Chem. Soc. Dalton Trans.* **1986**, 2545.

(88) Bergmeister, J. J. I.; Hanson, B. E.; Merola, J. S. *Inorg. Chem.* **1990**, *29*, 4831.

(89) Ochocki, J.; Kostka, K.; Zurowska, B.; Mrozinski, J.; Galdecka, E.; Galdecki, Z.; Reedijk, J. *J. Chem. Soc., Dalton Trans., N20, P2955* **1992**,

(90) Crabtree, R. H.; Felkin, H.; Khan, T.; Morris, G. E. *J. Organomet. Chem.* **1977**, *141*, 205.

(91) Crabtree, R. H.; Mihelcic, J. M.; Quirk, J. M. *J. Am. Chem. Soc.* **1979**, *101*, 7738.

(92) Crabtree, R. H.; Mellea, M. F.; Mihelcic, J. M.; Quirk, J. M. *J. AM. Chem. Soc.* **1982**, *104*, 107.

(93) Crabtree, R. H.; Demou, P. C.; Eden, D.; Mihelcic, J. M.; Parnell, C. A.; Quirk, J. M.; Morris, G. E. *J. Am. Chem. Soc.* **1982**, *104*, 6994.

(94) Luo, X.; Crabtree, R. H. *J. Am. Chem. Soc.* **1989**, *111*, 2527-2535.

(95) Luo, X. L.; Schulte, G. K.; Crabtree, R. H. *Inorg. Chem.* **1990**, *29*, 682.

(96) Novak, B. M.; Grubbs, R. H. *J. Am. Chem. Soc.* **1988**, *110*, 7542.

(97) O'Connor, C.; Wilkinson, G. *J. Chem. Soc. (A)* **1968**, 2665.

(98) Le, T. X.; Merola, J. S. *Organometallics* **1993**, *12*, 3798.

(99) Pearson, R. G. *J. Am. Chem. Soc.* **1963**, *85*, 3533.

(100) Greenwood, N. N.; Earnshaw, A., *Chemistry of the Elements* Pergamon Press: 1984.

(101) Merola, J. S. *Organometallics* **1989**, *8*, 2975.

(102) Rhodes, L. F.; Huffman, J. C.; Caulton, K. G. *J. Am. Chem. Soc.* **1984**, *106*, 6874.

(103) Johnson, C. E.; Fisher, B. J.; Eisenberg, R. *J. Am. Chem. Soc.* **1983**, *105*, 7772.

(104) Johnson, C. E.; Eisenberg, R. *J. Am. Chem. Soc.* **1985**, *107*, 3148.

(105) Birnbaum, E. R. *Inorg. Nucl. Chem. Lett.* **1971**, *7*, 233.

(106) Atkins, P. W., *Physical Chemistry*, 3rd ed., W. H. Freeman and Co., New York, **1986**, 824.

(107) Harding, P. A.; Preece, M.; Robinson, S. P.; Henrick, K.; *Inorg. Chim. Acta* **1986**, *118*, L31.

(108) Boniface, S. M.; Clark, G. R.; Collins, T. J.; Roper, W. R. *J. Org. Chem.* **1981**, *206*, 109.

Appendix: Calculation of K_{eq} Values of (1) in H_2O

Table A.1 ^{31}P NMR Integration Data for $IrH_2(PMe_3)_3Cl$

[Ir]	Int (-39)	Int (-49)
0.005	6.439	3.072
0.015	4.627	3.805
0.024	3.847	3.991
0.036	3.103	3.828
0.046	2.777	4.147
0.053	2.422	4.013
0.060	2.357	4.221
0.065	1.845	3.356

[Ir] = The initial molar concentration of $IrH_2(PMe_3)_3Cl$ in solution

Int (-39) = The integration area of the peak at -39 ppm in the ^{31}P NMR spectra of $IrH_2(PMe_3)_3Cl$ in H_2O

Int (-49) = The integration area of the peak at -49 ppm in the ^{31}P NMR spectra of $IrH_2(PMe_3)_3Cl$ in H_2O

Case 1 Equilibrium Calculations

Equilibrium Concentrations

$$2\ IrH_2P_3Cl \longrightarrow 2\ [IrH_2P_3(OH_2)]^+ + 2\ Cl^- \rightleftharpoons [H_2P_3Ir\text{-}Cl\text{-}IrP_3H_2]^+ + Cl^-$$

$$\downarrow \qquad \downarrow \qquad \downarrow \qquad \downarrow$$

$$(Ir_{init} - 2x) \qquad (Ir_{init} - x) \qquad (x) \qquad (Ir_{init} - x)$$

Ir_{init} = initial concentration of IrH_2P_3Cl in solution

$[H_2P_3Ir\text{-}Cl\text{-}IrP_3H_2]^+$ = 1/2(integration of peak at -49 ppm)

$[IrH_2P_3(OH_2)]^+$ = 1/2(integration of peak at -39 ppm)

$$(1) \qquad K_{eq} = \frac{\{[H_2P_3Ir\text{-}Cl\text{-}IrP_3H_2]^+\}}{\{[IrH_2P_3(OH_2)]^+\}^2\ \{Cl^-\}} = \frac{(x)}{(Ir_{init} - 2x)^2(Ir_{init} - x)}$$

$$(2) \qquad \frac{[H_2P_3Ir\text{-}Cl\text{-}IrP_3H_2]^+}{[IrH_2P_3(OH_2)]^+} = \frac{\text{(integration of peak at -49 ppm)}}{\text{(integration of peak at -39 ppm)}} = \mathbf{z}$$

The ratio **z** can be solved for numerically by inserting the relevant ^{31}P NMR integration values into the above equation. Thus

$$(3) \qquad \mathbf{z} = \frac{[H_2P_3Ir\text{-}Cl\text{-}IrP_3H_2]^+}{[IrH_2P_3(OH_2)]^+} = \frac{(x)}{(Ir_{init} - 2x)}$$

Solving for X in Equation 3, with **z** and Ir_{init} being known quantities, and then substituting into Equation 1, a value for K_{eq} is obtained.

Table A.2 Case 1 Equilibrium Species Concentrations

Trial #	Z	x	$[IrH_2P_3H_2O^+]$	$[Cl^-]$	$[Ir\text{-}Cl\text{-}Ir^+]$	Keq
1	0.4771	0.0012	0.0026	0.0038	0.0012	49339
2	0.8223	0.0047	0.0057	0.0103	0.0047	14028
3	1.0374	0.0081	0.0078	0.0159	0.0081	8358
4	1.2336	0.0128	0.0104	0.0232	0.0128	5123
5	1.4933	0.0172	0.0115	0.0288	0.0172	4499
6	1.6569	0.0204	0.0123	0.0326	0.0204	4131
7	1.7908	0.0235	0.0131	0.0365	0.0235	3742
8	1.8190	0.0255	0.0140	0.0395	0.0255	3285

Case 2 Equilibrium Calculations

Equilibrium Concentrations

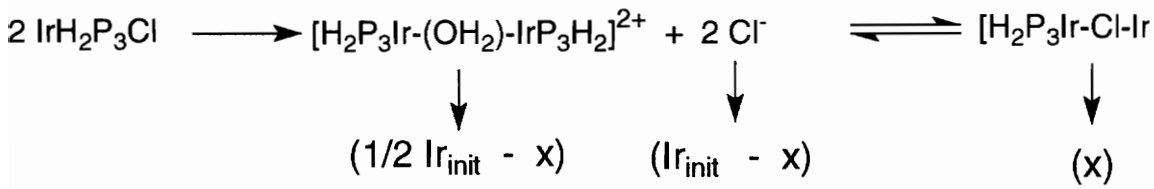

Ir_{init} = initial concentration of IrH_2P_3Cl in solution

$[H_2P_3Ir\text{-}Cl\text{-}IrP_3H_2]^+$ = 1/2(integration of peak at -49 ppm)

$[H_2P_3Ir\text{-}(OH_2)\text{-}IrP_3H_2]^{2+}$ = 1/4(integration of peak at -39 ppm)

$$(1) \qquad K_{eq} = \frac{\{[H_2P_3Ir\text{-}Cl\text{-}IrP_3H_2]^+\}}{\{[H_2P_3Ir\text{-}(OH_2)\text{-}IrP_3H_2]^{2+}\}\{Cl^-\}} = \frac{(x)}{(1/2\ Ir_{init} - x)(Ir_{init}}$$

$$(2) \qquad \frac{[H_2P_3Ir\text{-}Cl\text{-}IrP_3H_2]^+}{[H_2P_3Ir\text{-}(OH_2)\text{-}IrP_3H_2]^{2+}} = \frac{\text{(integration of peak at -49 ppm)}}{\text{1/2(integration of peak at -39 ppm)}}$$

The ratio **z** can be solved for numerically by inserting the relevant ^{31}P NMR integration values into Equation 2. Thus

$$(3) \qquad \mathbf{z} = \frac{[H_2P_3Ir\text{-}Cl\text{-}IrP_3H_2]^+}{[H_2P_3Ir\text{-}(OH_2)\text{-}IrP_3H_2]^{2+}} = \frac{(x)}{(1/2\ Ir_{init} - x)}$$

Solving for X in Equation 3, with **z** and Ir_{init} being known quantities, and ther substituting into Equation 1, a value for K_{eq} is obtained.

Table A.3 Case 2 Equilibrium Species Concentrations

Trial #	Z	x	[Ir-O-Ir^{2+}]	[Cl$^-$]	[Ir-Cl-Ir$^+$]	Keq
1	0.9542	0.0012	0.0013	0.0038	0.0012	252.5
2	1.6447	0.0047	0.0028	0.0103	0.0047	159.1
3	2.0749	0.0081	0.0039	0.0159	0.0081	130.5
4	2.4673	0.0128	0.0052	0.0232	0.0128	106.4
5	2.9867	0.0172	0.0058	0.0288	0.0172	103.8
6	3.3138	0.0204	0.0061	0.0326	0.0204	101.5
7	3.5817	0.0235	0.0065	0.0365	0.0235	98.0
8	3.6379	0.0255	0.0070	0.0395	0.0255	92.1

Case 3 Equilibrium Calculations

Equilibrium Concentrations

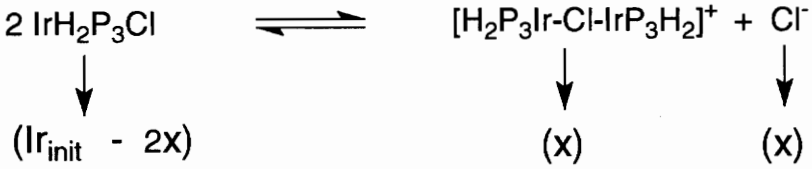

Ir_{init} = initial concentration of IrH_2P_3Cl in solution

$[IrH_2P_3Cl]$ = (integration of peak at -49 ppm)

$[H_2P_3Ir\text{-}Cl\text{-}IrP_3H_2]^+$ = 1/4(integration of peak at -39 ppm)

$$(1) \qquad K_{eq} = \frac{\{[H_2P_3Ir\text{-}Cl\text{-}IrP_3H_2]^+\}\ \{Cl^-\}}{\{[IrH_2P_3Cl]\}^2} = \frac{(x)\,(x)}{(Ir_{init} - 2x)^2}$$

$$(2) \qquad \frac{[H_2P_3Ir\text{-}Cl\text{-}IrP_3H_2]^+}{[IrH_2P_3Cl]} = \frac{1/4(\text{integration of peak at -39 ppm})}{(\text{integration of peak at -49 ppm})} = \mathbf{z}$$

The ratio **z** can be solved for numerically by inserting the relevant ^{31}P NMR integration values into Equation 2. Thus

$$(3) \qquad \mathbf{z} = \frac{[H_2P_3Ir\text{-}Cl\text{-}IrP_3H_2]^+}{[IrH_2P_3(OH_2)]^+} = \frac{(x)}{(Ir_{init} - 2x)}$$

Solving for X in Equation 3, with **z** and Ir_{init} being known quantities, and then substituting into Equation 1, a value for K_{eq} is obtained.

Table A.4 Case 3 Equilibrium Species Concentrations

Trial #	Z	x	$[IrH_2P_3Cl]$	$[Ir\text{-}Cl\text{-}Ir^+]$	$[Cl^-]$	Keq
1	0.5240	0.0013	0.0024	0.0013	0.0013	0.2746
2	0.3040	0.0028	0.0093	0.0028	0.0028	0.0924
3	0.2410	0.0039	0.0162	0.0039	0.0039	0.0581
4	0.2027	0.0052	0.0256	0.0052	0.0052	0.0411
5	0.1674	0.0058	0.0345	0.0058	0.0058	0.0280
6	0.1509	0.0061	0.0407	0.0061	0.0061	0.0228
7	0.1396	0.0065	0.0469	0.0065	0.0065	0.0195
8	0.1374	0.0070	0.0510	0.0070	0.0070	0.0189

Case 4 Equilibrium Calculations

Equilibrium Concentrations

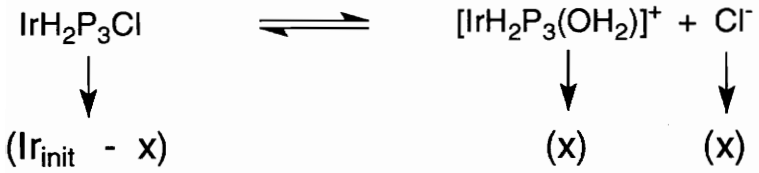

Ir_{init} = initial concentration of IrH_2P_3Cl in solution

$[IrH_2P_3Cl]$ = (integration of peak at -49 ppm)

$[IrH_2P_3(OH_2)]^+$ = 1/2(integration of peak at -39 ppm)

$$(1) \qquad K_{eq} = \frac{\{[IrH_2P_3(OH_2)]^+\}\{Cl^-\}}{\{[IrH_2P_3Cl]\}} = \frac{(x)(x)}{(Ir_{init} - x)}$$

$$(2) \qquad \frac{[IrH_2P_3(OH_2)]^+}{[IrH_2P_3Cl]} = \frac{1/2(\text{integration of peak at -39 ppm})}{(\text{integration of peak at -49 ppm})} = \mathbf{z}$$

The ratio **z** can be solved for numerically by inserting the relevant ^{31}P NMR integration values into Equation 2. Thus

$$(3) \qquad \mathbf{z} = \frac{[IrH_2P_3(OH_2)]^+}{[IrH_2P_3Cl]} = \frac{(x)}{(Ir_{init} - x)}$$

Solving for X in Equation 3, with **z** and Ir_{init} being known quantities, and then substituting into Equation 1, a value for K_{eq} is obtained.

Table A.5 Case 4 Equilibrium Species Concentrations

Trial #	Z	x	$[IrH_2P_3Cl]$	$[IrH_2P_3OH_2^+]$	$[Cl^-]$	Keq
1	1.048	0.0026	0.0024	0.0026	0.0026	0.0027
2	0.608	0.0057	0.0093	0.0057	0.0057	0.0034
3	0.482	0.0078	0.0162	0.0078	0.0078	0.0038
4	0.405	0.0104	0.0256	0.0104	0.0104	0.0042
5	0.335	0.0115	0.0345	0.0115	0.0115	0.0039
6	0.302	0.0123	0.0407	0.0123	0.0123	0.0037
7	0.279	0.0131	0.0469	0.0131	0.0131	0.0037
8	0.275	0.0140	0.0510	0.0140	0.0140	0.0039

Vita

The author was born in Pottsville, PA on June 19, 1966. He received his B.S. in Chemistry from Lehigh University in 1988 and began graduate studies under Professor Joseph S. Merola at Virginia Tech in 1989.